DISTORTIONAL BUCKLING OF COLD-FORMED STEEL COLUMNS

FINAL REPORT

August, 2000

a project sponsored by:
The American Iron and Steel Institute

research completed by:
B.W. Schafer

Distortional Buckling of Cold-Formed Steel Columns

(FINAL REPORT)

August 2000

APPENDICES

LIST OF TABLES

LIST OF FIGURES

1 Executive Summary

Research on the distortional buckling of cold-formed steel columns, primarily C and Z shapes is summarized below.

Defining distortional buckling:
- involves rotation at the web/flange juncture in typical members,
- exists at half-wavelengths intermediate between local and flexural or flexural-torsional buckling.

Existing research
- shows that post-buckling capacity exists in the distortional mode,
- has opened many questions about how distortional buckling interacts with other buckling modes,
- includes examples of how other specifications have incorporated distortional buckling.

Prediction by hand methods:
- local buckling of the member may be predicted using semi-empirical interaction models (see Appendix B),
- distortional buckling may be predicted using Schafer's approach or Hancock's approach (see Appendix B).

Prevalence of the distortional mode:
- narrow flanges (compared to the web depth) and wide flanges both lead to low distortional buckling stresses,
- short lips and very long lips (lip lengths as wide as the flange width) lead to low distortional buckling stresses,
- the majority of typical C and Z members suffer more from local buckling than distortional buckling,
- in members in which additional folds are added to break up the local buckling mode, distortional buckling is much more important and prevalent.

Ultimate strength in the distortional mode
- has lower post-buckling capacity than local buckling,
- has higher imperfection sensitivity than local buckling; but
- may be predicted by simple formulas when the distortional buckling stress is accurately known.

Comparison of the AISI (1996) Specification with existing data shows
- overall performance is on average 6% unconservative, but
- the error is not specifically due to distortional buckling, rather
- systematic error exists for high web slenderness (h/t) and/or high web height to flange width (h/b) ratios,
- the error is primarily due to the element approach which ignores all local buckling interaction.

Alternative design methods using an effective width approach:
- can lead to simpler design for local buckling,
- require the addition of a distortional buckling calculation,
- provide a means for effectively designing members prone to distortional failures,
- compared to the AISI (1996) method longer lips are encouraged and short lips discouraged.

Alternative design methods using a Direct Strength approach:
- remove systematic unconservative prediction in current methods,
- agree better with available experimental data,
- avoid the use of lengthy element by element calculations,
- provide a means for rationally incorporating numerical methods and optimizing member design,
- provide an explicit design check on both local and distortional buckling limit states,
- compared to the AISI (1996) method, encourages the use of longer lips and discourages the use of narrow members (high h/b) with slender webs (high h/t) and short lips (low d/b).

Recommendations for design and the AISI Specification:
- for immediate adoption, add new commentary language for B4.2 providing limits of the current method (see Appendix F.1 for proposed wording),
- for interim adoption, remove section B4.2, replace with k = 4 solution and add a distortional buckling check (see method C1 in Appendix B and proposed specification language in Appendix F.2),
- for interim adoption as an alternative design method, and for long-term adoption, adopt the Direct Strength design method and allow rational analysis (see methods C3 and C2 in Appendix B and proposed specification language in Appendix F.3).

2 Introduction

What is distortional buckling?

Distortional buckling, also known as "stiffener buckling" or "local-torsional buckling", is a mode characterized by rotation of the flange at the flange/web junction in members with edge stiffened elements. In members with intermediately stiffened elements distortional buckling is characterized by displacement of the intermediate stiffener normal to the plane of the element. This study focuses on distortional buckling of members with edge stiffened elements. Distortional buckling may be directly studied by finite strip analysis.

Consider the finite strip analysis of a lipped C in pure compression, Figure 1. The analysis proceeds by finding the lowest buckling mode at a variety of different longitudinal half sine waves (half-wavelengths). The minima of the curve reveal different buckling modes that exist for the member. In this case, distortional buckling exists at an intermediate half-wavelength, between local buckling and long half-wavelength flexural or flexural-torsional buckling. This intermediate length is a defining characteristic of distortional buckling.

As Figure 1 shows, for a typical lipped C member in pure compression local buckling often occurs at a lower buckling stress than distortional buckling. If the local buckling stress is significantly lower than the distortional buckling stress then it is possible that distortional buckling may be safely ignored. However, many situations exist in which distortional buckling must still be considered, even in routine design.

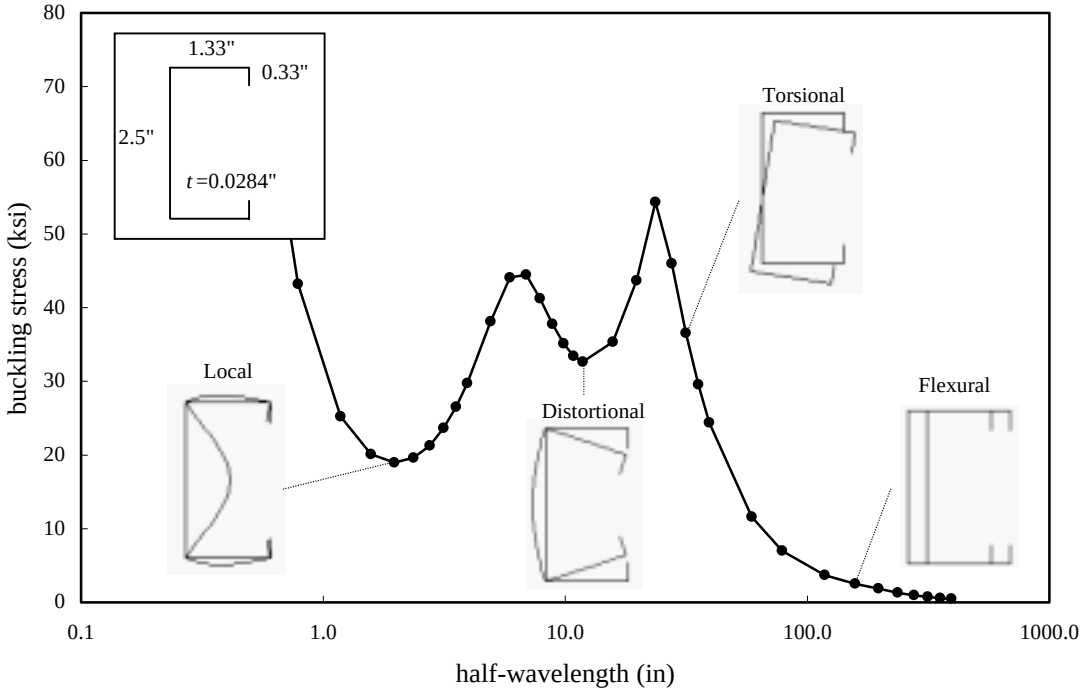

Figure 1 Finite Strip Analysis of a Drywall Stud

How does distortional buckling behave?

Intuition for local buckling behavior is a relatively straightforward – as width-to-thickness (*w/t*) ratios increase local buckling stress declines. This fact serves the engineer well in designing for local buckling. Similar intuition for distortional buckling is difficult to arrive at. A series of examples examining the distortional buckling stress of lipped C columns are summarized in Figure 2. (The distortional buckling stress was calculated using closed-form expressions derived in Schafer (1997), examples of this method are given in Appendix B). Figure 2 provides a means to develop a modest amount of intuition with respect to distortional buckling.

For distortional buckling:

Too little or too much flange is not good: Figure 2 (a) and (b) show results as the flange width is varied. In the examples, the highest distortional buckling stresses are achieved around a *b/h* ratio of 1/3; this conclusion is not general though, as different stiffener lengths yield a different optimum *b/h* (where *b* = flange width, *h* = web height and *d* = lip length). If the flange is too narrow local buckling of the web is at wavelengths near distortional buckling of the flange and the distortional mode easily forms at low stresses. If the flange is excessively wide local buckling is not the concern, but rather the size of the stiffener required to keep the flange in place is the concern. For practical stiffener lengths, wide flanges also lead to low distortional stresses.

Longer lips are usually better: Figure 2 (c) and (d) show results as the lip length is varied. The highest distortional buckling stresses are achieved when the lip length is nearly equal to the flange width ($d/b \sim 1$). Lips longer than this degrade the distortional buckling stress. From the standpoint of distortional buckling (ignoring the detrimental effects of long lips in local buckling modes) edge stiffener lengths should be longer than currently used in practice.

Deep webs lead to low stresses: Comparing the results from the 6 in. deep web to the 12 in. deep web given in Figure 2, the distortional buckling stress decreases approximately by a factor of 2 when the web depth is doubled. Actual decrease in the distortional buckling stress depends on the specific *d* and *b*. Distortional buckling is governed by the rotational stiffness at the web/flange juncture, deeper webs are more flexible and thus provide less rotational stiffness to the web/flange juncture. This results in earlier distortional buckling for deep webs. However, the trend appears approximately linear, as opposed to local buckling which changes as $(t/h)^2$ and thus local buckling stresses decrease at a faster rate with deeper webs.

As Figure 2 shows, the interaction of the flange, web, and lip in determining the distortional buckling stress is complex. Development of simple yet general criteria to incorporate this behavior has not proven successful to date.

Table 1 Summary of Research on Cold-Formed Steel Columns

	Overall	**Distortional Buckling**
1940's and 1950's	• Elastic plate stability formalized • Experimental work begins • Effective width for ultimate strength	• Known phenomena • Too complicated to predict analytically
1960's	• Early design methods formalized • Cold-formed steel material properties • Prediction of overall (global) buckling	• Approximate analytical methods from Aluminum researchers • Folded plate theory for distortional buckling
1970's	• Local and overall interaction • Design methods for unstiffened and edge stiffened elements • Finite Elements	• Observed in experiments, but often intentionally restricted • Elastic buckling criteria not accurate for predicting failure mode
1980's	• Imperfections and residual stresses • Effective width formalized • Finite strip • Distortional buckling problems	• Hand methods for elastic prediction • Experiments with unrestricted distortional buckling performed • Postbuckling reserve discovered
1990 to Present	• Distortional buckling problems • Distortional buckling design • Interaction & column boundary conditions • Generalized Beam Theory	• Hand methods for elastic prediction • Interaction of distortional with other buckling modes examined • Design: column curve or effective width? • Heightened imperfection sensitivity? • Inclusion in Design Standards

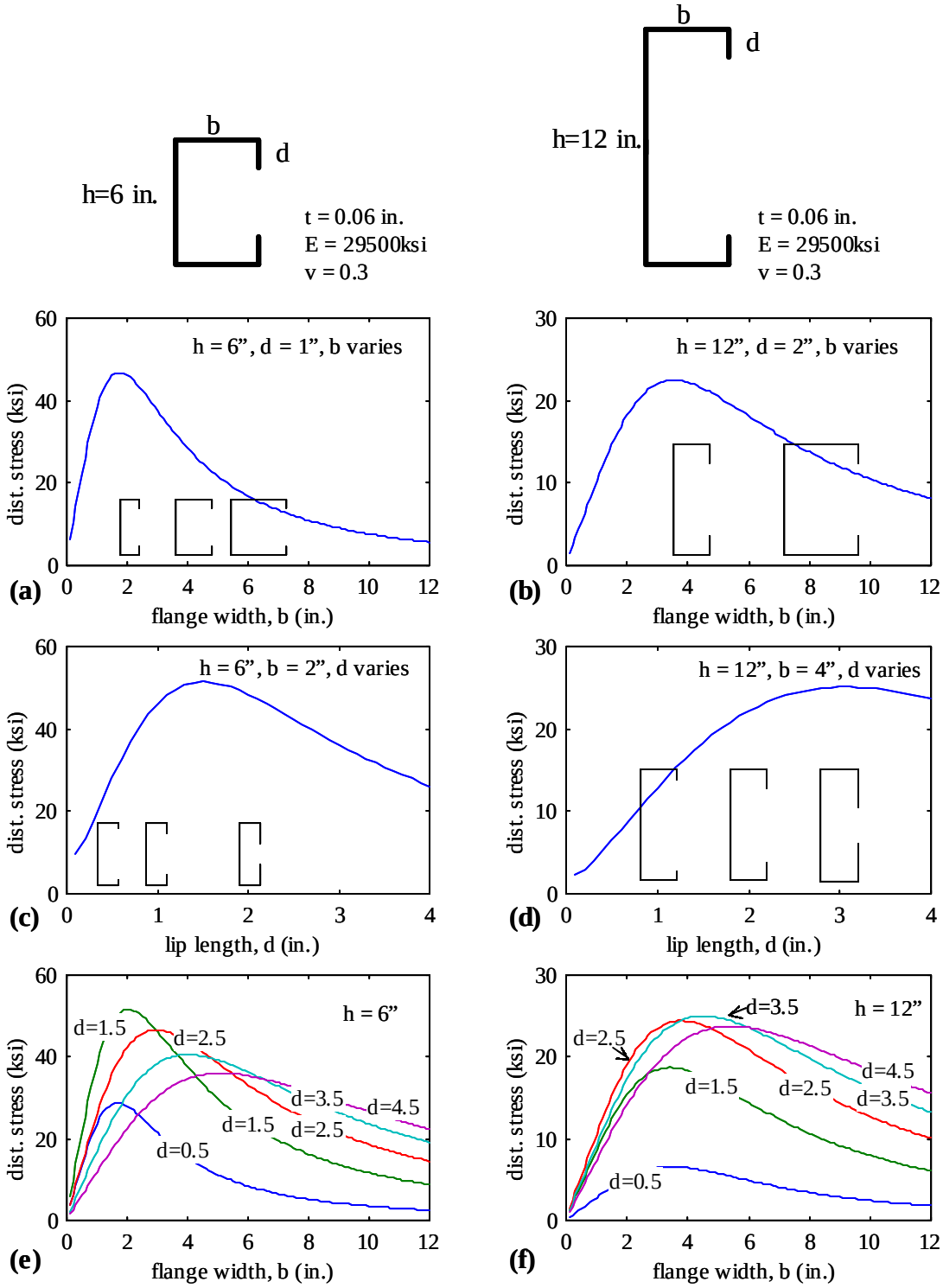

Figure 2 Behavior of Distortional Buckling Stress for Lipped C Columns (a-b) variation with respect to flange width, (c-d) variation with respect to lip length, (e-f) variation with respect to flange width for different lip lengths

What research has already been done for distortional buckling of columns?

Table 1 provides a summary of the history of research in cold-formed steel columns with an emphasis on distortional buckling. A full version of the history of distortional buckling in cold-formed steel column research may be found in Appendix A. Table 1 shows the basic trends in research and design specifications with respect to distortional buckling: notably, the 1990s saw the explicit introduction of distortional buckling into design specifications. Many questions remain to be completely answered: How does distortional buckling interact with other modes? Does the distortional mode exhibit a heightened imperfection sensitivity? How should distortional buckling be incorporated into specifications?

3 Hand Prediction of Column Buckling Modes

Illustrative examples, completed in Mathcad, for the hand prediction of the column buckling modes of Figure 1 are given in Appendix B. The following sections introduce the various prediction methods, and examine the accuracy of the proposed formula versus numerical methods.

3.1 Local Mode

Hand prediction of the local buckling mode may be done in two ways: the traditional, element approach; or a semi-empirical, interaction approach. The element approach is the classic isolated plate solution. For example, employing $k = 4$ for a "stiffened element" assumes it is a simply supported plate in pure compression. Local buckling of the entire member may be predicted by taking the minimum of the connected elements (very conservative approach), alternatively a weighted average may be used, or interaction of elements may be ignored and each element assumed to buckle independently, this is tacitly assumed in the AISI (1996) Specification.

The semi-empirical, interaction approach uses modified plate buckling coefficients (i.e., modified k's) to account for the influence of a single neighboring element. For instance, in Appendix B expressions are given for flange/web local buckling and for flange/lip local buckling. (*Note*: the expression for flange/web local buckling are newly derived for this work.) Local buckling of the entire member may be predicted by taking the minimum of these semi-empirical, interaction equations. A complete example for predictions in the local mode are given in Appendix B.

3.2 Distortional Mode

Closed-form "hand" models fro distortional buckling may be predicted via: current AISI (1996) methods, Lau and Hancock (1987), or Schafer (1997). The AISI (1996) method is based on the work of Desmond (1977) and its development is fully discussed in Appendix A and Schafer (1997). The approaches of Lau and Hancock (called Hancock's approach from hereon) and Schafer's approach are similar. The Hancock and Schafer models are conceptually the same for the flange, but differ in the methods used to treat the web. Schafer's method explicitly approximates the rotational stiffness at the web/flange juncture in the calculation of the distortional buckling stress.

Inaccuracy in the AISI (1996) approach lead to another simplified method for handling distortional buckling. The approach was created by the author – essentially an additional reduction is placed on the AISI k value for high web height to flange width ratios. This reduction approximately accounts for distortional buckling and local buckling interaction. The expression for the reduction, R, is given in the notes of Table 3.

A complete example for predictions in the distortional mode are given in Appendix B.

3.3 Flexural or Flexural-torsional Mode

Hand predictions for x-axis and y-axis flexural buckling as well as approximate hand prediction of flexural-torsional buckling is given in AISI (1996). Calculation of the 'warping' section properties is the only significant complication with these hand methods.

A complete example for predictions in the flexural or flexural-torsional mode are given in Appendix B.

3.4 Accuracy of Hand Predictions for Local and Distortional Buckling

A parametric study of 170 cross-sections is performed in order to assess the accuracy of available hand methods for prediction of local, distortional, and global buckling modes. The geometry of the studied members is shown in

Figure 3, summarized in Table 2 and detailed in Appendix C. A variety of C's and Z's are studied, including all of those listed in the AISI (1996) Design Manual as well as a group of commercially available drywall studs (selected primarily for their relatively high web slenderness). In addition, a group of members covering a large range of element slenderness, originally studied in Schafer (1997), is also included.

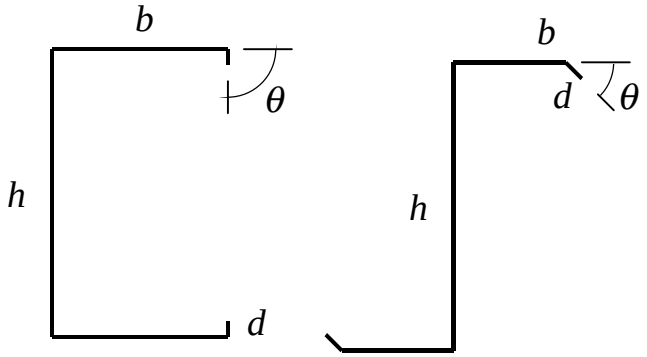

Figure 3 Geometry of Members for Elastic Buckling Study

Table 2 Summary of Member Geometry for Elastic Buckling Study

	h/b		h/t		b/t		d/t		
	max	min	max	min	max	min	max	min	count
Schafer (1997) Members	3.0	1.0	90	30	90	30	15.0	2.5	32
Commercial Drywall Studs	4.6	1.2	318	48	70	39	16.9	9.5	15
AISI Manual C's	7.8	0.9	232	20	66	15	13.8	3.2	73
AISI Manual Z's	4.2	1.7	199	32	55	18	20.3	5.1	50
	7.8	0.9	318	20	90	15	20.3	2.5	170

Overall performance of the prediction methods is shown for local buckling in Figure 4 and distortional buckling in Figure 5. Table 3 presents the summarized numerical information and Appendix C presents the detailed member by member results.

For local buckling prediction Table 3 and Figure 4 show that the semi-empirical interaction model (e.g., *k* calculated as a function of flange width to web width ratios) is clearly more accurate than the element model (each element, web, flange, lip treated separately). This is particularly true for moderate web height to flange width ratios. However, the element model is consistently conservative, and the semi-empirical interaction model may be unconservative for high web height to flange width ratios. This is more than offset by the increased accuracy in the practical range of sections. The semi-empirical interaction model predicts local buckling of the entire member with reasonable accuracy.

For distortional buckling prediction Table 3 and Figure 5 show that the AISI approach is flawed and that both Hancock's and Schafer's method work reasonably well. The existing AISI method is unconservative and inaccurate. Simple modifications proposed with an h/b correction (the R*AISI method) remove the overall unconservative nature of the prediction, but cannot provide the same level of accuracy as the more robust expressions of Hancock's and Schafer's method.

Distortional buckling prediction by Schafer's approach provides a slightly more accurate, but less conservative solution than Hancock's approach. In a finite strip analysis the distortional mode may not always exist as a minimum. In these cases the accuracy of the predictive methods cannot be directly assessed – and statistics for those members are not included in Table 3. However, Appendix C provides a direct member-by-member comparison of the distortional buckling predictions for Schafer's and Hancock's approach. As the web height to flange width ratio (*h/b*) increases (above approximately 4) Hancock's approach often yields a distortional buckling stress of zero. Thus, the method, conservatively indicates no strength exists in these sections. Schafer's approach yields a distortional buckling stress that is at or slightly above the web local buckling stress. Thus in this limit, Schafer's approach converges to the expected solution. This is a result of the more accurate treatment of the web's contribution to the rotational stiffness at the web/flange juncture.

Table 3 Performance of Prediction Methods for Elastic Buckling

		Local		Distortional			
		$\frac{(fcr)_{true}}{(fcr)_{element}}$	$\frac{(fcr)_{true}}{(fcr)_{interact}}$	$\frac{(fcr)_{true}}{(fcr)_{Schafer}}$	$\frac{(fcr)_{true}}{(fcr)_{Hancock}}$	$\frac{(fcr)_{true}}{(fcr)_{AISI}}$	$\frac{(fcr)_{true}}{(fcr)_{R*AISI}}$
All Data	avg.	**1.34**	**1.03**	**0.93**	**0.96**	**0.79**	**1.01**
	st.dev.	0.13	0.06	0.05	0.06	0.33	0.25
	max	1.49	1.15	1.07	1.08	1.45	1.70
	min	0.96	0.78	0.81	0.83	0.18	0.43
	count	149	149	89	89	89	89
Schafer (1997) Members	avg.	**1.16**	**1.02**	**0.92**	**0.96**	**1.09**	**1.16**
	st.dev.	0.15	0.08	0.07	0.06	0.16	0.22
Commercial Drywall Studs	avg.	**1.38**	**1.07**	**0.93**	**1.00**	**0.81**	**1.14**
	st.dev.	0.09	0.05	0.02	0.07	0.26	0.22
AISI Manual C's	avg.	**1.33**	**1.01**	**0.93**	**0.99**	**0.81**	**0.99**
	st.dev.	0.13	0.07	0.05	0.03	0.26	0.19
AISI Manual Z's	avg.	**1.39**	**1.04**	**0.92**	**0.92**	**0.41**	**0.81**
	st.dev.	0.03	0.04	0.03	0.06	0.18	0.24

$(fcr)_{element}$ = minimum local buckling stress of the web, flange and lip
$(fcr)_{interact}$ = minimum local buckling stress using the semi-empirical equations for the web/flange and flange/lip
$(fcr)_{Schafer}$ = distortional buckling stress via Schafer (1997)
$(fcr)_{Hancock}$ = distortional buckling stress via Lau and Hancock (1987)
$(fcr)_{AISI}$ = buckling stress for an edge stiffened element via AISI (1996)
$(fcr)_{R*AISI}$ = reduced buckling stress for an edge stiffened element, R=0.65/(h/b-1), h/b>1.65

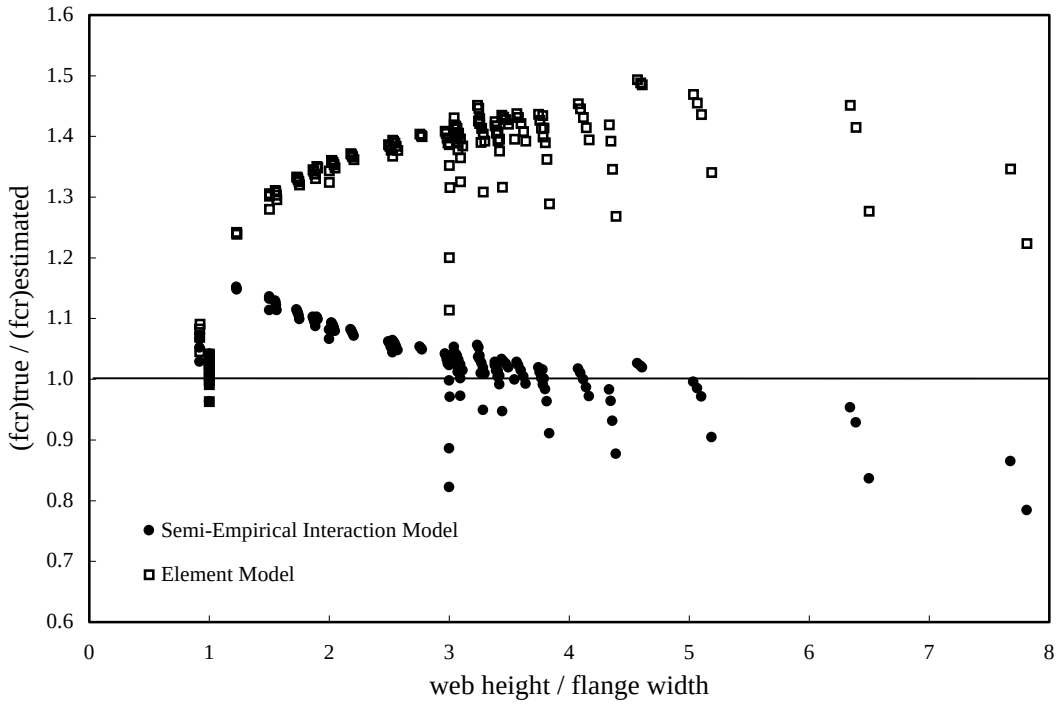

Figure 4 Performance of Local Buckling Prediction Methods

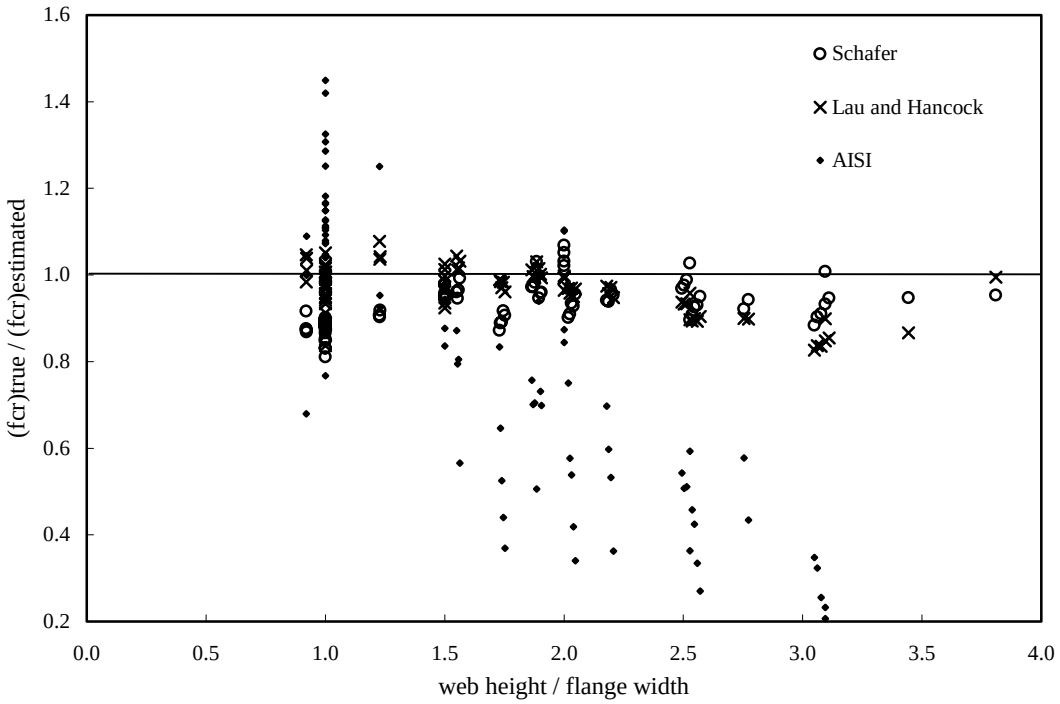

Figure 5 Performance of Distortional Buckling Prediction Methods

4 Understanding When the Distortional Mode is Prevalent

The AISI (1996) Specification does not explicitly treat distortional buckling as a separate mode of failure. Further, as the previous section indicated, existing AISI equations for predicting distortional buckling are inadequate for a large variety of common members. For columns, how important is this failure of the AISI Specification to predict distortional buckling? To answer this, and to provide more overall insight into distortional buckling we must answer the question: When is the distortional mode prevalent?

For lipped C's, the introduction, specifically Figure 2 and the related discussion, provide general guidance to address the issue of when the distortional mode is prevalent. Distortional buckling stresses are low when the flanges are very narrow (flange width less than approximately 1/6 the web height) or very wide (flange width greater than approximately 3/4 the web height). Members with narrow flanges are generally controlled by local buckling even though distortional buckling stresses are low because the web is much more slender than the flange and buckles locally first. If intermediate stiffeners are added in the web then members with narrow flanges are likely to suffer distortional failures.

Members with wide flanges (shapes approaching square) tend to have more problems with distortional buckling because as the shape approaches the square geometry distortional buckling stresses decrease while local buckling stresses increase. Eventually this leads to sections which are generally controlled by distortional limits.The distortional mode is not prevalent in members with long lips. Even though the distortional buckling stress eventually decreases for exceedingly long lips (see Figure 2 c and d) – the reductions in local buckling are more pronounced. Long lips retard the distortional mode and trigger the local mode.

Numerical examples follow to further reinforce these general concepts. Consider the members introduced in Table 2 and detailed in Appendix C. For all 170 of these members the buckling mode for the minimum elastic buckling stress (local vs. distortional) is determined via finite strip, and plotted against the web height (h) to flange width (b) ratio, as shown in Figure 6. For the vast majority of these members local buckling is the dominant mode of failure. In fact, for $h/b > 2$ essentially all of the members have a local buckling stress lower than distortional buckling. The exception is a couple of Z sections which have short sloping stiffeners, such a flange has little rotational stiffness to provide at the web/flange juncture.

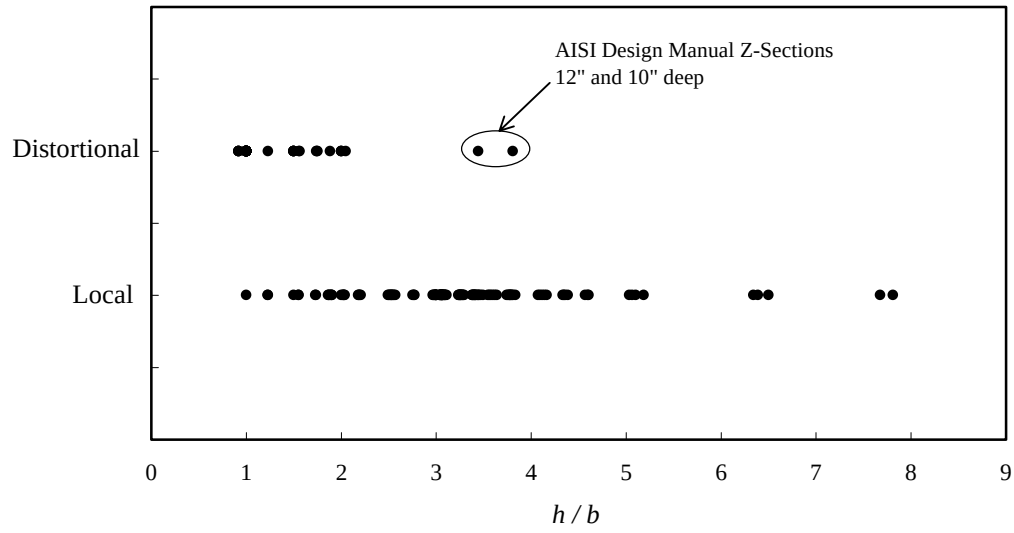

Figure 6 Minimum Elastic Buckling Mode for Studied Sections

4.1 In a Typical Lipped Channel Column

To better understand how local and distortional buckling are competing the studied members are broken into their specific cross-section type. In Figure 7 the buckling stress (via finite strip) in the local and distortional mode for both the AISI Lipped C sections (from the design manual) and a set of commercially available drywall studs are examined. Local buckling primarily follows a curve dominated by the web slenderness (h/t). For the majority of

these members the web is markedly more slender than the compression flange. The distortional buckling results exhibit a greater scatter than local buckling but for typical C sections members with $h/t < 100$ appear most prone to distortional buckling.

The points with a buckling stress of "zero" represent cases in which the finite strip analysis does not have a minimum in that mode. For instance, analysis of the members with high web slenderness typically only revealed a local buckling minimum, this is evidenced by the large number of distortional points along the "zero" line in the region of high web slenderness. In these situations investigation of higher modes will reveal the distortional buckling minimums; however this was not done in this case.

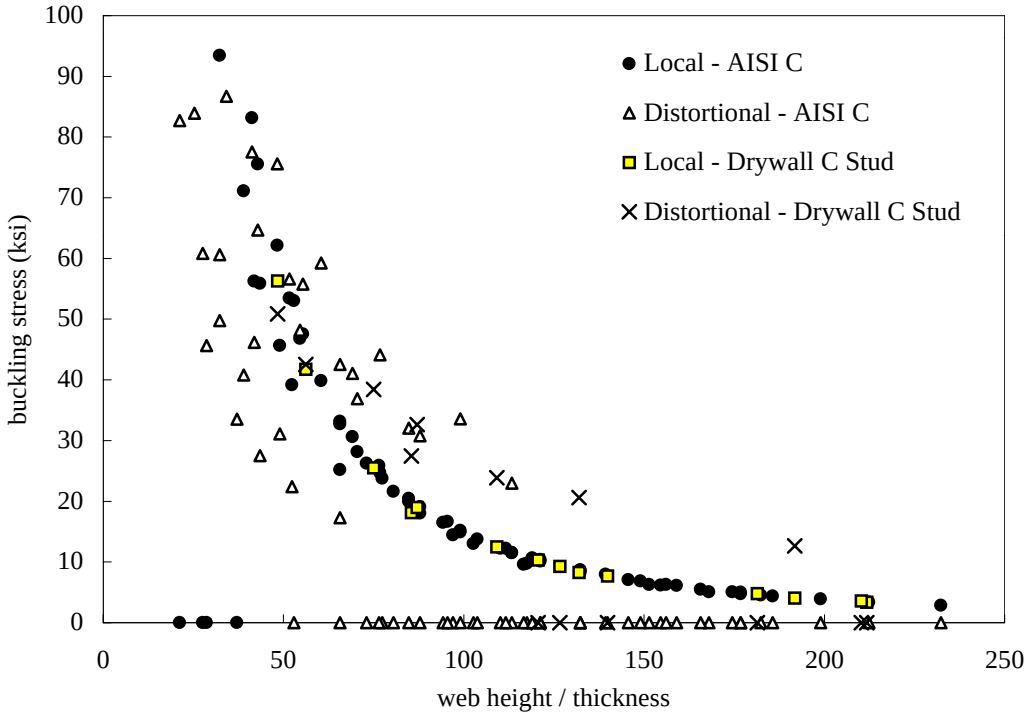

Figure 7 Local and Distortional Buckling of Lipped C's

4.2 In a Z section Column

A similar analysis, as conducted in the previous section, is performed for the Z sections in the AISI design manual, as shown in Figure 8. Local buckling of the entire member is again dominated by the web slenderness. As before, this is due to the fact that all of these members have web depths much greater than the flange width. Distortional buckling and local buckling occur at similar buckling stresses for a large variety of members. At first glance distortional buckling appears to follow the web slenderness closely as well, however closer inspection at h/t approximately 60 and 80 reveal that this is not always the case. Further, the sections used in the AISI Design Manual have little variation in the stiffener selection. Greater variation in the stiffener length, as done in Schafer (1997) reveals a scatter more like that of Figure 7. For standard Z sections distortional buckling appears most prevalent in the members with $h/t < 100$.

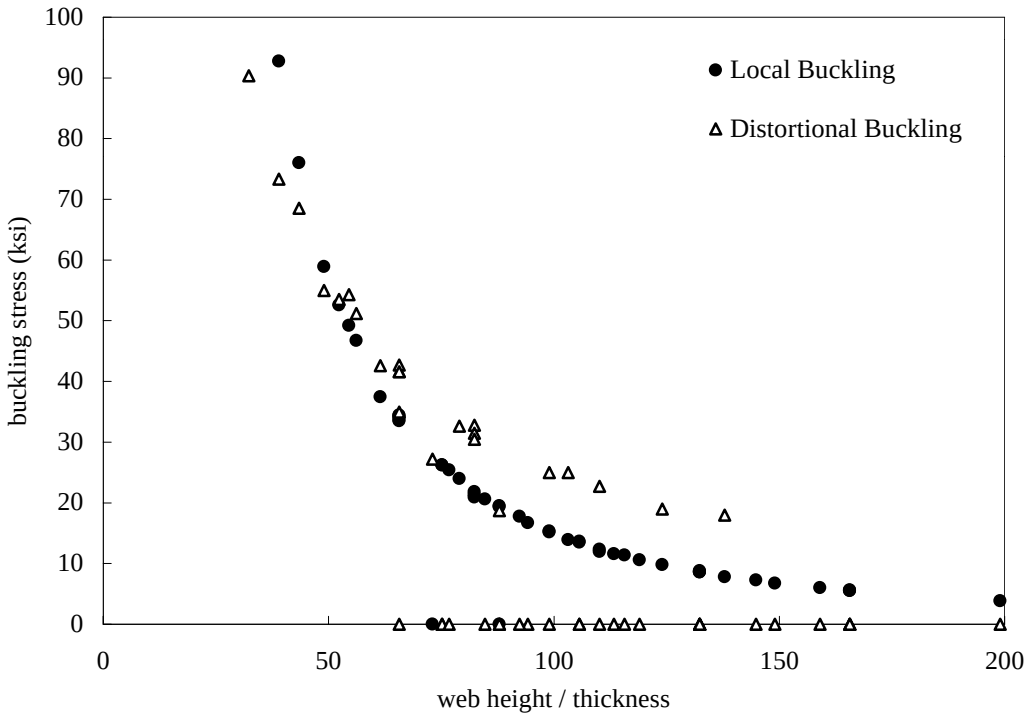

Figure 8 Local and Distortional Buckling of Z's

4.3 In Optimized Shapes

In typical Lipped C and Z shaped members the local mode is most prevalent. This is due to the slender nature of the web. An obvious way to eliminate this mode is to provide a longitudinal stiffener in the web and thus increase the local buckling stress. This idea has been experimentally studied in compression members by Thomasson (1978) and Kwon and Hancock (1992).

A parametric study which modifies the lipped C sections in the AISI Design Manual, as shown in Figure 9, is conducted here. A web stiffener with the same horizontal and vertical dimensions as the existing lip stiffener is introduced into the web. The resulting local and distortional modes are shown in Figure 10. The numerical results, depicted in Figure 11, indicate that while the stiffener markedly increases the local buckling stress now distortional buckling is not only prevalent, but is a far more dominant mode of behavior than the local mode.

In Figure 11 the curve for local buckling without a stiffener is also shown. For $h/t > 60$ there is an improvement in the elastic buckling stress of all the members; the stiffener provides a benefit. However, the cost is that the mode of failure is now a distortional one (Figure 10(b)) and thus significantly different than local buckling without the intermediate stiffener. Experimental and analytical evidence indicates that the distortional mode is more imperfection sensitive and has a reduced post-buckling capacity. From an elastic buckling standpoint the improvement due to the intermediate stiffener is clear; however it is not clear what the exact ultimate benefit is.

Optimization of the cross-section through adding additional folds may greatly benefit the ultimate strength, but also often directly leads to a need to more prominently consider the distortional mode.

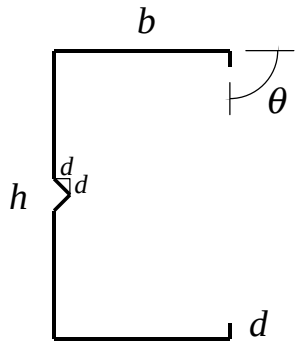

Figure 9 Geometry of Lipped C's with a Web Stiffener

(a) Local Buckling (b) Distortional Buckling

Figure 10 Local and Distortional Buckling of Lipped C with a Web Stiffener

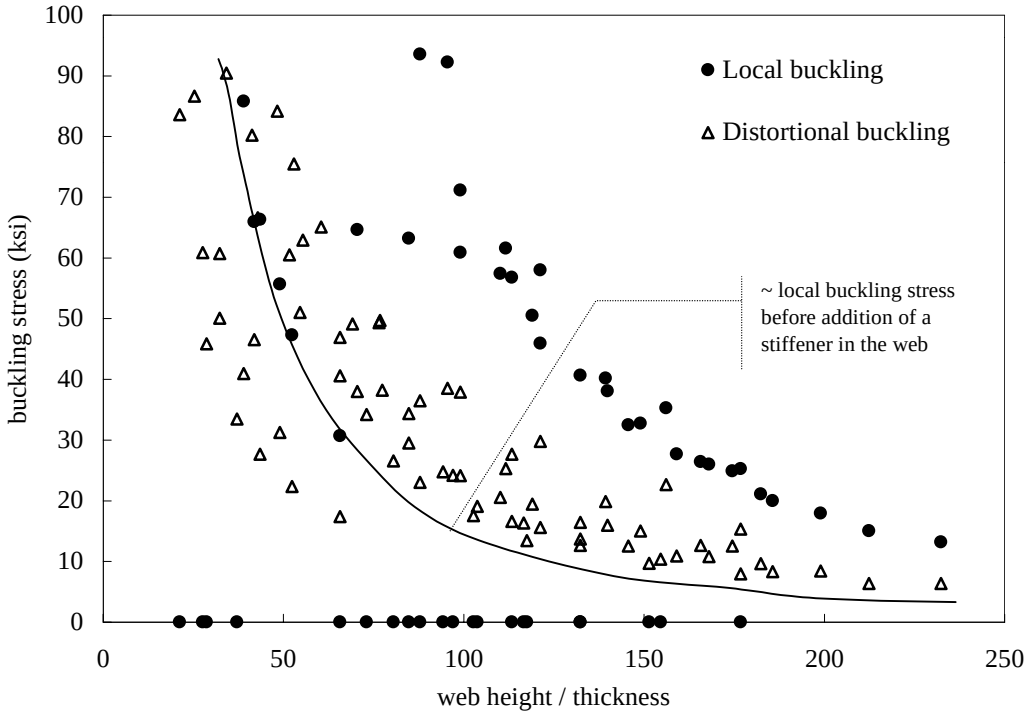

Figure 11 Local and Distortional Buckling of Lipped C's with a web stiffener

5 Ultimate Strength in the Distortional Mode

5.1 Numerical Studies

Finite element analysis of the ultimate strength of cold-formed steel elements and members was investigated in Schafer (1997). Examination of the ultimate strength of isolated edge stiffened elements with a variety of geometric dimensions demonstrated that:

- distortional failures have lower post-buckling capacity than local buckling modes of failure, see Figure 12,
- distortional buckling may control failure even when the elastic distortional buckling stress (load) is higher than the elastic local buckling stress (load), see Figure 13, and
- distortional failures have higher imperfection sensitivity, see Figure 14.

As a result of these facts the distortional mode has a lower strength curve than local buckling (i.e., Winter's curve is unconservative), lower ϕ factors may be needed for strength prediction in the distortional mode, and since elastic buckling is not a direct indicator of the final failure mode - complications arise in the prediction of the actual failure mode.

Numerical analysis of a series of lipped channel columns demonstrate that the ultimate strength of columns which fail in the distortional buckling mode can be predicted through knowledge of the elastic distortional buckling stress (load) of the column. The geometry of the studied columns is presented in Figure 15 and Table 4. The ultimate strength of the columns is shown in Figure 16.

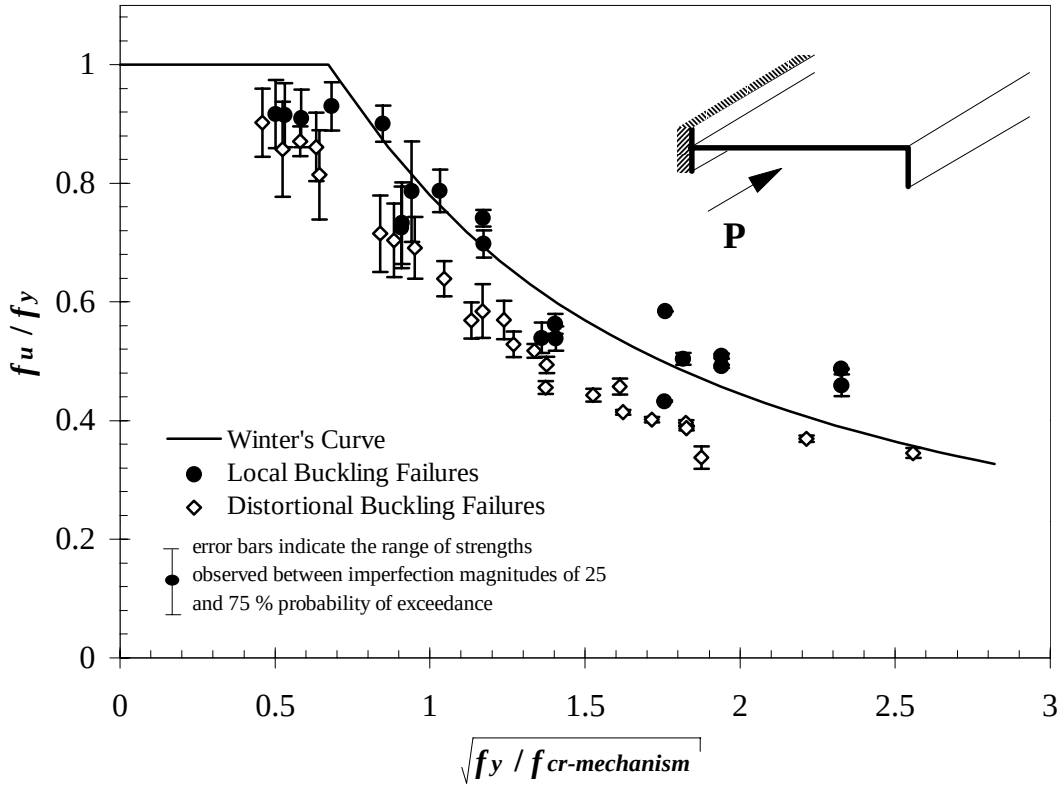

Figure 12 Lower post-buckling capacity in distortional mode: finite element analysis of edge stiffened element

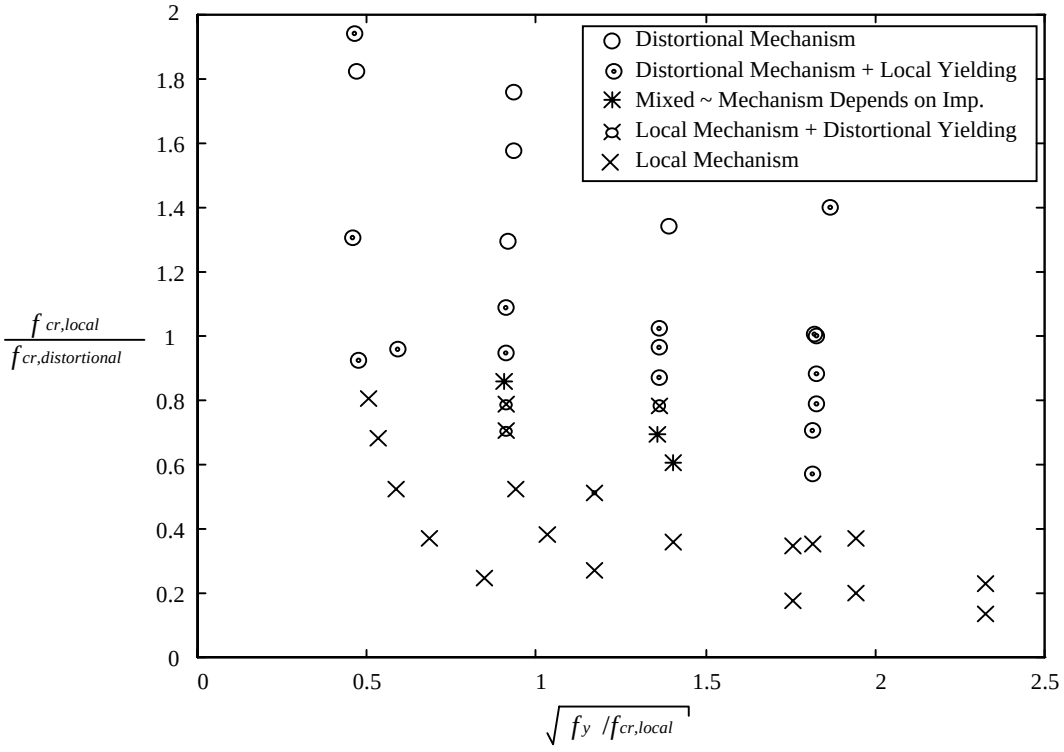

Figure 13 Minimum elastic buckling stress does not predict failure mode: finite element analysis of edge stiffened element

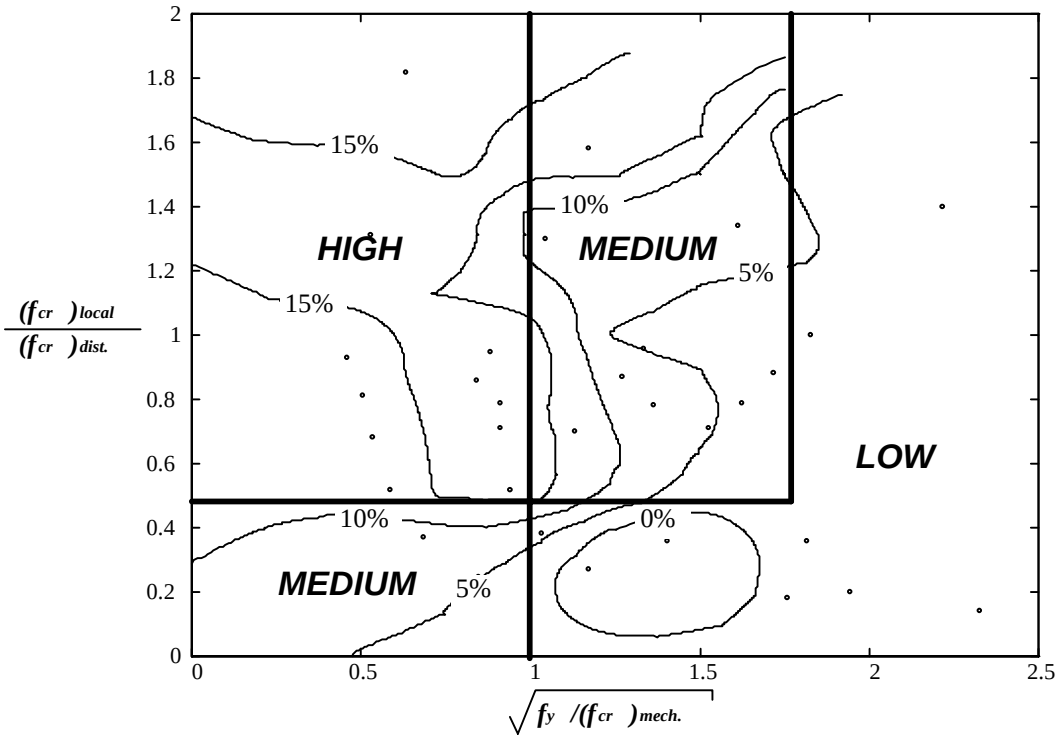

Figure 14 Heightened imperfection sensitivity in distortional failures: finite element analysis of edge stiffened element

Table 4 Geometry of members in pure compression studied via finite element analysis

H	*B*	*D*	θ
30	30	2.5,5	45,90
60	30	2.5,5	45,90
	60	2.5,5,10	45,90
90	30	2.5,5	45,90
	60	2.5,5,10	45,90
	90	2.5,5,10,15	45,90

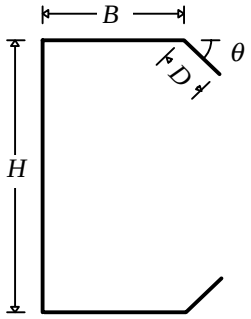

Figure 15 Geometry of members in pure compression studied via finite element analysis

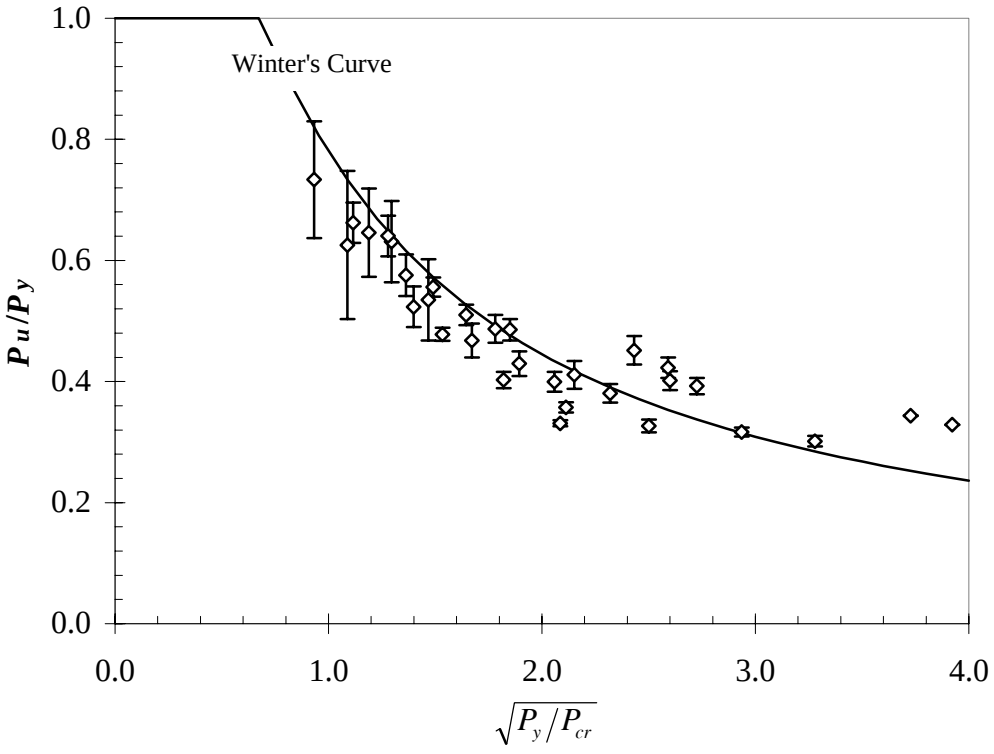

Figure 16 Ultimate strength of columns in pure compression failing in distortional buckling, studied via finite element analysis (Note, error bars indicate the range of strength between imperfection magnitudes of 25 and 75 % probability of exceedance.)

5.2 Experimental Data

The most convincing experimental evidence for the prediction of the strength of cold-formed steel columns failing in the distortional mode is derived from the work conducted at the University of Sydney: Lau and Hancock (1987), Kwon and Hancock (1992) as summarized in Hancock et al. (1994). Compression tests were conducted on: (a) lipped channels, (b) rack column uprights, (c) rack column uprights with additional outward edge stiffeners, (d) hats, and (e) lipped channels with a web stiffener as shown in Figure 17. The ultimate strength is reported in Figure 18.

The expression fit to the distortional buckling failures of Figure 18 is known as the Modified Winter Curve or "Hancock's curve" and may be expressed as:

$$\frac{P_n}{P_y} = \left(1 - 0.25\left(\frac{P_{crd}}{P_y}\right)^{.6}\right)\left(\frac{P_{crd}}{P_y}\right)^{.6} \quad \text{where } \sqrt{\frac{P_y}{P_{crd}}} > 0.561, \text{ otherwise } \frac{P_n}{P_y} = 1 \ .$$

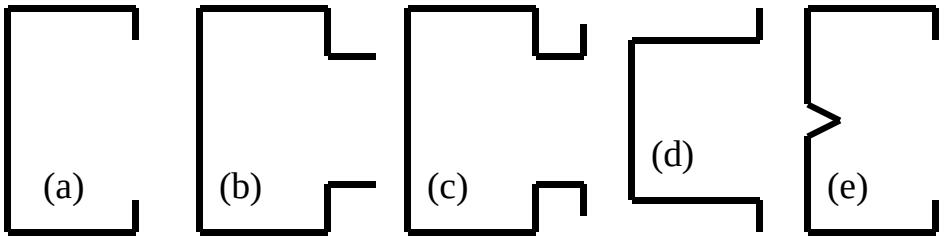

Figure 17 Geometry of columns studied at U. of Sydney

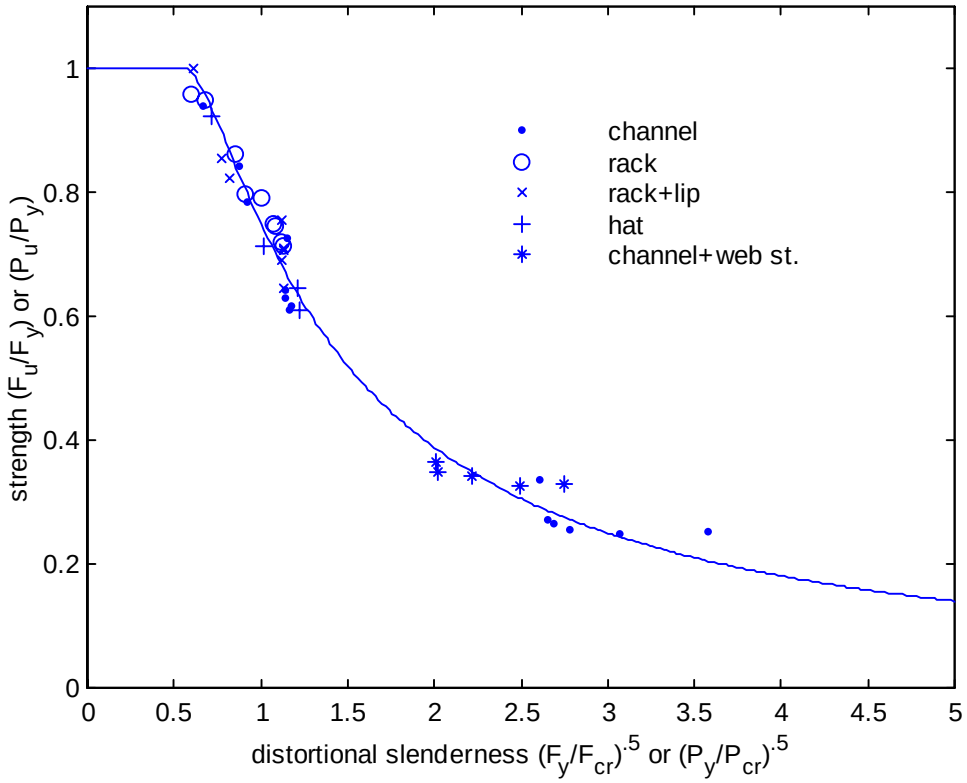

Figure 18 Ultimate strength of columns failing in distortional buckling (U. of Sydney tests)

where:

P_n is the nominal capacity
P_y is the squash load ($A_g f_y$)
P_{crd} is the critical elastic distortional buckling load

Figure 18 provides strong evidence that *if the failure is known to occur in the distortional mode*, then the elastic distortional buckling load (stress) may be used to predict the ultimate strength. This fact appears true for a variety of different cross-sections. Note that the current AISI (1996) Specification has no rules which would govern the strength of many of the investigated members.

The prevalence of the distortional failure mode in these tests is increased due to the use of high strength steel. For two members with identical geometry, but different yield stress, a high strength steel member will have the greater slenderness - as Figure 13 shows, as slenderness increases the prevalence of the distortional mode increases.

Recent additional work on rack columns such as Figure 17(c), but with perforations, have also investigated distortional buckling (Baldassino and Hancock 1999). Based on comparisons to hand methods for the prediction of distortional buckling, they found that use of the minimum net area for computation of the distortional buckling strength, was unconservative – instead they used an effective area which accounts for local buckling. Based on this result they concluded that local and distortional buckling may interact in perforated rack columns.

6 Design Methods

Consider the general design problem of a cold-formed steel column. Identification of the possible limit states for the column, with consideration for interaction between modes creates a large variety of different possible failure mechanisms:

- local,
- distortional,
- long column Euler buckling,
- local interaction with distortional,
- local interaction with Euler,
- distortional interaction with Euler, and
- all three basic modes: local, distortional, Euler interacting.

Currently, the AISI (1996) Specification uses an effective width approach to accommodate local buckling. In the AISI approach, interaction with Euler buckling is handled by limiting the stress in the effective width determination to the nominal column buckling stress (F_n). Distortional buckling is not directly treated in the AISI approach, and interaction with distortional buckling and other modes is not considered.

Table 6 presents a general outline to the various possibilities of the design of cold-formed steel columns. Each limit state is identified. Methods for examining elastic buckling and the ultimate strength are identified. The methods presented in Table 6 summarize current “element” approaches to the design of cold-formed steel as well as the member level “direct strength” approaches that have been recently investigated for cold-formed steel bending members (Schafer and Peköz 1998). All new design methods are investigated for various combinations presented in Table 6.

Eleven different design methods are selected for investigation, as detailed in Table 5. Four basic types of design methods are considered:

A. the current AISI approach and small variations, e.g. adding a distortional check,

B. methods which consider local interaction with long column buckling, but ignore any distortional interactions,

C. methods which consider local or distortional interaction with long column buckling, and

D. methods which consider local and distortional interaction as well as local or distortional interaction with long column buckling.

In each of types B through D, three types of design methods are considered.

1. "Element" type solutions, where local buckling is considered by finding the effective width of each isolated element and using Winter's curve to determine the strength (similar to AISI in concept, but local buckling is always assumed, for instance the flange of an edge stiffened element always uses k = 4, not a modified k); distortional buckling is considered as either a separate failure mode (member level solution) or compared versus the elastic local buckling stress (element level solution).

2. "Member" solutions where a local buckling stress (load) is determined for the member as a whole and a local buckling strength is found by using an alternative strength curve (i.e., $P_n/P_y=(1-0.15(P_{crL}/P_y)^{0.4})(P_{crL}/P_y)^{0.4}$). Distortional buckling stress (load) is also determined for the member as a whole and a different strength curve (Hancock's curve) is used. In this solution hand methods are used for all calculations.

3. Identical to, 2, except finite strip solutions are used for the buckling stress (load) in local and distortional buckling instead of hand methods.

Appendix D provides a design example for each of the 11 separate methods.

Table 5 Key to investigated design methods (indices refers to methods outlined in Table 6)

Label	(L)ocal	(D)istortional	(E)uler	L+D	L+E	D+E
A1	1.a.i.a.i	-	3.a.i.a.i	-	5.a.i.a	-
A2	1.a.i.a.i	2.b.i.b.ii	3.a.i.a.i	-	5.a.i.a	-
B1	1.a.ii.a.i	2.b.i.b.ii	3.a.i.a.i	-	5.a.ii.a	-
B2	1.b.i.b.ii	2.b.i.b.ii	3.a.i.a.i	-	5.b.i.b(1.b.i)	-
B3	1.b.ii.b.ii	2.b.ii.b.ii	3.a.i.a.i	-	5.b.i.b(1.b.ii)	-
C1	1.a.ii.a.i	2.a.ii.a.ii	3.a.i.a.i	-	5.a.ii.a	6.b.i.b(2.b.i)
C2	1.b.i.b.ii	2.b.i.b.ii	3.a.i.a.i	-	5.b.i.b(1.b.i)	6.b.i.b(2.b.i)
C3	1.b.ii.b.ii	2.b.ii.b.ii	3.a.i.a.i	-	5.b.i.b(1.b.ii)	6.b.i.b(2.b.ii)
D1	1.a.ii.a.i	2.a.ii.a.ii	3.a.i.a.i	4.a.ii.a(2.a.ii)	5.a.ii.a	6.b.i.b(2.b.i)
D2	1.b.i.b.ii	2.b.i.b.ii	3.a.i.a.i	4.b.i.b(1.b.i,2.b.i)	5.b.i.b(1.b.i)	6.b.i.b(2.b.i)
D3	1.b.ii.b.ii	2.b.ii.b.ii	3.a.i.a.i	4.b.i.b(1.b.ii,2.b.ii)	5.b.i.b(1.b.ii)	6.b.i.b(2.b.ii)

For example, A1=AISI method, local, Euler, and local+Euler interaction is considered; local buckling strength is completed by the method outlined in 1.a.i.a.i in Table 3, Euler buckling strength is completed by the method outlined in 3.a.i.a.i in Table 3, and Local and Euler interaction is completed by 5.a.i.a in Table 3.

Table 6 Summary of Design Method Possibilities for Cold-Formed Steel Column

COLD-FORMED STEEL COLUMNS BASIC LIMIT STATES AND STRENGTH DETERMINATION		
Failure Mode/Mechanism	**Elastic Buckling Calculation**	**Ultimate Strength determination**
1. Local (considered in design)	a. element by element (f_{crL}) i. AISI expressions ii. local only, "k=4" solutions	a. effective width determimed using f_{crL} and f_y i. Winter's curve: $b_{eff}=\rho b$, $\rho=(1-0.22(f_{crL}/f_y)^{0.5})(f_{crL}/f_y)^{0.5}$ ii. alternative strength curves
	b. member (P_{crL}) i. hand solutions ii. numerical (finite strip)	b. strength directly determined using P_{crL} and P_y i. Winter's curve: $P_{ult}=\rho P_y$, $\rho=(1-0.22(P_{crL}/P_y)^{0.5})(P_{crL}/P_y)^{0.5}$ ii. alternative curves, e.g.: $\rho=(1-0.15(P_{crL}/P_y)^{0.4})(P_{crL}/P_y)^{0.4}$
	c. back calc. from stub column test	c. from stub colun test
2. Distortional (mostly ignored in design)	a. element by element (f_{crD}) i. AISI expressions approx. this ii. hand solutions (Hancock or Schafer) iii. numerical finite strip	a. effective width determined using f_{crD} and f_y i. Winter's curve: $b_{eff}=\rho b$, $\rho=(1-0.22(f_{crD}/f_y)^{0.5})(f_{crD}/f_y)^{0.5}$ ii. Winter's curve with f_{crD} lowered to $R_d f_{crD}$ iii. Hancock's curve: $\rho=(1-0.25(f_{crD}/f_y)^{0.6})(f_{crD}/f_y)^{0.6}$ iv. alternative strength curves
	b. member (P_{crD}) i. hand solutions (Hancock or Schafer) ii. numerical (finite strip)	b. strength directly determined using P_{crD} and P_y i. Winter's curve with P_{crD} lowered to $R_d P_{crD}$ ii. Hancock's curve: $\rho=(1-0.25(P_{crD}/P_y)^{0.6})(P_{crD}/P_y)^{0.6}$ iii. alternative strength curves
3. Long (Euler) (considered in design)	a. member (f_{crE} or P_{crE}) i. AISI expressions ii. numerical (finite strip)	a. strength using f_{crE} and f_y or P_{crE} and P_y i. AISI column curve, e.g.: $f_{nE}=0.877 f_{crE}$ or $P_n=0.877 P_{crE}$
4. Local+Distortional (mostly ignored in design)	a. element by element (f_{crL} and f_{crD}) i. "AISI" - f_{crL} by 1.a.i. and f_{crD} by 2.a.i. ii. f_{crL} by 1.a.ii and f_{crD} by 2.a.ii or iii	a. effective width with local post-buckling limited by f_{nD} (i.e. replace f_y with f_{nD} in 1.a-a) f_{nD} is inelastic distortional stress determine f_{nD} from $f_{nD}=\rho f_y$ and an expression in 2.a.-a.
	b. member (P_{crL} and P_{crD}) i. P_{crL} by 1.b. or 1.c and P_{crD} by 2.b.	b. direct strength with local post-buckling limited by P_{nD} (i.e. replace P_y with P_{nD} in 1.b-b) P_{nD} is inelastic distortional load determine P_{nD} from $P_{nD}=\rho P_y$ and an expression in 2.b.-b.
5. Local+Long (considered in design)	a. element by element (f_{crL} and f_{crE}) i. AISI - f_{crL} by 1.a.i. and f_{crE} by 3.a. ii. f_{crL} by 1.a.ii and f_{crE} by 3.a.	a. effective width with local post-buckling limited by f_{nE} (i.e. replace f_y with f_{nE} in 1.a-a) f_{nE} is inelastic Euler buckling stress determine f_{nE} from expression in 3.a.-a.
	b. member (P_{crL} and P_{crE}) i. P_{crL} by 1.b. or 1.c and P_{crE} by 3.a.	b. direct strength with local post-buckling limited by P_{nE} (i.e. replace P_y with P_{nE} in 1.b-b) P_{nE} is inelastic Euler buckling load determine P_{nE} from expression in 3.a.-a.
6. Distortional+Long (mostly ignored in design)	a. element by element (f_{crD} and f_{crE}) i. f_{crD} by 2.a.ii or iii and f_{crE} by 3.a.	a. effective width with distortional post-buckling limited by f_{nE} (i.e. replace f_y with f_{nE} in 2.a-a) f_{nE} is inelastic Euler buckling stress determine f_{nE} from expression in 3.a.-a.
	b. member (P_{crD} and P_{crE}) i. P_{crD} by 2.b. and P_{crE} by 3.a.	b. direct strength with distortional post-buckling limited by P_{nE} (i.e. replace P_y with P_{nE} in 1.b-b) P_{nE} is inelastic Euler buckling load determine P_{nE} from expression in 3.a.-a.
7. Local+Dist.+Long (ignored)	Interaction of all 3 modes is currently ignored. The inelastic buckling stress would have to consider multiple modes; e.g. local post-buckling limited by inelastic buckling stress for distortional and long column interaction.	

7 Experimental Data: Lipped Channels and Z's

Unlike the experimental data conducted at the University of Sydney, the majority of experiments do not identify the failure mode of the column. Thus, distortional buckling must be examined within the context of general strength prediction of cold-formed steel columns, rather than as an isolated event.

7.1 Lipped Channels

Experimental data on cold-formed lipped C columns was collected from Mulligan (1983), Thomasson (1978), and Loughlan (1979) as summarized in Peköz (1987). Additional tests on lipped C's were also collected from Miller and Pekoz (1994). Only unperforated sections, with 90 degree edge stiffeners, tested in a pin-pin configuration were selected for this study. The geometry of the tested sections is summarized in Table 7, where *h*, *b*, and *d* are centerline dimensions defined in Figure 15, and $\theta = 90$.

The experimental data on lipped channels represents a wide variety of sections; in particular, slender webs, slender flanges, and relatively long lips are all tested. However, in the vast majority of the sections (95 out of 102) *h/b* is greater than 1.6 – only in 4 specimens is h/b less than 1. Thus, in essentially all of the tested sections the web is significantly more slender than the flange - in this case, local buckling is more dominant than the distortional mode of behavior (given a reasonable choice of lip length). Thus, this data set provides an examination of columns with *h/b* greater than 1.6, but for typical rack columns or other columns approaching a more square configuration the available data is incomplete. The behavior of rack columns and those sections approaching a more square configuration motivated the original testing on distortional buckling at the University of Sydney (see Figure 18).

Table 7 Geometry of experimental data on lipped channel columns

	h/b		*h/t*		*b/t*		*d/t*		
	max	min	max	min	max	min	max	min	count
Loughlan (1979)	5.0	1.6	322	91	80	30	33	11	33
Miller and Pekoz (1994)	4.6	2.5	170	46	38	18	8	5	19
Mulligan (1983)	2.9	1.0	207	93	93	64	16	14	13
Mulligan (1983) Stub Columns	3.9	0.7	353	65	100	33	22	7	24
Thomasson (1978)	3.0	3.0	472	207	159	69	32	14	13
	5.0	0.7	472	46	159	18	33	5	102

7.2 Z-Sections

A set of experiments on Z-section columns is compiled in Polyzois and Charnvarnichborikarn (1993). The geometry is shown in Figure 19 and summarized in Table 8. The tested sections have right angle (θ=90) edge stiffeners rather than the typical 50° sloping lip stiffeners. Work on elastic buckling with sloping edge stiffeners indicate distortional buckling is more prevalent in members with sloping lips vs. right angle lips (Schafer 1997). The *h*/*b* ratios are similar to those of the lipped channel columns – and thus this data suffers from the same limitations cited above for the lipped channel columns.

The researchers specifically investigated the case of small, or no edge stiffening lip at all. For small edge stiffeners distortional buckling may control the failure mode, even when the *h*/*b* ratio is high (i.e., even when the web slenderness is significantly greater than the flange slenderness.). The experiments show that as the edge stiffener length is increased the strength increases until a limiting maximum is reached. This basic behavior is the motivation for the current AISI Specification rules developed based on tests by Desmond (1977). Unlike the data on lipped channels, this experimental database was not used to calibrate the existing AISI Specification rules for columns; therefore it provides an independent set of data for examination of current procedures.

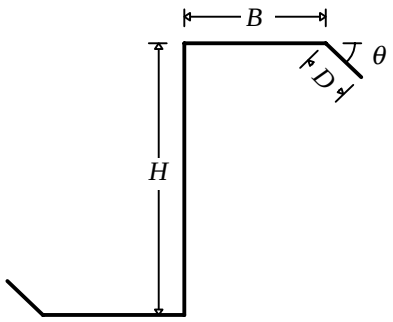

Figure 19 Geometry of Z section columns (θ=90 in selected data)

Table 8 Geometry of experimental data on Z section columns

	h/b		*h/t*		*b/t*		*d/t*		
	max	min	max	min	max	min	max	min	count
Polyzois and Charnvarnichborikarn (1993)	2.7	1.5	137	76	56	30	36	0	85

8 Performance of Design Methods for Lipped C and Z Sections

Using the collected experimental data eleven different design methods were selected for investigation, as detailed in Table 5 and shown in Appendix D. Four basic types of design methods are considered:

A. the current AISI approach and small variations, e.g. adding a distortional check,

B. methods which consider local interaction with long column buckling, but ignore any distortional interactions,

C. methods which consider local or distortional interaction with long column buckling, and

D. methods which consider local and distortional interaction as well as local or distortional interaction with long column buckling.

In each of types B through D, three types of design methods are considered.

1. "Element" type solutions, where local buckling is considered by finding the effective width of each isolated element and using Winter's curve to determine the strength (similar to AISI in concept, but local buckling is always assumed, for instance the flange of an edge stiffened element always uses k = 4, not a modified k); distortional buckling is considered as either a separate failure mode (member level solution) or compared versus the elastic local buckling stress (element level solution).

2. "Member" solutions where a local buckling stress (load) is determined for the member as a whole and a local buckling strength is found by using an alternative strength curve (i.e., $P_n/P_y=(1-0.15(P_{crL}/P_y)^{0.4})(P_{crL}/P_y)^{0.4}$). Distortional buckling stress (load) is also determined for the member as a whole and a different strength curve (Hancock's curve) is used. In this solution hand methods are used for all calculations.

3. Identical to, 2, except finite strip solutions are used for the buckling stress (load) in local and distortional buckling instead of hand methods.

8.1 Overall – for Lipped C and Z Sections

For the investigated design methods, the mean test to predicted ratios for tests on lipped C and Z sections is given in Table 9; in addition the mean test to predicted ratio broken down by limit state is given in Table 10. Methods A1 (current AISI Specification) through C3 all perform reasonably well. However, the "D" methods perform poorly

(overly conservative). This indicates that in the available test data, local and distortional interaction is not significant.

Distortional buckling is not a prevalent failure mode in the experimental data set on lipped C's. Based on the prediction of method C3 (a Direct Strength method with different strength curves for local and distortional modes), only 18 of 102 experiments are identified as having lower strength in the distortional mode than the local mode. This is consistent with the geometry of these members which have wide webs and reasonably sized flanges and lip stiffeners.

Distortional buckling is more prevalent in the experimental data set on Z sections. Based on method C3, 25 of 85 experiments are identified as having lower strength in the distortional mode than the local mode. The increased prevalence of distortional failures in the data on lipped Z's vs. C's is due in part to the ineffectiveness of sloping lip stiffeners and because the researchers systematically varied lip length in these specimens (from no lip up to lip lengths nearly as wide as the flange width) . The specimens with small lips (or no lip at all) are identified as failing in the distortional mode, as the lip length increases local buckling quickly controls – this is accentuated by the fact that the *h/b* ratio is never less than 1.5, and local buckling generally controls for even moderately sized lips in this case.

Table 9 Test to predicted ratio for lipped channels and Z sections (st. dev. in parentheses)

limit states checked*?	L+E	L+E, D	L+E, D			L+E, D+E			L+D, L+E, D+E		
design method**:	A1	A2	B1	B2	B3	C1	C2	C3	D1	D2	D3
Lipped Channels											
Loughlan (1979)	**0.97**	**0.97**	**0.97**	**1.11**	**1.08**	**0.97**	**1.11**	**1.08**	**1.25**	**1.43**	**1.41**
	(0.04)	(0.04)	(0.04)	(0.07)	(0.07)	(0.04)	(0.07)	(0.06)	(0.15)	(0.21)	(0.20)
Miller and Pekoz (1994)	**0.86**	**0.86**	**0.86**	**1.01**	**1.00**	**0.88**	**1.01**	**1.02**	**1.46**	**1.77**	**1.86**
	(0.04)	(0.04)	(0.04)	(0.07)	(0.07)	(0.05)	(0.07)	(0.12)	(0.12)	(0.14)	(0.22)
Mulligan (1983)	**0.86**	**0.86**	**0.83**	**0.94**	**0.92**	**0.84**	**0.94**	**0.92**	**0.94**	**1.06**	**1.08**
	(0.12)	(0.12)	(0.12)	(0.12)	(0.13)	(0.12)	(0.12)	(0.13)	(0.13)	(0.17)	(0.19)
Mulligan (1983) Stub Col.	**1.05**	**1.06**	**1.06**	**1.15**	**1.13**	**1.06**	**1.15**	**1.14**	**1.47**	**1.64**	**1.76**
	(0.06)	(0.06)	(0.06)	(0.09)	(0.11)	(0.07)	(0.09)	(0.11)	(0.21)	(0.37)	(0.50)
Thomasson (1978)	**0.99**	**1.00**	**1.00**	**1.01**	**1.00**	**1.03**	**1.02**	**1.03**	**1.06**	**1.08**	**1.09**
	(0.23)	(0.23)	(0.23)	(0.22)	(0.22)	(0.22)	(0.22)	(0.22)	(0.24)	(0.26)	(0.28)
Z-Sections											
Polyzois at al. (1993)	**0.93**	**0.98**	**0.94**	**0.99**	**0.96**	**0.96**	**1.01**	**0.98**	**1.10**	**1.20**	**1.24**
	(0.10)	(0.14)	(0.14)	(0.13)	(0.13)	(0.16)	(0.15)	(0.15)	(0.23)	(0.26)	(0.29)
All Data	**0.94**	**0.96**	**0.94**	**1.01**	**0.99**	**0.95**	**1.02**	**1.01**	**1.15**	**1.28**	**1.32**
st. dev of all data	(0.13)	(0.14)	(0.15)	(0.14)	(0.15)	(0.16)	(0.15)	(0.16)	(0.27)	(0.34)	(0.39)
weighted st. dev.	(0.09)	(0.10)	(0.11)	(0.11)	(0.12)	(0.12)	(0.12)	(0.13)	(0.20)	(0.25)	(0.29)

* L=Local, D=Distortional, E=Euler

** A1=AISI (1996) Specification, A2=AISI (1996) with a distortional buckling check, B3 and C3 and D3 are direct strength methods, based on finite strip results, with the strength considering different interactions.

Table 10 Test to Predicted Ratios for all 11 Solution Methods, Broken Down by Controlling Limit State

design method:	A1: AISI (1996) Specification								
limit state[1]:	L+E			-			-		
test to predicted stats[2]:	**mean**	std	count	**mean**	std	count	**mean**	std	count
Loughlan (1979)	**0.97**	0.04	13						
Miller and Pekoz (1994)	**0.86**	0.04	13						
Mulligan (1983)	**0.86**	0.12	33						
Mulligan (1983) Stub Col.	**1.05**	0.06	24						
Thomasson (1978)	**0.99**	0.23	19						
Polyzois at al. (1993)	**0.93**	0.10	85						
All Data	**0.94**	0.13	187						

design method:	A2: AISI (1996) Specification with Distortional Check								
limit state[1]:	L+E			D			-		
test to predicted stats[2]:	**mean**	std	count	**mean**	std	count	**mean**	std	count
Loughlan (1979)	**0.97**	0.04	13						
Miller and Pekoz (1994)	**0.86**	0.04	13						
Mulligan (1983)	**0.86**	0.12	33						
Mulligan (1983) Stub Col.	**1.06**	0.06	20	**1.10**	0.09	4			
Thomasson (1978)	**1.00**	0.24	18	**0.98**		1			
Polyzois at al. (1993)	**0.92**	0.10	60	**1.12**	0.12	25			
All Data	**0.93**	0.13	157	**1.11**	0.11	30			

design method:	B1: Effective Width Method with L+E and D Check								
limit state[1]:	L+E			D			-		
test to predicted stats[2]:	**mean**	std	count	**mean**	std	count	**mean**	std	count
Loughlan (1979)	**0.97**	0.04	13						
Miller and Pekoz (1994)	**0.86**	0.04	13						
Mulligan (1983)	**0.83**	0.12	33						
Mulligan (1983) Stub Col.	**1.05**	0.06	19	**1.10**	0.07	5			
Thomasson (1978)	**1.00**	0.24	18	**0.98**		1			
Polyzois at al. (1993)	**0.87**	0.08	47	**1.03**	0.16	38			
All Data	**0.91**	0.14	143	**1.04**	0.15	44			

design method:	B2: Hand Based Direct Strength Method with L+E & D								
limit state[1]:	L+E			D			-		
test to predicted stats[2]:	**mean**	std	count	**mean**	std	count	**mean**	std	count
Loughlan (1979)	**1.11**	0.07	13						
Miller and Pekoz (1994)	**1.01**	0.07	13						
Mulligan (1983)	**0.94**	0.12	33						
Mulligan (1983) Stub Col.	**1.15**	0.09	24						
Thomasson (1978)	**1.01**	0.22	19						
Polyzois at al. (1993)	**0.95**	0.12	60	**1.09**	0.11	25			
All Data	**1.00**	0.15	162	**1.09**	0.11	25			

design method:	B3: Numerical Direct Strength Method with L+E & D								
limit state[1]:	L+E			-			-		
test to predicted stats[2]:	**mean**	std	count	**mean**	std	count	**mean**	std	count
Loughlan (1979)	**1.08**	0.07	13						
Miller and Pekoz (1994)	**0.99**	0.06	12	**1.09**		1			
Mulligan (1983)	**0.92**	0.13	33						
Mulligan (1983) Stub Col.	**1.10**	0.09	20	**1.28**	0.04	4			
Thomasson (1978)	**1.00**	0.23	18	**1.02**		1			
Polyzois at al. (1993)	**0.92**	0.12	60	**1.05**	0.10	25			
All Data	**0.97**	0.14	156	**1.08**	0.12	31			

design method:	C1: Effective Width Method with L+E and D+E Check								
limit state[1]:	L+E			D+E			-		
test to predicted stats[2]:	**mean**	std	count	**mean**	std	count	**mean**	std	count
Loughlan (1979)	**0.97**	0.04	12	**0.94**		1			
Miller and Pekoz (1994)	**0.85**	0.04	8	**0.93**	0.03	5			
Mulligan (1983)	**0.84**	0.12	32	**0.74**		1			
Mulligan (1983) Stub Col.	**1.04**	0.06	18	**1.10**	0.07	6			
Thomasson (1978)	**1.04**	0.25	14	**0.97**	0.10	5			
Polyzois at al. (1993)	**0.87**	0.08	47	**1.07**	0.17	38			
All Data	**0.91**	0.14	131	**1.04**	0.16	56			

design method:	C2: Hand Based Direct Strength with L+E & D+E								
limit state[1]:	L+E			D+E			-		
test to predicted stats[2]:	**mean**	std	count	**mean**	std	count	**mean**	std	count
Loughlan (1979)	**1.12**	0.05	12	**0.94**		1			
Miller and Pekoz (1994)	**1.01**	0.07	13						
Mulligan (1983)	**0.94**	0.12	33						
Mulligan (1983) Stub Col.	**1.15**	0.09	24						
Thomasson (1978)	**1.01**	0.25	14	**1.04**	0.09	5			
Polyzois at al. (1993)	**0.96**	0.12	57	**1.12**	0.15	28			
All Data	**1.00**	0.15	153	**1.10**	0.15	34			

design method:	C3: Numerical Direct Strength Method with L+E & D+E								
limit state[1]:	L+E			D+E			-		
test to predicted stats[2]:	**mean**	std	count	**mean**	std	count	**mean**	std	count
Loughlan (1979)	**1.09**	0.05	12	**1.00**		1			
Miller and Pekoz (1994)	**0.99**	0.06	12	**1.38**		1			
Mulligan (1983)	**0.92**	0.13	33						
Mulligan (1983) Stub Col.	**1.10**	0.10	18	**1.26**	0.06	6			
Thomasson (1978)	**1.07**	0.30	9	**1.00**	0.13	10			
Polyzois at al. (1993)	**0.92**	0.12	60	**1.12**	0.10	25			
All Data	**0.97**	0.15	144	**1.11**	0.14	43			

design method:	D1: Effective Width with L+E, D+E, and L+D Checks								
limit state[1]:	L+E			D+E			L+D		
test to predicted stats[2]:	**mean**	std	count	**mean**	std	count	**mean**	std	count
Loughlan (1979)							**1.25**	0.15	13
Miller and Pekoz (1994)							**1.46**	0.12	13
Mulligan (1983)	**0.94**	0.16	7				**0.94**	0.13	26
Mulligan (1983) Stub Col							**1.47**	0.21	24
Thomasson (1978)	**1.04**	0.25	14				**1.12**	0.24	5
Polyzois at al. (1993)	**0.86**	0.05	11				**1.14**	0.22	74
All Data	**0.96**	0.20	32				**1.19**	0.26	155

design method:	D2: Hand Based Direct Strength with L+E, D+E, & L+D								
limit state[1]:	L+E			D+E			L+D		
test to predicted stats[2]:	**mean**	std	count	**mean**	std	count	**mean**	std	count
Loughlan (1979)							**1.43**	0.21	13
Miller and Pekoz (1994)							**1.77**	0.14	13
Mulligan (1983)	**1.01**	0.16	7				**1.07**	0.17	26
Mulligan (1983) Stub Col							**1.64**	0.37	24
Thomasson (1978)	**1.03**	0.27	12	**1.08**	0.04	2	**1.21**	0.27	5
Polyzois at al. (1993)	**0.88**	0.07	11				**1.25**	0.24	74
All Data	**0.97**	0.20	30				**1.34**	0.33	155

design method:	D3: Numerical Direct Strength with L+E, D+E, and L+D								
limit state[1]:	L+E			D+E			L+D		
test to predicted stats[2]:	**mean**	std	count	**mean**	std	count	**mean**	std	count
Loughlan (1979)							**1.41**	0.20	13
Miller and Pekoz (1994)							**1.86**	0.22	13
Mulligan (1983)	**0.99**	0.21	4				**1.09**	0.19	29
Mulligan (1983) Stub Col							**1.76**	0.50	24
Thomasson (1978)	**1.07**	0.30	9	**0.95**	0.14	5	**1.27**	0.28	5
Polyzois at al. (1993)							**1.24**	0.29	85
All Data	**1.05**	0.27	13				**1.35**	0.39	169

[1] L=Local buckling, D=Distortional buckling, E=Euler (overall) buckling, L+E =Limit State that consider Local buckling interaction with Euler (overall) buckling, etc.

[2] test to predicted ratios are broken down by the controlling limit state

8.2 AISI Performance (A1)

Experimental data on lipped channels and Z sections indicates that the overall performance of the current AISI (1996) Specification is good, but 6% unconservative.

Within the limitations of the experimental data, the AISI Specification does not exhibit poor performance related specifically to the distortional mode. The addition of a separate distortional check (method A2) provides little change to the results; compare A1 and A2 in Table 9, or note in Table 10 that the distortional check almost never controls (only 5 times in 102 lipped channels). Further, Figure 20 presents the test to predicted ratio for the AISI method vs. the ratio of the distortional slenderness/local slenderness for the data. As the ratio of the distortional slenderness/local slenderness increases the distortional mode becomes more prevalent. No trend exists in the data to suggest that members more prone to distortional modes are problematic for the AISI Specification. (Note, slenderness is the square root of the inelastic Euler buckling stress F_n divided by the critical buckling stress for the appropriate mode.)

Systematic error does exist in the current AISI Specification approach for columns. Investigation of the performance vs. *h/t*, or *h/t·h/b* shows this behavior. Consider Figure 21 which shows the data for lipped channels vs. the slenderness of the web, *h/t*. As *h/t* increases the AISI method is prone to yield unconservative solutions. If *h/t* and *h/b* is high, such that the web is contributing a large percentage to the overall strength, then the behavior is more pronounced. This behavior is primarily one of local web/flange interaction, not distortional buckling. Since the AISI method uses an element approach, *no matter how high the slenderness of the web becomes* it has no effect on the solution for the flange.

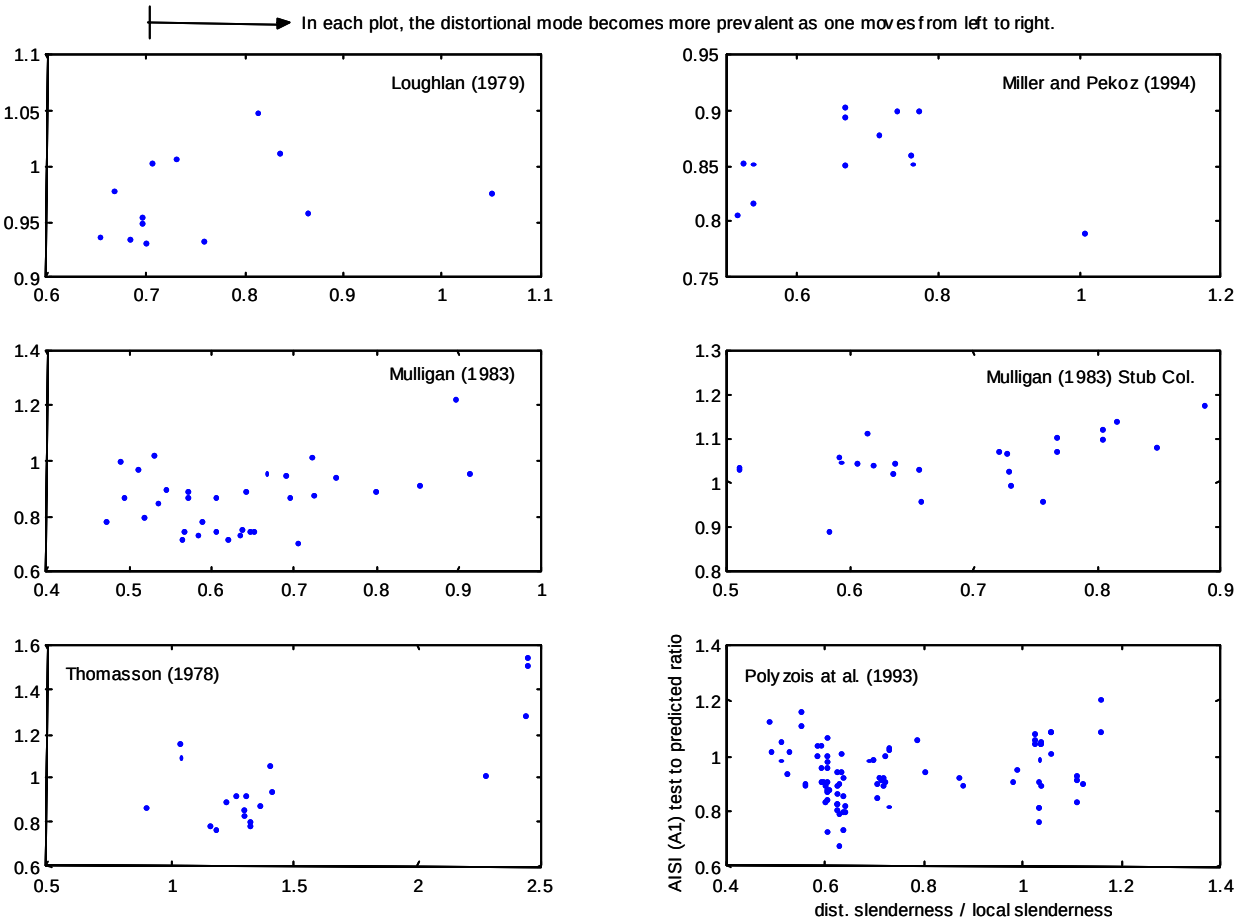

Figure 20 Performance of the AISI Specification (A1) vs. distortional/local slenderness

The data on Z-sections performed by Polyzois et al. (1993) shows another aspect of the AISI Specification that is inconsistent and in some cases unconservative. For small to intermediate lip lengths the AISI prediction in some tests is significantly unconservative (e.g., $d \sim 20$ in Figure 22). For longer lip lengths the Specification under-predicts the observed strength. The reduction in the AISI strength prediction occurs due to an expression that decreases k as $d/b > 0.25$ (expression B4.2-8 in AISI (1996) Specification). In addition the double reduction on the lip, first for its own effective width, then due to the ratio of supplied to adequate stiffener moment of inertia further penalizes longer lips. For longer lips the Specification appears overly conservative.

Performance of the AISI Specification is generally good, and no distinct problems with respect to distortional buckling are identified by the studied data. However, members with large h/t, particularly when $h/b \sim> 2$ tend to have unconservative predictions. Experimental data on Z-sections indicates that intermediate length lip stiffeners may have unconservative predictions while; at the same time predictions for long lip lengths are generally overly conservative.

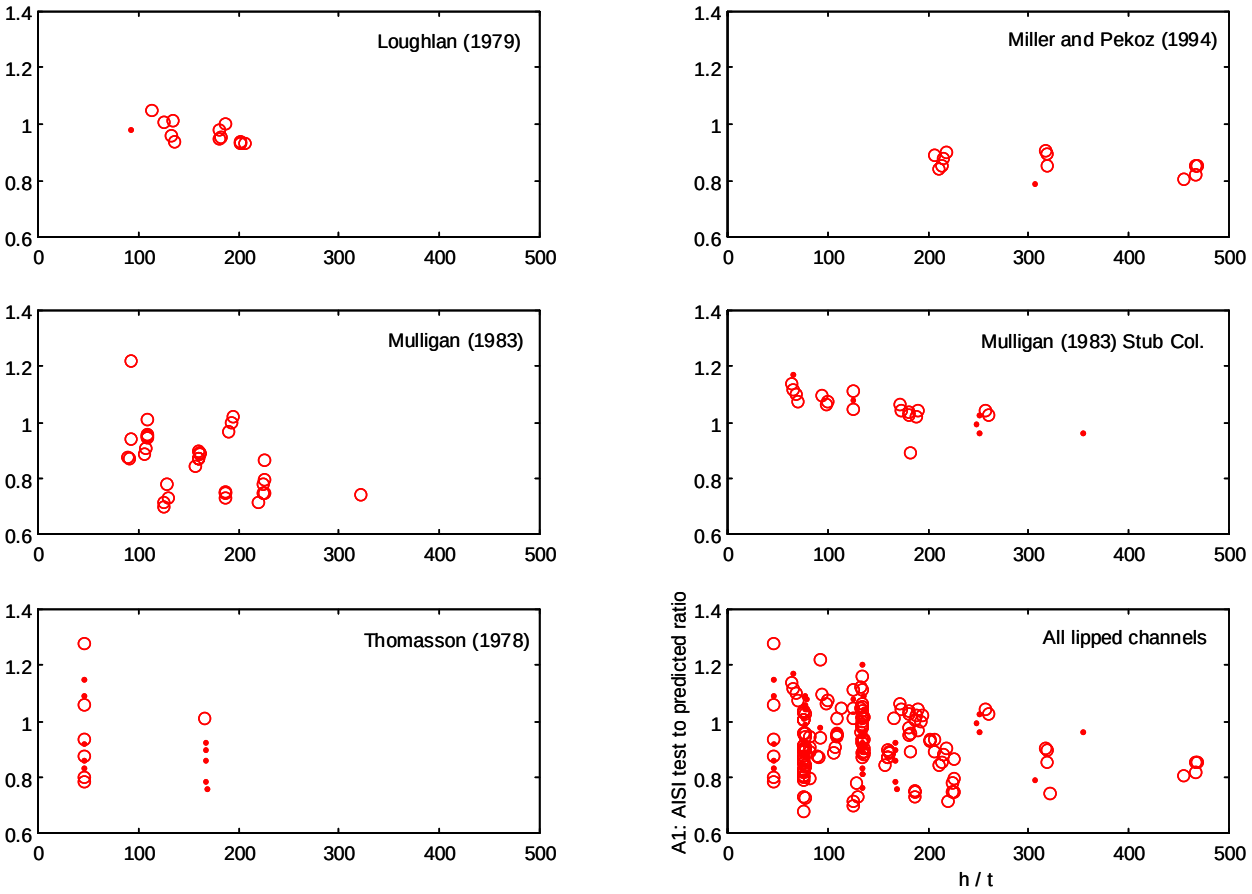

Figure 21 Performance of the AISI Specification (A1) vs. web slenderness (circles indicate members preficted to fail in a local mode by method C3, dots indicate members predicted to fail in a distortional mode by method C3)

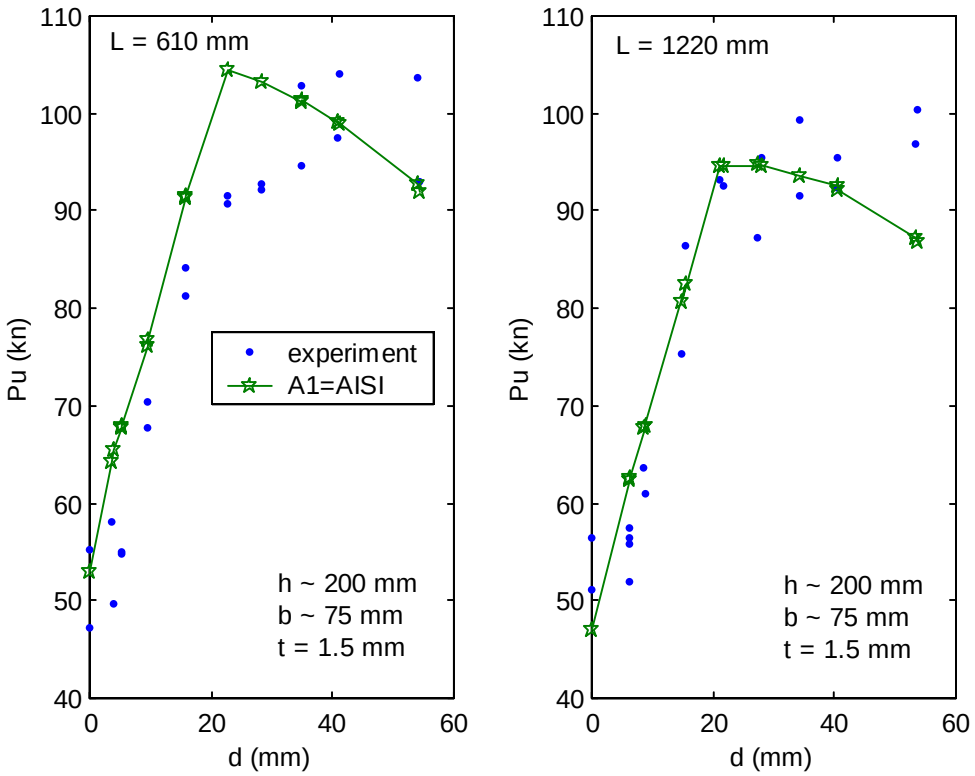

Figure 22 Performance of the AISI Specification for Z Sections

8.3 AISI with a distortional check (A2)

The experimental data on lipped C and Z Sections indicates that the AISI Specification would not significantly benefit from the addition of a separate distortional buckling check. Error in the current AISI Specification is not a function of distortional buckling, and instead relates primarily to web/flange interaction in local buckling Existing rules work reasonably well for the majority of simple lipped C and Z Sections.

However, rack sections, sections with intermediate web stiffeners, and a variety of other optimized shapes which are more prone to distortional buckling (see Figure 18) still require accurate design methods. These shapes would benefit from the proper inclusion of distortional buckling into the Specification, even a simple additional check, such as investigated in this design approach.

8.4 Alternative Effective Width Method B1

The current AISI Specification uses an effective width method for determining strength in local buckling. However, the effective width is based on expressions, such as those in AISI Specification Section B4.2 for edge stiffened elements, that include aspects of local buckling and distortional buckling. If distortional buckling is treated separately, then only local buckling need be considered in determination of the local buckling effective width. For example, in a lipped channel, the flange would always use k = 4, for local buckling, instead of a modified *k* value.

This basic approach is investigated in methods B1, C1 and D1 - considering various interactions amongst the modes. The simplest of which, B1, uses a separate check for distortional buckling and considers local and Euler buckling interaction. Figure 23 shows how B1 predicts the experiments on Z sections. The predicted strength is the minimum of the distortional buckling curve and the local buckling curve (which includes Euler buckling interaction.) The method provides a reasonable upper bound to the data and demonstrates that if a separate distortional check is made, the complicated rules for determining *k*, in Specification section B4.2 could be abandoned and a simple *k* = 4 value could be used for local buckling of edge stiffened elements.

The results of Table 9 show that in general this approach (B1) can work as well as existing design rules. Table 10 shows that members identified to fail in the distortional mode are well predicted by the method; however, members failing in the local mode are not predicted as accurately. The systematically unconservative predictions for lipped C's with high web slenderness (*h/t*) exhibited by the AISI Specification is slightly reduced using method B1, but not eliminated. The local web/flange interaction that occurs in the members with high *h/t* ratios is not well predicted by this method, because the element based effective width methods assume the *k* (plate buckling coefficient) for each element is independent.

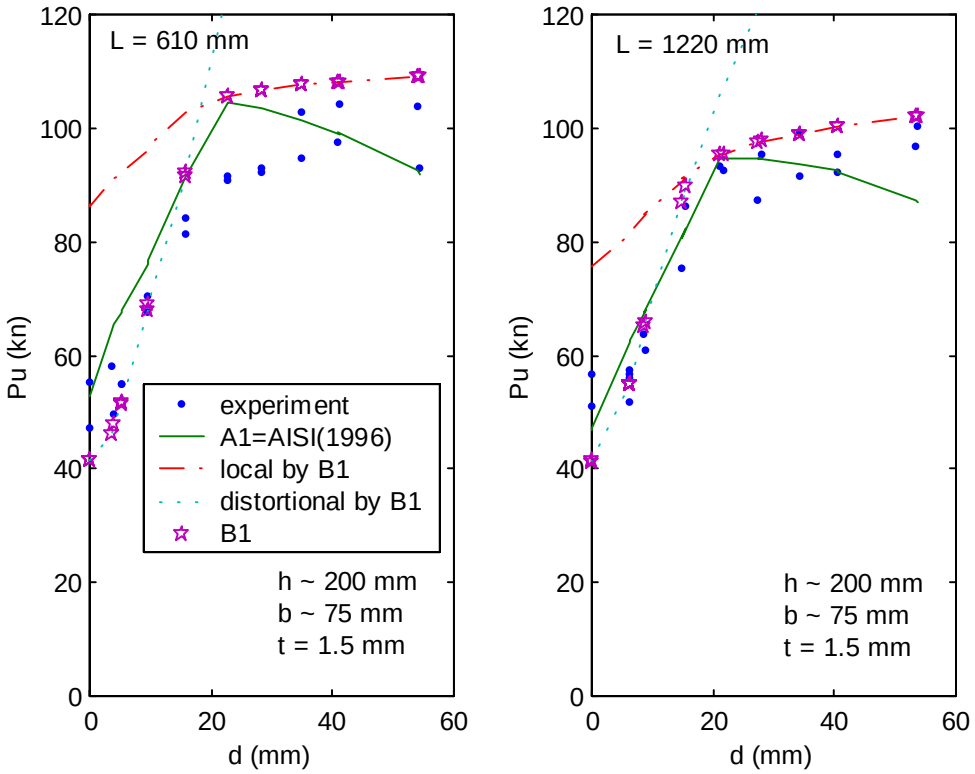

Figure 23 Performance of method B1 for sample of Z-Section Data

8.5 Hand Solutions, Direct Strength Method B2

Hand solutions for the elastic local and distortional buckling of C's and Z's that account for the interaction of the elements are available (see Appendix B for examples). Those hand solutions may be used to determine the slenderness in the local and distortional modes. Two different strength curves are postulated, one for local buckling (e.g., if no Euler interaction $P_n/P_y=(1-0.15(P_{crL}/P_y)^{0.4})(P_{crL}/P_y)^{0.4}$) and one for distortional buckling (e.g., if no Euler interaction $P_n/P_y=(1-0.25(P_{crD}/P_y)^{0.6})(P_{crD}/P_y)^{0.6}$) in order to predict the strength in these modes.

For the lipped C and Z section data the performance of the strength curves may be gauged in a simple plot of slenderness vs. strength, as shown in Figure 24 for method B2 (statistical rather than graphical summaries are in Table 9 and Table 10). Overall the method works well, and given typical scatter in column data, appears to be a good predictor over a wide range of slenderness. Examination of Table 10 shows that the increased accuracy of the method (over methods A1, A2 and B1) occurs due to improvements in the local buckling prediction – i.e. web/flange and flange/lip interaction are included in the local buckling calculation of method B2.

Figure 25 shows how the results od method B2, for the same Z section data in which the lip length is systematically increased. The presented method (B2) provides a good average prediction of the experimental data. Examination of all the experiments with respect to *h/t* and *h/t·h/b* as well as other variables reveals no systematic error in the method. Test to predicted ratios (Table 9) indicate that the basic approach (methods B2, C2, and D2) is sound, as long as local and distortional interaction (method D2) is ignored.

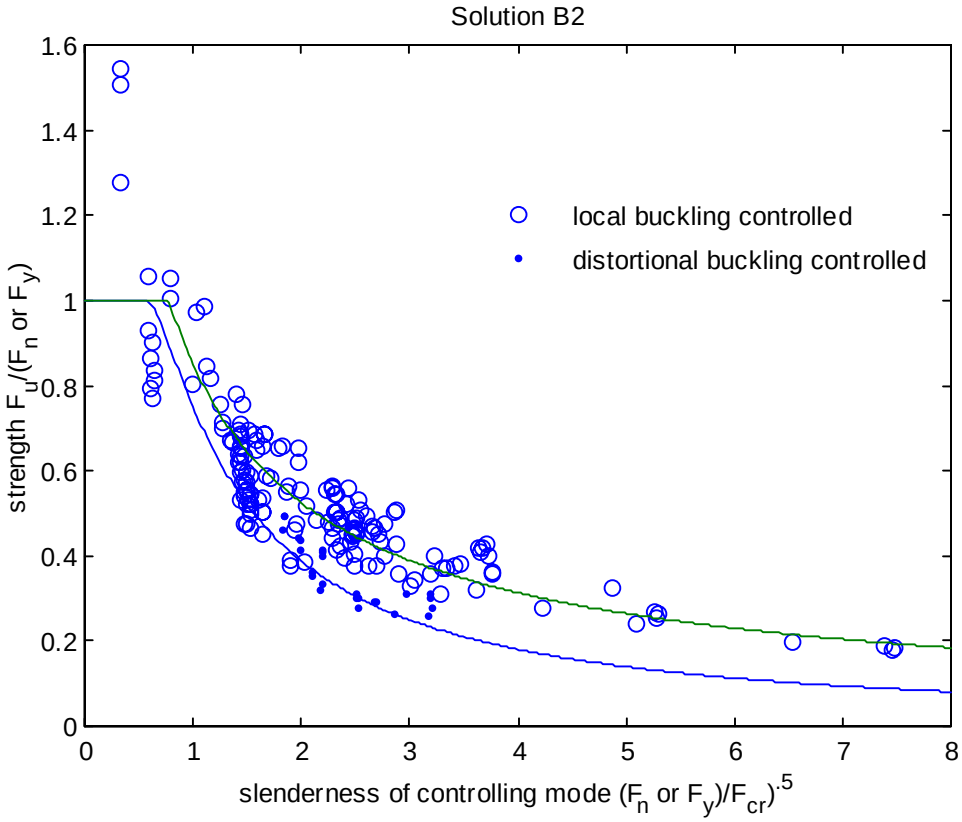

Figure 24 Slenderness vs. strength for method B2

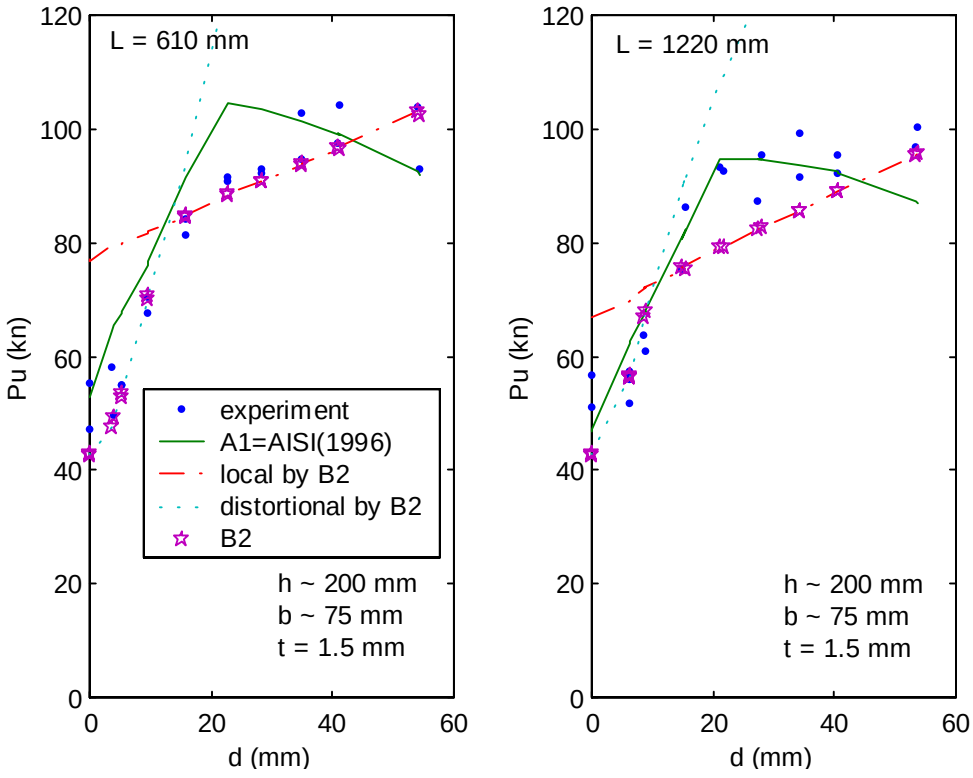

Figure 25 Performance of method B2 for sample of Z-Section data

8.6 Numerical Solutions, Direct Strength Method B3

The Direct Strength Method postulates that if the elastic critical buckling loads in the local and distortional mode are known for the entire member, this may be used to directly determine the member strength. A hand method implementation of this approach (method B2) agrees well with the experiments. Numerical implementation, in which the local and distortional buckling loads are determined from finite strip analysis performs as well or better. Consider a plot of slenderness vs. strength for the collected data for prediction method B3 (Figure 26).

Comparison against the Z section data is given in Figure 27. Figure 27 and Figure 22 underscore that the large difference between the various presented design methods is a function of how local buckling interaction is handled, not how distortional buckling is dealt with. Table 10 also demonstrates this same point, as the test to predicted ratios for local bucking are far more influential in assessing the overall accuracy of the method. Method B3 provides a good average prediction of the experimental data. Examination of all the experiments with respect to *h/t* and *h/t·h/b* as well as other variables reveals no systematic error. Test to predicted ratios (Table 9) indicate that overall the basic approach (methods B3, C3, and D3) is sound, as long as local and distortional interaction (method D3) is ignored.

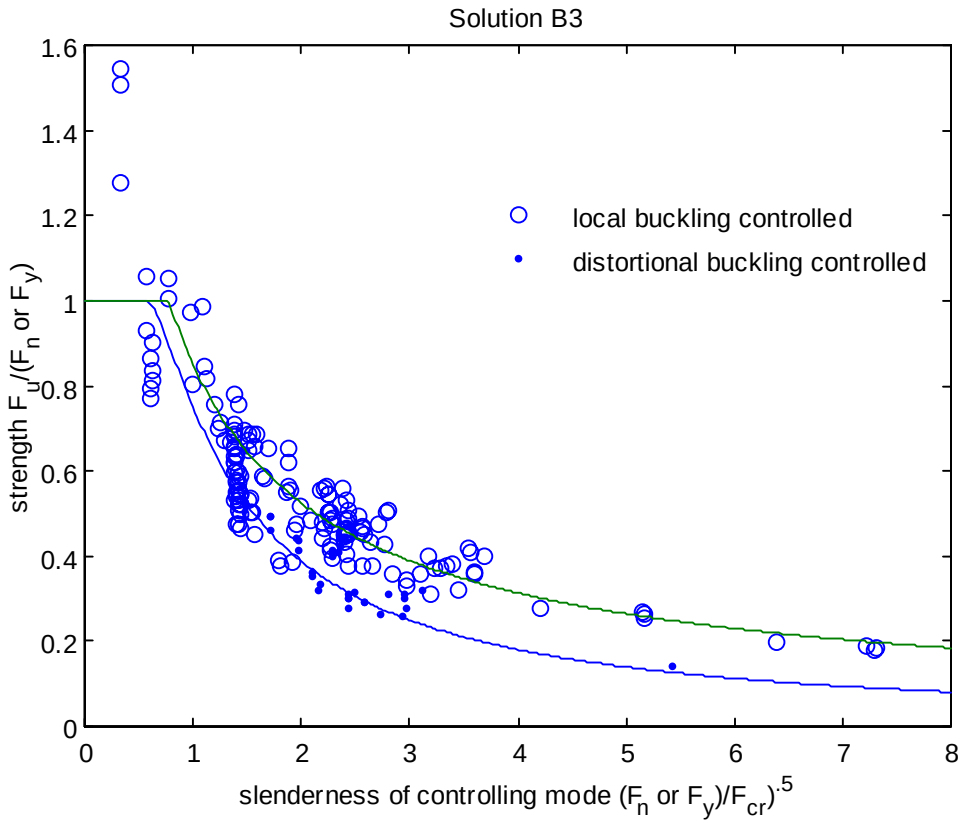

Figure 26 Slenderness vs. strength for C and Z sections, method B3

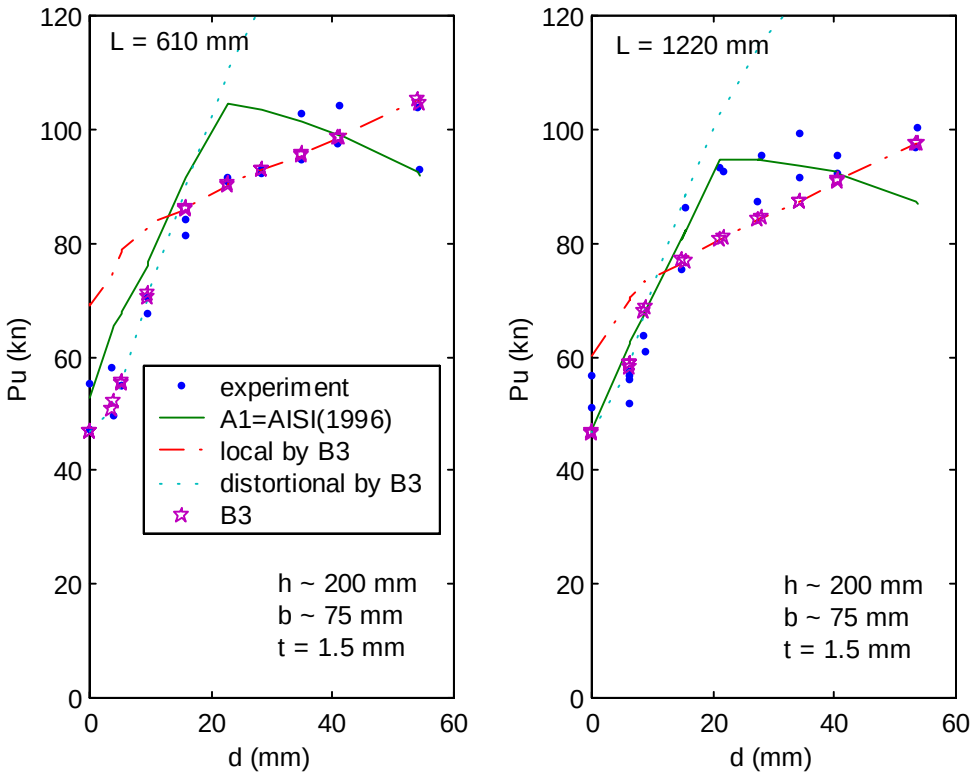

Figure 27 Performance of method B3 for sample of Z-Section data

8.7 Methods which allow Distortional and Euler Interaction (C1, C2, C3)

Design methods C1, C2, and C3 are nearly identical to their counterparts, methods B1, B2, and B3 respectively, except that in the strength calculation for distortional buckling the possibility of interaction with Euler (overall long-column) buckling is recognized (see Appendix D for design examples). Comparing the mean test to predicted ratios in Table 9 shows that for the studied experimental data of lipped C and Z sections little overall difference occurs when distortional and Euler interaction is considered. Looking at the more detailed results in Table 10 shows that the local buckling predictions remain essentially unchanged and the distortional buckling predictions are slightly more conservative (as expected). Interaction of distortional buckling with Euler buckling cannot be definitively recognized nor rejected from the available data.

For members with small edge stiffeners distortional and Euler interaction seems plausible, because the deformations and wavelengths involved are similar to the ones that initiate local and Euler buckling interaction (in pin-ended columns). However, for members with intermediate stiffeners or other additional folds, the amount of interaction for distortional and Euler buckling would seem to be much lower, particularly given the long wavelengths that distortional buckling occurs at in these members. For example, the experimental data on channels with intermediate stiffeners and racks with large compound lips (Figure 18) ignores this interaction.

Including Euler interaction in the distortional buckling calculation is conservative. Further, the inclusion of Euler buckling does not complicate the procedure, since it must already be considered for the local mode. A plot of slenderness vs. strength for method C3 is given in Figure 28, comparison with Figure 26 provides a means to assess the impact of including the interaction. In Figure 28 the slenderness is defined as the square root of the inelastic Euler column buckling stress (F_n) divided by the local or distortion buckling stress, and strength is simply normalized by F_n. (Note, Figure 28 is identical for load (P) or stress (f) since ratios are used for both the x and y axes).

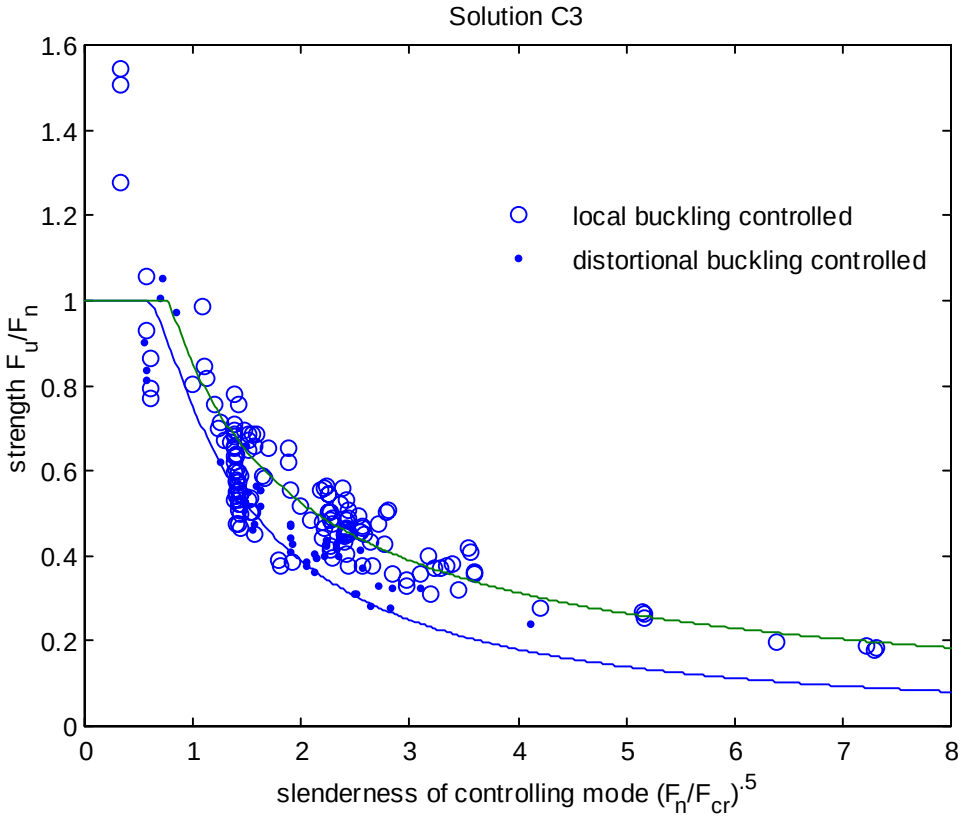

Figure 28 Slenderness vs. strength for C and Z sections, method C3

8.8 Methods which allow Local and Distortional Interaction (D1, D2, and D3)

The "D" methods (D1, D2 and D3) allow local and distortional interaction by setting the limiting inelastic stress for local buckling to the inelastic distortional buckling stress (see Appendix D for design examples). The "D" methods perform poorly (overly conservative) – see Table 9 and Table 10. In the majority of cases local plus distortional interaction is identified as the controlling limit state, but predicted strengths are significantly lower than tested capacities. This evaluation does not indicate that no interaction exists between these two modes, but in the available data, local and distortional interaction does not appear significant.

Based on this finding it is recommended that local and distortional interaction be ignored for routine design. Note, other data may indicated interaction between these two modes, for example as stated earlier, some evidence exists for perforated rack columns that local and distortional modes may interact (Baldassino and Hancock 1999).

9 Performance for Additional Experimental Data

9.1 Lipped Channel with Web Stiffeners

Thomasson (1978) tested a series of cold-formed columns with up to two stiffeners in the web, with geometry as shown in Figure 29 and summarized in Table 11. (The members without intermediate web stiffeners are included in the group of experimental data on lipped channels previously presented.) Thomasson investigated channels with very slender webs, flanges, and lips. The thickness was as low as 0.63 mm (0.025 in.) in some specimens, which lead to the high width to thickness ratios, presented in Table 11.

Figure 29 shows attachments to the lips of the channels with one or two intermediate stiffeners. When Thomasson initially tested the specimens with an intermediate stiffener they buckled in a distortional mode:

> "The provision of one or two stiffeners in the wide flange [the web] confers on the panel both an elevated load bearing capacity and an elevated stiffness. The consequences of improving the stiffness of the wide flange were not entirely favourable. . ..In order that the improved properties of the wide flange may be utilised, steps must be taken to prevent the occurrence of the torsional mode. By connecting the narrow flanges of the panels by means of 30 x 3 mm flats at 300 mm centres, the symmetrical torsion mode [Figure 30 (a)] was eliminated. This measure does not prevent the occurrence of the anti-symmetrical mode [Figure 30 (b)]." Thomasson (1978)

Numerical prediction of the elastic buckling stress (load) of the anti-symmetrical distortional mode may be approximated by modeling only ½ of the member and enforcing anti-symmetry at mid-width of the web.

Due to the more complicated cross-section only design methods B3 and C3, the numerical Direct Strength methods, are investigated for this data. The test to predicted ratios presented in Table 12 indicate that (a) the experimental results are generally lower than the predicted values and (b) including distortional interaction with Euler buckling (method C3) provides better mean predictions of the strength. The slenderness vs. strength for this data presented in Figure 31 indicates that including the long column interaction (method C3) also provides a different prediction of the failure mode for a number of the members.

The tested members are quite slender. Nonetheless, the predicted strength without intermediate web stiffeners is excellent for methods B3 or C3, see Table 9. In the members with intermediate web stiffeners, the addition of the straps to restrict symmetrical distortional buckling makes prediction of the strength slightly more complicated. Nonetheless, predictions are adequate, particularly if long column interaction (method C3) is included.

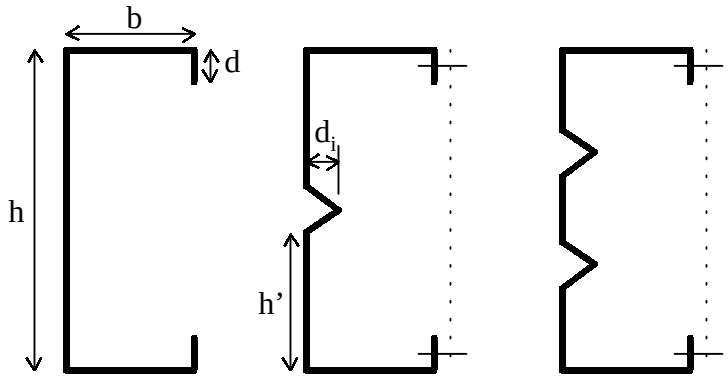

Figure 29 Geometry of lipped channels tested by Thomasson (1978)

Table 11 Summary of geometry of lipped channels tested by Thomasson (1978)

	h/b		h/t		b/t		d/t		
	max	min	max	min	max	min	max	min	count
Thomasson (1978)	3.1	3.0	489	205	160	68	33	14	46
					d_i/d		h'/t		
					max	min	max	min	count
	no intermediate web stiffeners				-	-	-	-	14
	one intermediate web stiffener				0.94	0.39	222	91	16
	two intermediate web stiffeners				0.94	0.47	145	57	16

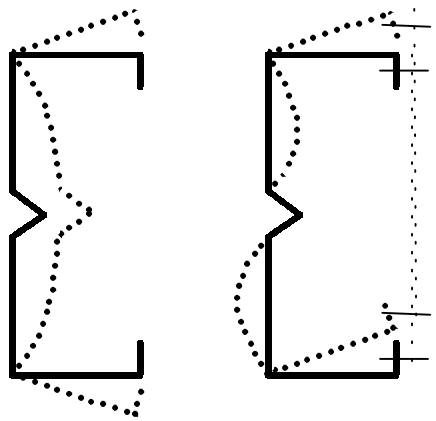

Figure 30 Distortional buckling modes (a) modeobserved in initial testing with web stiffener in place (b) mode observed after addition of flat bars connecting lip stiffeners

Table 12 Test to predicted ratio for Thomasson (1978) channels with intermediate web stiffeners

limit states checked?	L+E	L+E, D	L+E, D			L+E, D+E			L+D, L+E, D+E		
design method:	A1	A2	B1	B2	B3	C1	C2	C3	D1	D2	D3
Channels with int. stiffeners and straps* Thomasson (1978)											
1 int. web stiffener	-	-	-	-	**0.83**	-	-	**0.85**	-	-	-
	-	-	-	-	(0.10)	-	-	(0.07)	-	-	-
2 int. web stiffeners	-	-	-	-	**0.85**	-	-	**0.95**	-	-	-
	-	-	-	-	(0.12)	-	-	(0.16)	-	-	-

* lips of edge stiffeners strapped together, thus restricting symmetrical distortional buckling

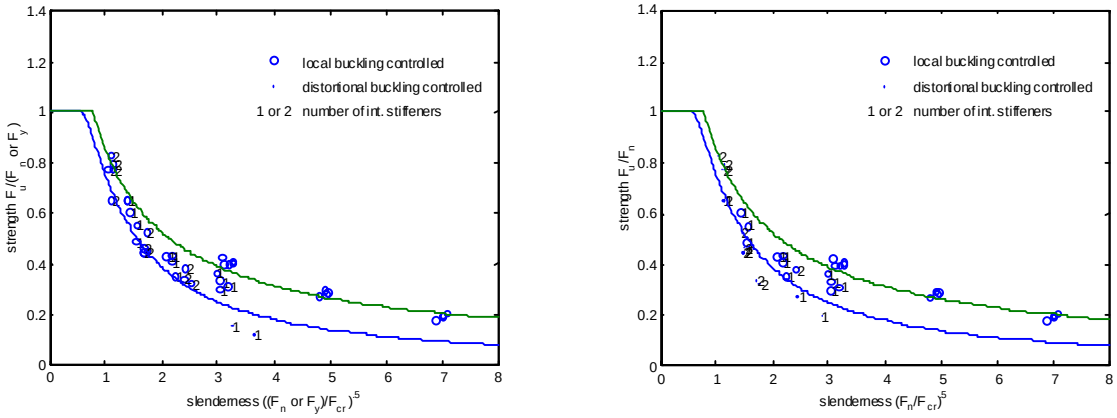

(a)method B3 (b) method C3

Figure 31 Slenderness vs. strength for Thomasson(1978) tests

9.2 All available data

The Thomasson (1978) data and The University of Sydney experimental data (see Section 5.2) is added to the data on lipped C and Z sections. The slenderness vs. strength plot for method C3 is completed in order to provide a presentation of the overall strength prediction for the Direct Strength Method for available column data. Though scatter certainly exists the plot demonstrates that such an approach is viable as a general method for prediction of the

strength of cold-formed steel columns in local, or distortional buckling with consideration of interaction with long column Euler buckling.

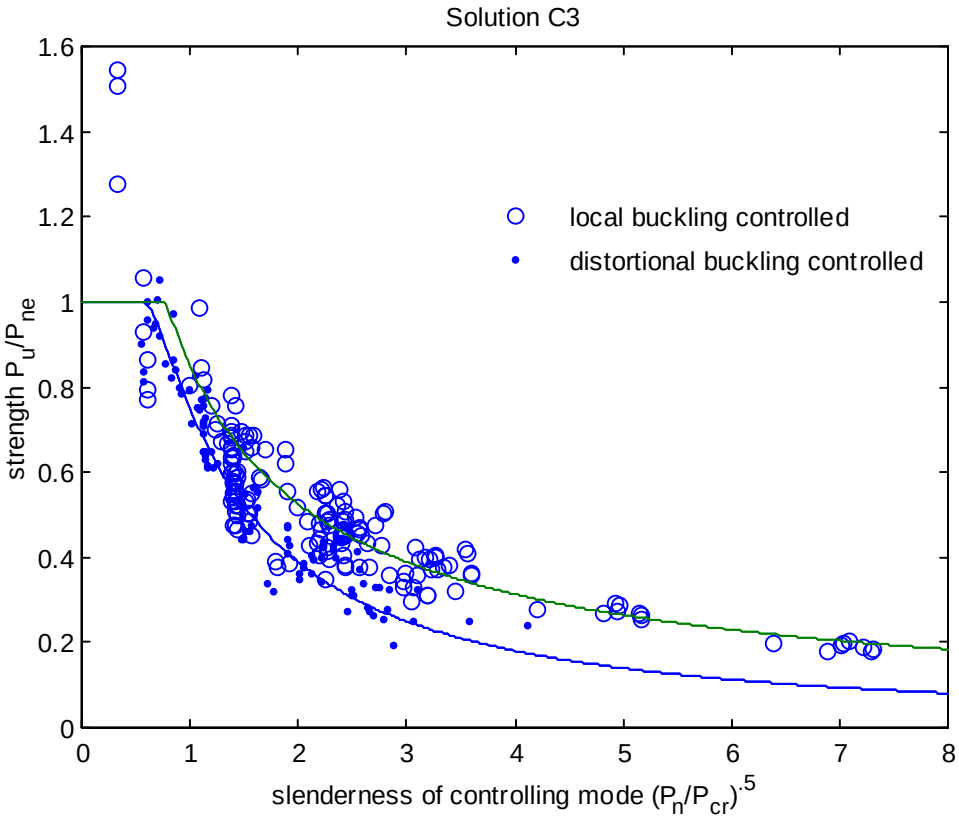

Figure 32 Slenderness vs. strength all available column data (C's, Z's, C's with int. web stiffeners, racks, racks with compound lips)

10 Discussion

10.1 Reliability of examined methods (ϕ factors)

The reliability of the 11 design methods was assessed by calculating the resistance factor (ϕ) for a β of 2.5 via the guidelines of Section F in the AISI Specification. The results are given in Table 13. Variability in the data is relatively high, and the resulting ϕ factors are consistent with current practice of $\phi = 0.85$.

If local and distortional buckling are treated as different limit states then the possibility of using two different ϕ factors exists. The experimental data suggests lower ϕ factors for local buckling limit states than distortional buckling. However, this does not reflect the variability in the data (Table 10 shows the variability in the 2 methods is generally about the same – if not a little higher for distortional failure modes) but rather reflects the higher test to predicted ratios for currently proposed formula in the distortional mode.

Numerical studies presented in Section 5.1 suggest that distortional failures have a greater imperfection sensitivity and thus lower ϕ factors may be needed for this mode. This observation may be true, but it is not borne out by this data. Continued use of $\phi \sim 0.85$ appears appropriate for cold-formed steel columns.

Table 13 Calculated Resistance Factors (ϕ) for the 11 Methods by Limit State

Design method	L+E	D or D+E	L+D	All Data[1]
A1: AISI (1996) Specification	0.79			**0.82**
A2: AISI (1996) plus distortional check	0.78	0.94		**0.83**
B1: Effective width with distortional check	0.75	0.84		**0.81**
B2: Direct Strength by hand w/ dist. check	0.82	0.92		**0.86**
B3*: Direct Strength numerical wi/ dist. check	0.79	0.90		**0.84**
C1: same as B1 but consider D+E interaction	0.75	0.84		**0.81**
C2: same as B2 but consider D+E interaction	0.82	0.89		**0.86**
C3*: same as B3 but consider D+E interaction	0.80	0.89		**0.84**
D1: same as C1 but consideer D+L interaction	0.72		0.81	**0.88**
D2: same as C2 but consider D+L interaction	0.73	0.99	0.80	**0.89**
D3: same as C3 but consider D+L interaction	0.66	0.70	0.70	**0.85**

[1] resistance factor calculations for "all data" use a weighted standard deviation, i.e., the standard deviation for all the data is weighted by the number of samples conducted by each researcher.
* resistance factors calculated for methods B3 and C3 include Thomasson's data as well as all the cited University of Sydney data. Other methods only include the lippped channel and Z's used in this report.

10.2 Understanding when the distortional mode is prevalent – redux

Section 4 of this report provides elastic buckling analysis to answer the question: when is the distortional mode prevalent? Experiments suggest ultimate strength in the local and distortional mode is different, therefore elastic buckling analysis does not provide a complete answer to the above question. The overall pervasiveness of distortional buckling may be assessed by examination of Table 10, which shows the predicted number of failures in the competing modes. For the majority of the studied members local buckling is the predicted failure mode.

A parametric study of member dimensions ranging from *h/b* of 0.1 to 6, *d/b* from 0.01 to 0.5 and *b/t* of 30, 60 and 90 with f_y = 50 ksi is performed using the Direct Strength design method B2 to further investigate ultimate strength in the two modes. The mode with the lower strength is identified in Figure 33. For each *b/t* ratio (30, 60 and 90) figures are provided as a function of *h/b* vs. *d/b* as well as *h/t* vs. *d/t*. Note these figures are dependent on the yield stress selected as well as the dimensional ratios. The difficulty of ascribing simple dimensional limits to determine when local or distortional buckling will control is conveyed by the complexity and changing nature of the border that separates the two limit states in Figure 33.

The distortional mode controls the predicted strength over a relatively large range of dimensions. Members with stocky flanges (fully effective) are more prone to distortional failures than those with slender flanges; however as we learned in Figure 2 there is a limit to this line of thinking, flanges should not be too wide nor too narrow. In most cases members with short lips are prone to distortional failures; however the boundary of what a “short” lip depends on the other dimensions of the column and the yield stress. The border between local and distortional for members with high *h/b* ratios is somewhat misleading, because local and distortional buckling of very narrow members are quite similar phenomena – almost completely driven by the web deformation.

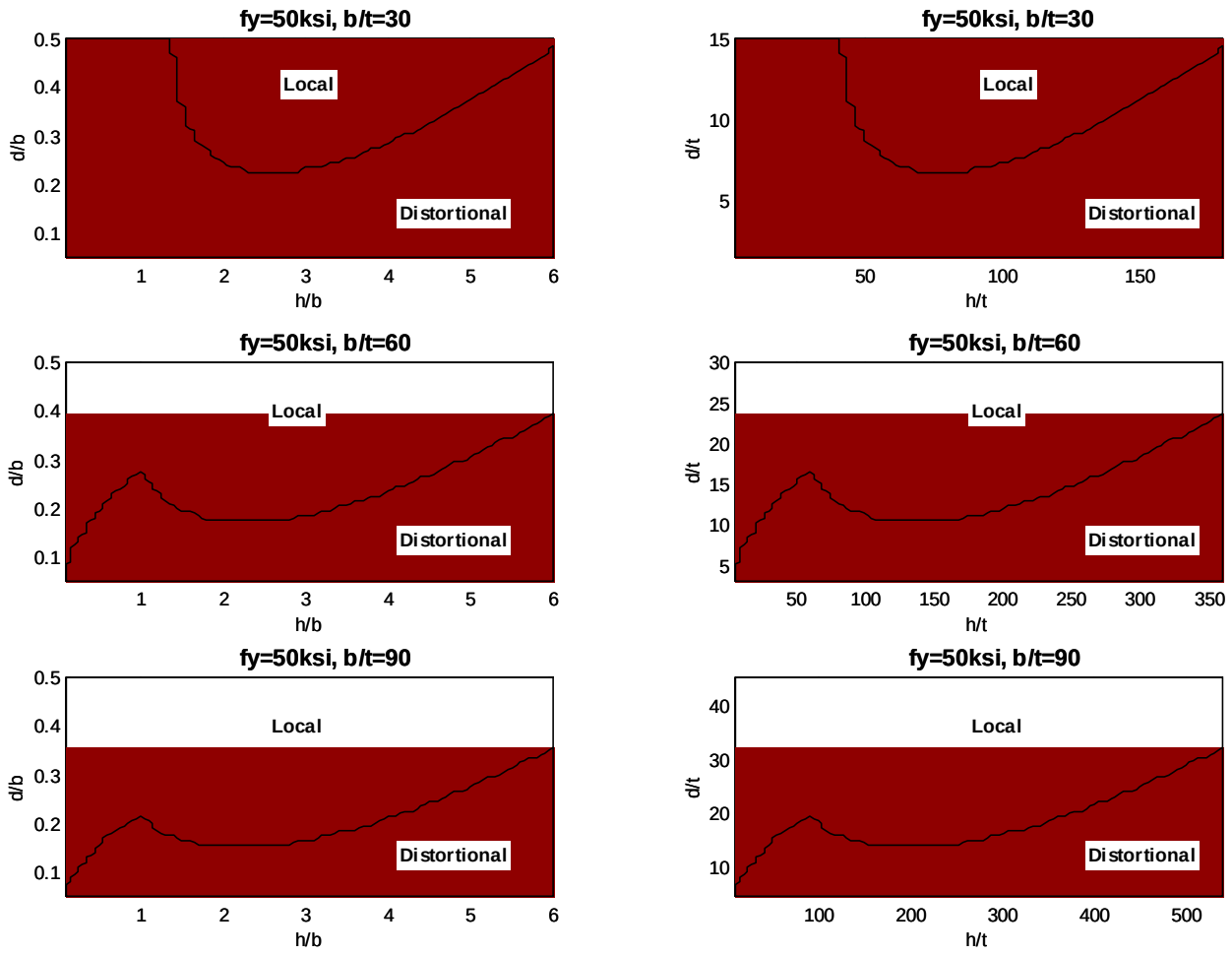

Figure 33 Predicted Failure Modes based on Direct Strength Design Method B2

10.3 Restriction of the Distortional Mode

One factor not explicitly discussed in the majority of this work is the restriction of the distortional mode through bracing or other means. Attachments to sheeting, as well as discrete braces may be used to hinder the distortional mode and thus increase the strength of the member. The analysis of Thomasson's tests in Section 9.1 provides insight on how to use anti-symmetry in numerical analysis for certain special cases of restricted distortional buckling; however, general guidance on including bracing or other attachments that restrict the distortional mode is lacking.

Completely ignoring bracing that restricts the distortional mode can lead to overly conservative design. For discrete braces the best current practice is to compare the unbraced length with the half-wavelength of the mode. If the unbraced length is less than the half-wavelength then it may be used in the hand formulas for prediction of the distortional buckling stress – or the shorter unbraced length may be directly considered in the numerical analysis. The bracing should restrict the rotation of the flange and cause the buckling wave to occur in the unbraced segment.

10.4 Specification Directions?

The current AISI Specification has at least 4 paths that can be taken to address the findings of this work:

1. do nothing / add commentary language only,
2. add an additional strength check for distortional buckling on top of the existing Specification methods,

3. remove section B4.2 and instead always use k=4 for local buckling of edge stiffened elements, and then add a distortional check,
4. adopt a completely new procedure (hand or numerical) which accounts for interaction amongst the elements for local buckling and includes a check on distortional buckling.

Option 1

As the data shows (Table 9) doing nothing, i.e., no change to the Specification, will work reasonably well for a variety of conventional situations. Commentary, or even dimensional limits, could be added to indicate that members with high web slenderness and narrow flanges are likely to yield unconservative solutions with current methods due to local buckling interaction, and members with low web slenderness and wide flanges (shapes approaching square) are likely to yield unconservative solutions with current methods due to distortional buckling. The expressions in B4.2 could even be tweaked to eliminate some of the problems demonstrated in Figure 22 for intermediate length lip stiffeners. However, inherent in this approach is the fact that local buckling interaction (web/flange, flange/lip) and distortional buckling are currently ignored. Further, innovations such as adding stiffeners in the web, or using more efficient stiffening lips are retarded by continued use of current approaches.

Option 2

If distortional buckling was the primary problem with strength predictions for columns then adopting a distortional check on top of current Specification rules would be a viable fix, but it is not. The addition of a distortional check without further modification to the Specification will only complicate, not improve, design. This option should be rejected.

Option 3

Current use of the effective width approach in the Specification essentially necessitates an element by element treatment of the member. If this method is to be maintained the best approach is to simplify the local buckling portion of the procedure (remove section B4.2 and replace with k = 4) and add a distortional buckling check (this is method B1 or C1). Similar design procedures have been proposed for distortional buckling of beams (Hancock et al. 1996, Schafer and Peköz 1999) and shown to provide reliable predictions. This solution accounts for issues related to distortional buckling effectively, but ignores problems related to local buckling interaction.

Option 4

Adopting completely new procedures for cold-formed steel column design requires significant changes in current practice and thinking. The member based, or Direct Strength, methods (B2, C2, D2 and B3, C3, D3) that are investigated herein do not fit well in the current Specification methodology. Instead of breaking the design of a member into detailed calculations of each element the entire cross-section is treated as a whole. “Treating the member as a whole” implies that calculations for local and distortional buckling properly consider the interaction of the elements making up the cross-section. Closed-form expressions and numerical methods are provided for completing this task. The elastic buckling information is used in combination with strength curves to generate the capacity for the member. The accuracy of methods B2, B3, C2, and C3 demonstrate the viability of this approach.

Adoption of the Direct Strength method holds several advantages over current methods: calculations do not have to be performed for individual elements, interaction of the elements in both local and distortional buckling is accounted for, distortional buckling is explicitly treated as a unique limit state, an obvious means for introducing rational analysis through numerical prediction of elastic buckling is provided, and a rational analysis procedure is provided for members with stiffener configurations or other geometries that current rules do not apply to. The Direct Strength method removes systematic errors that exist in the current AISI (1996) method. The method provides a means for integrating known behavior into a straightforward design procedure and should increase innovation of cold-formed steel member cross-sections.

10.5 Recommendations

Based on the findings of this report the following three recommendations are made for improving current practice in cold-formed steel design.

1. Proposed for immediate adoption:

The commentary in AISI Specification Section B4.2 should be revised to provide general guidance on member cross-sections that may be unconservatively predicted by current design methods. Updated references to research that provide design methods for local and distortional buckling should be added. (see Appendix F.1).

2. Proposed for interim adoption

As long as the AISI Specification still follows effective width procedures it is proposed that the existing rules for B4.2 be removed, to be replaced with k = 4 for local buckling of edge stiffened elements and a separate distortional buckling check for all members which have edge stiffened elements in the cross-section be added. (Thus, this recommendation is for interim adoption of design method C1, see Appendix D for a full example and Appendix F.2 for proposed Specification language – this procedure has previously been shown to work for beams as well as columns, see discussion in the previous section).

3. Proposed for long-term adoption and interim adoption as an alternative procedure

Adopt the Direct Strength method for the design of columns as an alternative design procedure, and move towards this procedure in the future. Design method C2 provides a closed-form, "hand" implementation of this method and design method C3 provides the same method with numerical analysis via the finite strip method for predicting the elastic buckling. Method C3 is proposed for adoption with a rational analysis clause to be used for prediction of the elastic buckling loads. The design formula of method C2 could be provided in an Appendix as one form of rational analysis, finite strip and finite element analysis would be other acceptable forms of rational analysis for prediction of elastic buckling. (see Appendix D for complete design examples using methods C2 and C3 and Appendix F.3 for proposed Specification language).

10.6 Industry Impact of Adopting Recommendations

The following discussion relates primarily to changes in the strength prediction of cold-formed steel members due to adoption of the proposed methods. Detailed discussions of the errors in current methods and the advantages of the proposed methods can be found in Section 8 and 9.

Impact of Proposal 1 "for immediate adoption"

Adding additional commentary language will not change the letter of the Specification, but it may change the interpretation slightly. Recognizing the limitations of the current methods in the commentary at least gives the user some knowledge of current findings and the additional references provide guidance as to where more information can be obtained.

Impact of Proposal 2 "for interim adoption"

Adoption of Proposal 2 (in essence, design method C1) will make local buckling calculations simpler - but it will add significant effort to the design due to calculation of the distortional buckling stress. Due to its complexity, the addition of a separate distortional buckling check will encourage a rational analysis clause. This method generally encourages better designs by explicitly recognizing and calculating the distortional mode.

The impact on strength predictions is provided in the detailed summary in Appendix E – which includes a column which compares methods C1 (Proposal 2) to A1 (current AISI 1996 method), and in Figure 34 which plots the ratio of the two methods vs. different geometric quantities. Compared to the current AISI (1996) method adoption of method C1 will favor members with longer lips, and discourage members with small lips. Members with lip length to flange width ratios (*d/b*) less than 0.2 may anticipate significant reductions in strength, while members with *d/b* greater than 0.4 may see large increases. The overall average impact on test to predicted ratios for the studied members is less than 1%.

Impact of Proposal 3 "for long-term adoption and interim adoption as an alternative procedure"

Adoption of the Direct Strength method holds several advantages over current methods: calculations do not have to be performed for individual elements, interaction of the elements in both local and distortional buckling is accounted for and thus systematic error in current methods is removed, distortional buckling is explicitly treated as a unique

limit state, an obvious means for introducing rational analysis through numerical prediction of elastic buckling is provided, and a rational analysis procedure is provided for members with stiffener configurations or other geometries that current rules do not apply to. The method provides a means for integrating known behavior into a straightforward design procedure and should increase innovation of cold-formed steel member cross-sections.

The impact on strength predictions is provided in the detailed summary in Appendix E – which includes a column which compares methods C3 (Proposal 3) to A1 (current AISI 1996 method), and in Figure 35 which plots the ratio of the two methods vs. different geometric quantities. The Direct Strength Method (method C3) provides markedly different strength predictions than current methods. In the studied members of lipped C's and Z's the predicted strength can be as much as 16% higher than the current AISI (1996) method, but on average adoption entails a strength loss of 7%. Compared to the current AISI (1996) method, narrow members (high *h/b*) with slender webs (high *h/t*) and short lips (low *d/b*) will be specifically discouraged. Members with longer lips (higher *d/b*) are encouraged. The method removes systematic error that exist in the current AISI (1996) approach and the overall test to predicted ratio is 1.01.

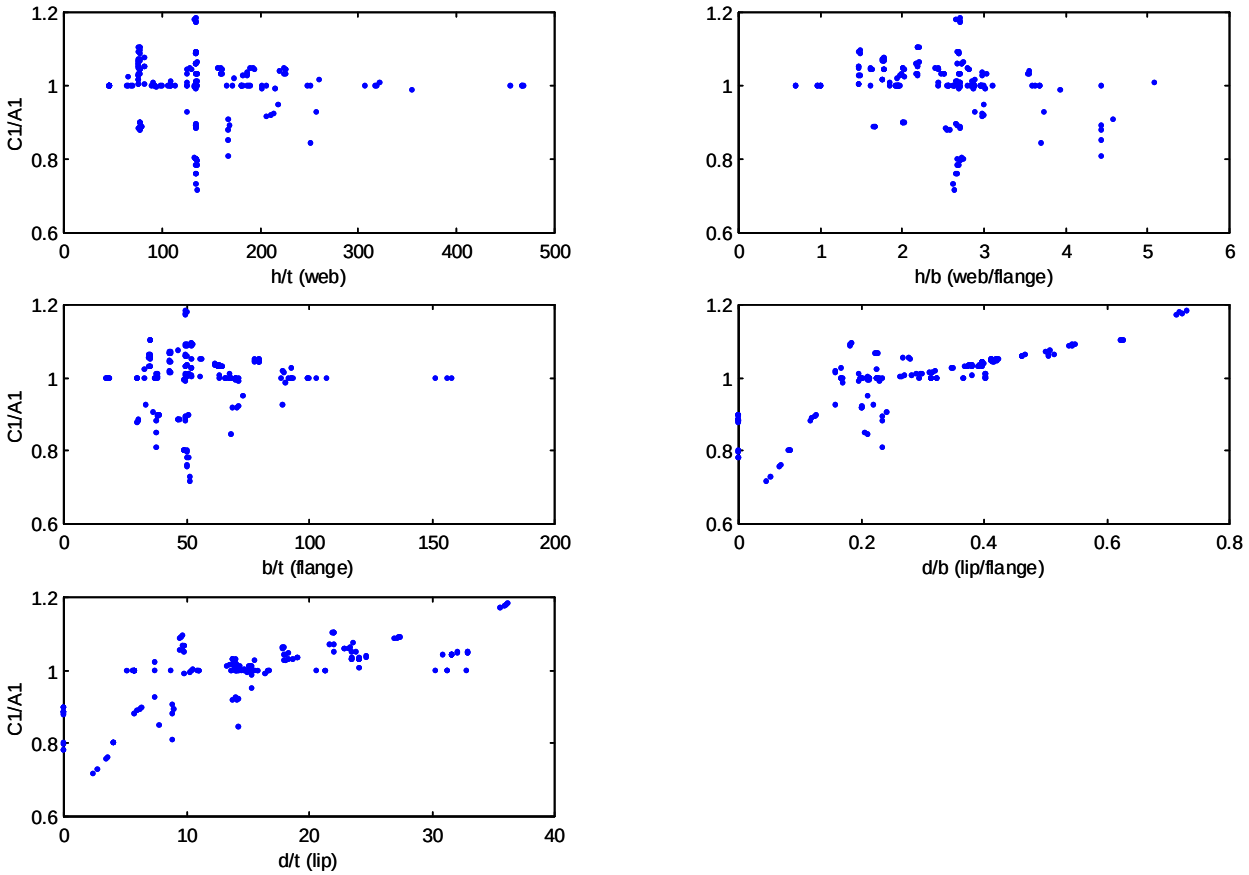

Figure 34 Impact of Adopting Proposal 2 an Alternative Effective Width Method, Shown as Ratio of Proposal 2 (C1) / AISI (A1) for the Lipped Channels and Z's Studied in this Report

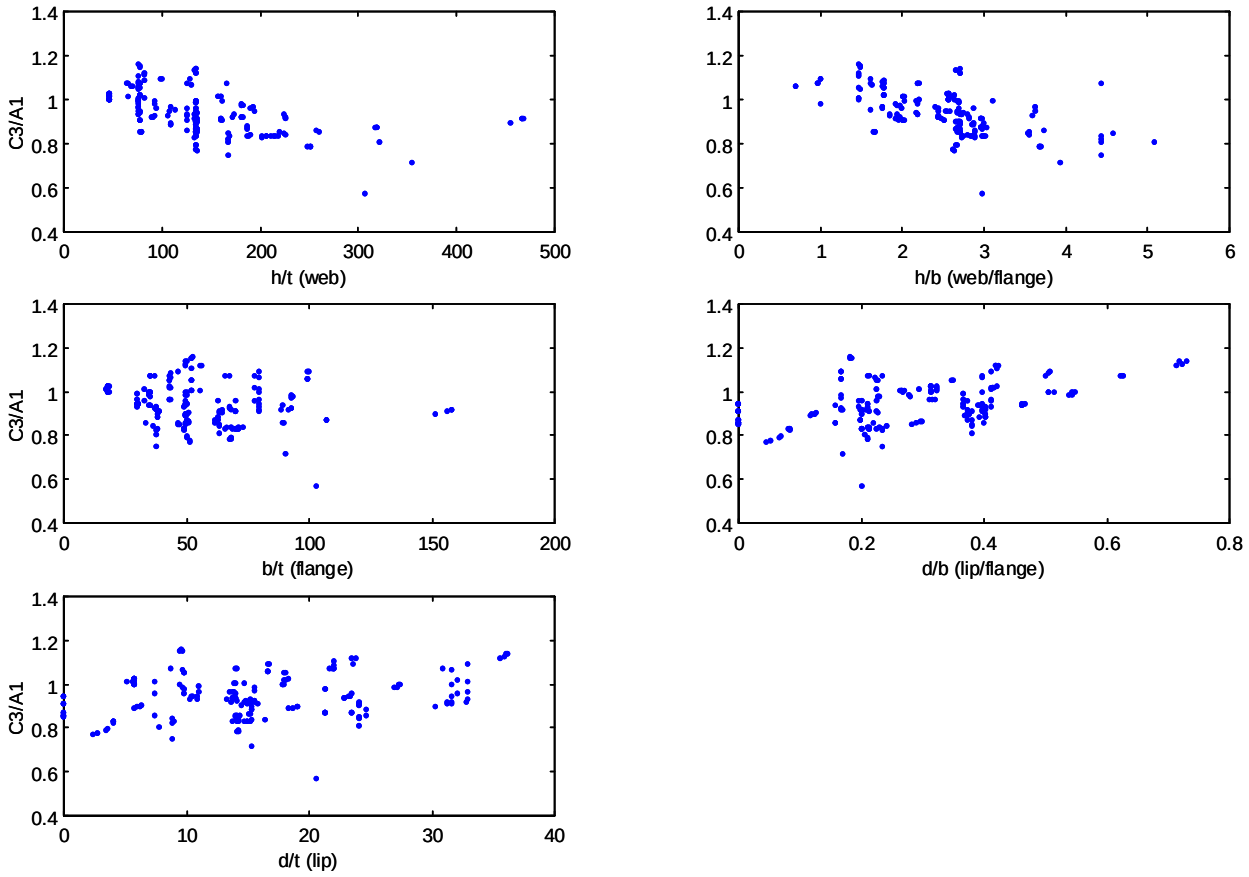

Figure 35 Impact of Adopting Proposal 3 the Direct Strength Method, Shown as Ratio of Proposal 3 (C3) / AISI (A1) for the Lipped Channels and Z's Studied in this Report

11 Conclusions

Ultimate strength of columns failing in the distortional mode is worthy of attention because distortional failures have lower post-buckling capacity than local modes of failure, distortional buckling may control failure even when the elastic distortional buckling stress (load) is higher than the elastic local buckling stress (load), and distortional failure modes have higher imperfection sensitivity. Existing experimental data demonstrates that if the failure is known to occur in the distortional mode, then the elastic distortional buckling stress (load) may be used to predict the ultimate strength.

Local buckling is the most common failure mode for the majority of existing lipped C and Z section columns. This is due to the fact that these members have slender webs, and as a result local buckling is a more common limit state than distortional buckling. Rack sections and other members with *h/b* ratios around 1, members with intermediate stiffeners in the web, and members with particularly small edge stiffeners, are all examples of columns that are prone to distortional failures. For these members explicit checks on distortional buckling are required for successful design.

The current AISI Specification provides a reasonable average prediction of standard lipped C and Z sections (on average nominal strength prediction is 6% unconservative). However, the AISI Specification exhibits systematic error for members with high *h/t* ratios (slender webs) and high *h/b* ratios (slender web with narrow flange). Further, AISI Specification predictions for tested Z sections over-predict the strength capacity of intermediate length edge stiffeners, and under-predict the strength capacity of long edge stiffeners. Issues related to local web/flange interaction, not distortional buckling are the primary source of errors in the AISI Specification. The addition of a simple distortional buckling check on top of existing AISI Specification rules does not remove the errors. Based on

these findings commentary language addressing the limits of the current AISI (1996) Specification is suggested for immediate adoption (see Appendix F.1).

A variety of alternative methods are shown to provide predictions that are as good or better than current design rules. However, design methods that continue the current effective width methodology of performing calculations separately for each element inherently suffer from an inability to consider the interaction of elements in local buckling. Nonetheless, since this is the currently accepted design procedure a method based on the effective width approach that properly incorporates distortional buckling was determined. This method (method C1 in Appendix D) is given in Appendix F.2 and is suggested for interim adoption into the AISI Specification.

The Direct Strength method (method C2 and C3 in Appendix D) given in Appendix F.3 is suggested as a long term solution for column design. Advantages of the Direct Strength method include: calculations do not have to be performed for individual elements, interaction of the elements in both local and distortional buckling is accounted for, distortional buckling is explicitly treated as a unique limit state, an obvious means for introducing rational analysis through numerical prediction of elastic buckling is provided, and a rational analysis procedure is provided for members with stiffener configurations or other geometries that current rules do not apply to. The Direct Strength method removes systematic errors that exist in the current AISI (1996) method. The method provides a means for integrating known behavior into a straightforward design procedure and will increase innovation of cold-formed steel member cross-sections.

12 References

American Iron and Steel Institute (1996). Cold-Formed Steel Design Manual. *American Iron and Steel Institute*.

Baldassino, N., Hancock, G. (1999). "Distortional Buckling of Cold-Formed Steel Storage Rack Section including Perforations."

Desmond, T.P. (1977). The Behavior and Design of Thin-Walled Compression Elements with Longitudinal Stiffeners. Ph.D. Thesis, Cornell University, Ithaca, New York.

Hancock, G.J., Kwon, Y.B., Bernard, E.S. (1994). "Strength Design Curves for Thin-Walled Sections Undergoing Distortional Buckling". *J. of Constructional Steel Research*, Elsevier, 31(2-3), pp. 169-186.

Hancock, G.J., Rogers, C.A., Schuster, R.M. (1996). "Comparison of the Distortional Buckling Method for Flexural Members with Tests." *Proceedings of the Thirteenth International Specialty Conference on Cold-Formed Steel Structures*, St. Louis, Missouri.

Kwon, Y.B., and Hancock, G.J., (1992) "Strength Tests of Cold-Formed Channel Sections undergoing Local and Distortional Buckling",*Jour Struct Engg,* ASCE, 117(2),, pp 1786 – 1803.

Lau, S.C.W., and Hancock, G.J (1987).,"Distortional Buckling Formulas for Channel Columns", *Journal of Structural Engineering*,ASCE,1987, 113(5), pp 1063 – 1078.

Loughlan, J. (1979). Mode Interaction in Lipped Channel Columns under Concentric or Eccentric Loading. Ph.D. Thesis. University of Strathclyde, Glasgow.

Miller, T.H., Peköz, T. (1994). "Load-Eccentricity Effects on Cold-Formed Steel Lipped- Channel Columns." *J. of Struct. Eng.*, ASCE, 120(3), pp. 805-823.

Mulligan, G.P. (1983). The Influence of Local Buckling on the Structural Behavior of Singly-Symmetric Cold-Formed Steel Columns. Ph.D. Thesis. Cornell University. Ithaca, New York.

Peköz, T. (1987). *Development of a Unified Approach to the Design of Cold-Formed Steel Members.* American Iron and Steel Institute Research Report, CF 87-1.

Polyzois, D., Charnvarnichborikarn, P. (1993). "Web-Flange Interaction in Cold-Formed Steel Z-Section Columns". *J. of Struct. Eng.* ASCE, 119(9), pp. 2607-2628.

Schafer, B.W. (1997). Cold-Formed Steel Behavior and Design: Analytical and Numerical Modeling of Elements and Members with Longitudinal Stiffeners. Ph.D. Thesis. Cornell University. Ithaca, New York.

Schafer, B.W., Peköz, T. (1998). "Direct Strength Prediction of Cold-Formed Steel Members using Numerical Elastic Buckling Solutions." *Fourteenth International Specialty Conference on Cold-Formed Steel Structures.* St. Louis, Missouri.

Schafer, B.W., Peköz, T. (1999). "Laterally Braced Cold-Formed Steel Flexural Members with Edge Stiffened Flanges." *Journal of Structural Engineering*. 125(2).

Thomasson, P. (1978). "Thin-walled C-shaped Panels in Axial Compression". *Swedish Council for Building Research.* D1:1978, Stockholm, Sweden.

A Detailed History of Distortional Buckling of Columns

A History of Distortional Buckling of Cold-Formed Steel Columns

Benjamin Schafer, Ph.D. and Gregory Hancock, Ph.D.

Research in the behavior of cold-formed steel columns spans approximately fifty years. Through that time distortional buckling, under many different names, has come in and out of the spotlight. This brief account highlights the major experimental work in cold-formed steel column research. Theoretical trends are also briefly mentioned, particularly as they relate to distortional buckling. Though distortional buckling in beams and columns is intimately tied together an attempt is made to focus only on the column research.

Summary

	Overall	**Distortional Buckling**
1940's and 1950's	• Elastic plate stability formalized • Experimental work begins • Effective width for ultimate strength	• Known phenomena • Too complicated to predict analytically
1960's	• Early design methods formalized • Cold-formed steel material properties • Prediction of overall (global) buckling	• Approximate analytical methods from Aluminum researchers • Folded plate theory for distortional buckling
1970's	• Local and overall interaction • Design methods for unstiffened and edge stiffened elements • Finite Elements	• Observed in experiments, but often intentionally restricted • Elastic buckling criteria not accurate for predicting failure mode
1980's	• Imperfections and residual stresses • Effective width formalized • Finite strip • Distortional buckling problems	• Hand methods for elastic prediction • Experiments with unrestricted distortional buckling performed • Postbuckling reserve discovered
1990 to Present	• Distortional buckling problems • Distortional buckling design • Interaction & column boundary conditions • Generalized Beam Theory	• Hand methods for elastic prediction • Interaction of distortional with other buckling modes examined • Design: column curve or effective width? • Heightened imperfection sensitivity? • Inclusion in Design Standards

The 1940's and 1950's

Cold-formed steel column research began in the 1940's with proprietary testing at Cornell University (Winter 1940, Winter 1943). Winter (1949) summarized the state of the art for the 1940's. Chilver (1951, 1953) and Harvey (1953) summarized the experimental and theoretical thin-walled column research in Britain. After fifty years of progress, modern column research is still similar to Chilver's work: elastic stability solutions for local plate buckling and "effective width" for the ultimate strength.

The elastic plate buckling solution was based on Lundquist and Stowell (1943) who extended the work of Timoshenko and Gere (1936) by providing practical methods for calculating the stability of connected plates. The "effective width" solution was based on von Kármán et al. (1932) and the experimental corrections of Winter (1947). Notably, both Chilver and Harvey properly included the interaction of elements in determining the local buckling stress. Also, for lipped channels Chilver stated that the reinforcing "lip" should be sufficiently stiff to insure local buckling (and thus avoid distortional buckling), but gave no criteria for achieving this.

The 1960's

At Cornell, cold-formed steel column research in the 1960's primarily ignored distortional buckling as work focused on material properties (Karren 1965, Karren and Winter 1967, Uribe and Winter 1969), and the behavior of long columns (Chajes et al. 1966, Peköz 1969). Karren showed significant variation in engineering properties around the cross-section; notable, since this fact is widely ignored in current research on distortional buckling. The experimental method used by Karren – compression testing of back to back connected specimens – would also later be used by Cornell researchers. At the same time researchers in Canada examined optimizing the geometry of cold-formed columns and edge stiffeners (Divakaran 1964, Venkataramaiah 1971).

Aluminum researchers in the 1960's investigated lipped channels and hats experimentally (Dwight 1963) and analytically (Sharp 1966). Sharp presented an early theoretical treatment of distortional buckling, or as he termed it "overall" buckling. Under simplifications about the rotational restraint at the web/flange juncture the distortional buckling stress of a lipped channel was approximated. Dwight's experiments were used for verification.

A folded plate method was developed at Purdue University (Goldberg, Bogdanoff and Glauz 1964) to predict the lateral and torsional buckling of thin-walled beams including sectional distortion. The method demonstrated distortional buckling of open sections under both compressive axial and bending load. At about the same time, an exact stiffness method was developed in the UK by Wittrick (1968a, 1968b) for studying the buckling of stiffened panels in compression. Although only stiffened panels, and not open section members, were investigated, distortional buckling modes (called torsional modes) were discovered.

The 1970's

Across the world, column research in the 1970's focused on the interaction between local and overall (i.e, global – flexural, torsional, flexural-torsional) buckling modes (DeWolf 1974, Klöppel and Bilstien 1976, Rhodes and Harvey 1977, Peköz 1977, Loughlan 1979). At Cornell, work also continued on unstiffened elements (Kalyanaraman et al. 1977) and on intermediate and edge stiffeners (Desmond 1977). In Germany isolated edge stiffeners were studied experimentally and analytically by physically replacing the web/flange juncture with a simple support, thus providing known boundary conditions (Kloppel and Unger 1970).

Desmond's (1977) work forms the basis for the modern AISI (1996) Specification on edge stiffened elements. In that work, the term "stiffener" buckling describes the distortional mode. For design purposes, Chilver stated that a "lip" should have sufficient stiffness to insure that local buckling occurs. Desmond recognized that elastic buckling criteria (i.e, ensuring that "stiffener" buckling is a higher critical stress than local buckling) does not meet Chilver's criteria. Using experimental data Desmond empirically formulated rules for an adequate "lip" stiffener. An adequate stiffener is not always economical and thus Desmond provided a single empirical solution for the buckling coefficient, *k*, of an edge stiffened element in either local or "stiffener" buckling. As a result, distortional buckling was incorporated into the AISI Specification as another local mode and was not treated as explicitly different from local plate buckling. Desmond's (and Kalyanaraman's) experimental studies, followed Karren, and thus the specimens were formed by connecting two members back to back. In the resulting specimen, the web thickness is twice that of the flange. The distortional buckling stress is artificially elevated due to higher than normal rotational stiffness at the web/flange juncture provided by the web.

In Sweden, Thomasson (1978) performed experiments on lipped channels with slender webs. In order to elevate the local buckling stress of the webs small groove stiffeners were folded in. This eliminated the local buckling problem, but created what Thomasson called a "local-torsional" problem – i.e, distortional buckling. This is a recurring theme for distortional buckling – optimization to remove a local mode creates a distortional problem. Thomasson considered this "local-torsional" mode undesirable and thus put closely spaced braces from lip to lip, insuring that distortional buckling did not occur and therefore making the local mode again dominant.

The 1980's

At Cornell research focused on imperfections and residual stresses (Dat 1980, Weng 1987), local buckling interaction (Mulligan 1983), beam-columns (Loh 1985), and the formalization of a unified effective width approach (Peköz 1987). Mulligan (1983) encountered distortional buckling in testing, and followed Thomasson's terminology thus calling the mode "local-torsional". Mulligan observed that Desmond's adequate moment of inertia criteria did not appear to restrain this local-torsional mode in many cases. However, in the end, Mulligan chose to provide braces in a manner similar to Thomasson and distortional buckling was restricted in order to study local buckling phenomena

In Europe, researchers such as Batista et al. (1987) continued to provide strong evidence for interaction of local and overall column buckling. At the University of Strathclyde research on local and overall interaction continued (Rhodes and Loughlan 1980, Zaras and Rhodes 1987) as well as studies on the behavior of isolated lip stiffened elements (Lim 1985, Lim and Rhodes 1986). Lim (1985) took the same experimental approach as Klöppel and Unger (1970). The "torsional" mode (distortional buckling) for these flanges may be accurately predicted due to the special boundary conditions.

In the 1980's some researchers began to focus on distortional buckling. This trend was most evident at the University of Sydney. The need to investigate the behavior of cold-formed steel storage racks lead to work on distortional buckling (Hancock 1985, Lau 1988). The optimized nature of storage rack columns insured that distortional buckling often dominated. Hancock extended and popularized Cheung's (1976) finite strip analysis as a tool for understanding the buckling modes in thin-walled members. The specific version of the finite strip method which

could account for both plate flexural buckling and membrane buckling in thin-walled members was developed by Plank and Wittrick (1974). Lau extended the finite strip buckling capabilities to the spline finite strip method (Cheung and Fan, 1983) to allow for fixed-ended boundary conditions, performed experiments in which distortional buckling was the failure mechanism (Lau and Hancock, 1990), and generated a hand method (Lau and Hancock, 1987) for predicting the elastic distortional buckling stress. The hand method used classical analytical techniques similar to Sharp (1966) but included web instability in the model which had not been considered by Sharp.

In Japan, several authors (Hikosaka, Takami and Maruyama, 1987, Takahashi 1988) published papers on the prediction of distortional buckling of thin-walled members with polygonal cross-section.

In the USA, Sridharan (1982) developed the finite strip method to study post-buckling in the distortional mode (called local-torsional) and demonstrated the rapid increase in membrane stress at the tips of edge-stiffening lips after distortional buckling. This indicated that the post-buckling reserve in the distortional mode may not be as great as the local mode since yielding would occur earlier in the post-buckling range.

1990 to Present

In Europe, column testing continued, Moldovan (1994). Eurocode 3 Part 1.3 (1996) provided a method for predicting the distortional buckling of simple lipped sections such as channels accounting for the restraint provided by the web and the flange to the lip buckling as a strut. This method accounted for the distortional deformations of the web and flange but used a column curve for the failure of the lip so that there was no post-buckling reserve in the distortional mode. Testing of HSS Channels was performed at the Technical Research Centre of Finland (Salmi and Talja, 1993) and the sections underwent distortional buckling in some cases. The results were compared with the Eurocode method including modifications to improve it.

At the University of Missouri-Rolla work on the effect of strain rate on columns was conducted (Kasser et al. 1992). At Cornell, further research on load eccentricity effects and web perforations were conducted (Miller and Peköz 1994). Research in Canada and at Texas-Austin examined Z section columns and provided further experimental evidence of distortional failures and problems in the AISI Specification (Polyzois and Sudharampal 1990, Purnadi et al. 1990, Polyzois and Charvarnichborikarn 1993).

University of Sydney research on distortional buckling continued in the 1990's (Kwon 1992, Kwon and Hancock 1992, Hancock et al. 1994). Kwon conducted experiments on lipped channels with and without groove stiffeners in the web. The distortional mode was unrestricted and the tests showed that interaction of distortional buckling with other modes is weak. Distortional buckling was experimentally observed to have lower post-buckling capacity than local buckling. The results were summarized and new column strength curves suggested for distortional failures in Hancock et al. (1994). Research also continued on local and overall column buckling interaction. Rasmussen and Hancock (1991) showed the importance of different end fixity on the post-buckling behavior. Young (1997) experimentally demonstrated that fixed ended columns do not suffer the same interaction problems as pin ended columns. Young also observed that the interaction of distortional buckling with other modes is weak.

The University of Strathclyde conducted studies directly related to "torsional" buckling, i.e., distortional buckling (Seah 1989, Seah et al. 1991, Seah and Rhodes 1993). Seah investigated hats and channels with compound lips. Seah developed hand methods for the prediction of distortional buckling similar to Lau's and Sharp's treatments. For ultimate strength Seah and Rhodes's treated the distortional mode in a manner similar to local buckling. Thus, they proposed an effective width approach rather than the column curve approach proposed by Sydney researchers. In addition, Chou, Seah and Rhodes (1996) summarized the state of the art prediction abilities of cold-formed steel design specifications. Limitations and discrepancies were found in all major design specifications.

In the 1990's Generalized Beam Theory (GBT) (theory: Schardt 1989, Davies et al. 1994) has become a useful tool to study distortional buckling of columns (applications: Schardt 1994, Davies and Jiang 1996). Using GBT, Davies and Jiang argued that distortional buckling has weak interactions with other modes. GBT is currently only applicable in elastic problems, but Davies and Jiang endorsed the column strength curves of Hancock et al. (1994) for ultimate strength prediction.

Using finite strip and finite element analysis Schafer (1997) demonstrated that the distortional mode has greater imperfection sensitivity than local modes. Schafer also observed that distortional failures have lower post-buckling strength than local failures. New hand methods for predicting distortional buckling that are a hybrid of the finite strip method and the classic hand methods used by Sharp (1966) are presented and verified. Schafer (1998) explicitly showed that the AISI Specification equations (via Desmond) over-predict the distortional buckling stress, particularly as the ratio of the web height to flange width becomes large.

The Australian Standard for Steel Storage Racking (1993) and the Australian/New Zealand Standard for Cold-Formed Steel Structures (1996) were developed to contain explicit design rules for distortional buckling in compression.

Batista, E., Rondal, J., Maquoi, R. (1987). "Column Stability of Cold-Formed U and C Sections". *Proc. of the Int'l Conf. on Steel and Aluminum Structures*. Cardiff, U.K.

Chajes, A., Fang, J., Winter, G. (1966). "Torsional Flexural Buckling, Elastic and Inelastic, of Cold Formed Thin Walled Columns". *Cornell Engineering Research Bulletin*, 66(1).

Cheung, Y.K. (1976). *Finite Strip Method in Structural Analysis*. Pergamon Press, New York.

Cheung,Y.K. and Fan, S.C. (1983),"Static Analysis of Right Box Girder Bridges by the Spline Finite Strip Method",*Proc Inst Civ Engrs*, Part 2, 75, June, pp 311 – 323.

Chilver, A.H. (1951). "The Behavior of Thin-Walled Structural Members in Compression". *Engineering*, pp. 281-282.

Chilver, A.H. (1953). "The Stability and Strength of Thin-Walled Steel Struts". *The Engineer*, pp. 180-183.

Chou, S.W., Seah, L.K., Rhodes, J. (1996). "Accuracy of Some Codes of Practice in Predicting the Load Capacity of Cold-Formed Columns". *J. of Constructional Steel Research*, Elsevier, 37(2), pp. 137-172.

Comite Europeen de Normalisation (1996),"Eurocode 3: Design of Steel Structures, Part 1.3: General Rules",*European Prestandard ENV 1993-1-3*.

Dat, D.T. (1980). The Strength of Cold-Formed Steel Columns. Ph.D. Thesis. Cornell University. Ithaca, New York.

Davies, J.M., Jiang, C. (1996). "Design of Thin-Walled Columns for Distortional Buckling". *Proc. of the 2nd Int'l Conf. on Coupled Instabilities in Metal Structures*, Imperial College Press, Liege, Belgium.

Davies, J.M., Leach, P., Heinz, D. (1994). "Second-Order Generalised Beam Theory". *J. of Constructional Steel Research*, Elsevier, 31(2-3), pp. 221-242.

Desmond, T.P. (1977). The Behavior and Strength of Thin-Walled Compression Elements with Longitudinal Stiffeners. Ph.D. Thesis. Cornell University. Ithaca, New York.

Dewolf, J.T., Peköz, T., Winter, G. (1974). "Local and Overall Buckling of Cold-Formed Members". *J. of the Structural Div.*, ASCE, 100(ST10), pp. 2017-2036.

Divakaran, S. (1964). The Influence of Shape on the Strength of open Thin-Walled Columns. M.S. Thesis. McMaster University. Hamilton, Ontario, Canada.

Dwight, J.B. (1963). "Aluminum Sections with Lipped Flanges and Their Resistance to Local Buckling". *Proc., Symposium on Aluminum in Structural Eng.,* London, England.

Goldberg, J.E., Bogdanoff, J.L. and Glauz, W.D., "Lateral and Torsional Buckling of Thin-Walled Beams",*Proceedings*, IABSE, Vol. 24, 1964, pp 91 –100.

Hancock, G.J. (1985). "Distortional Buckling of Steel Storage Rack Columns". *J. of Structural Eng.*, ASCE, 111(12), pp. 2770-2783

Hancock, G.J., Kwon, Y.B., Bernard, E.S. (1994). "Strength Design Curves for Thin-Walled Sections Undergoing Distortional Buckling". *J. of Constructional Steel Research*, Elsevier, 31(2-3), pp. 169-186.

Harvey, J.M. (1953). "Structural Strength of Thin-Walled Channel Sections". *Engineering*, pp. 291-293.

Hikosaka,H.,Takami,K. and Maruyama,Y. (1987),"Analysis of Elastic Distortional Instability of Thin-Walled Members with Open Polygonal Cross Section", *Proceedings of Japan Society of Civil Engineers*, Structural Eng./Earthquake Eng., Vol. 4, No. 1, April, pp 31 – 40.

Kalyanaraman, V., Peköz, T., Winter, G. (1977). "Unstiffened Compression Elements". *J. of the Structural Div.*, ASCE, 103(ST9), pp. 1833-1848

Karren, K.W. (1965). Effects of Cold-Forming on Light-Gage Steel Members. Ph.D. Thesis, Cornell University. Ithaca, New York.

Karren, K.W., Winter, G. (1967). "Effects of Cold-Forming on Light-Gage Steel Members". *J. of the Structural Div.*, ASCE, 93(ST1), pp. 433-469.

Kassar, M., Pan, C.L., Yu, W.W. (1992). "Effect of Strain Rate on Cold-Formed Steel Stub Columns". *J. of Structural Eng.*, ASCE, 118(11), pp. 3151-3168.

Klöppel, K. Bilstein, W. (1976). "Untersuchungen zur linearn und nichtlinearen Beultheorie mit Beulwerttafeln fur dunnwandige U, C und Hut-Profile und Tafeln fur mitwirkende Breiten und Tragspannungen von dreiseitig und vierseitig gelenkig gelagerten Reckteckplatten nach der nichtlinearen Beultheorie". *Stahlbau*, 45(2), pp. 33-38.

Klöppel, K., Unger, B. (1970). "Das Ausbeulen einer am freien Rand verstuiften, dreiseitig momentenfrei gelagerten Platte unter Verwendung der nichtlinearen Beultheorie, Teill II: Experimentelle Untersuchungen, Bergleich der experimentellen mit den theoretischen Ergebnissen". *Der Stahlabu*, 39, pp. 115-123

Kwon, Y.B. (1992). Post-Buckling Behaviour of Thin-Walled Channel Sections. Ph.D. Thesis. University of Sydney. Sydney, Australia.

Kwon, Y.B., and Hancock, G.J., "Strength Tests of Cold-Formed Channel Sections undergoing Local and Distortional Buckling",*Jour Struct Engg*, ASCE, 117(2),, pp 1786 – 1803.

Lau, S.C.W. (1988). Distortional Buckling of Thin-Walled Columns. Ph.D. Thesis, University of Sydney. Sydney, Australia.

Lau, S.C.W., and Hancock, G.J (1987).,"Distortional Buckling Formulas for Channel Columns", *Journal of Structural Engineering,*ASCE,1987, 113(5), pp 1063 – 1078.
Lau, S.C.W. and Hancock, G.J (1990).,"Inelastic Buckling of Channel Columns in the Distortional Mode", *Thin-Walled Structures,* 10(1), pp 59-84.
Lim, B.S. (1985). Buckling behaviour of asymmetric edge stiffened plates. Ph.D. Thesis, University of Strathclyde, Glasgow.
Lim, B.S., Rhodes, J. (1986). "Buckling Behaviour of Asymmetric Edge Stiffened Plates". *Applied Solid Mechanics,* Elsevier, 1, pp. 351-375.
Loh, T.S. (1985). Combined Axial Load and Bending in Cold-Formed Steel Members. Ph.D. Thesis, Cornell University. Ithaca, New York.
Loughlan, J. (1979). Mode Interaction in Lipped Channel Columns under Concentric or Eccentric Loading. Ph.D. Thesis. University of Strathclyde, Glasgow.
Lundquist, E.E., Stowel, E.Z. (1943). "Principles of Moment Distribution Applied to the Stability of Structures Composed of Bars or Plates". *NACA*, L-326.
Miller, T.H., Peköz, T. (1994). "Load-Eccentricity Effects on Cold-Formed Steel Lipped-Channel Columns." *J. of Struct. Eng.*, ASCE, 120(3), pp. 805-823.
Moldovan, A. (1994). "Compression Tests on Cold-Formed Steel Columns with Monosymmetrical Section". *Thin-Walled Structures*, Elsevier, 20(1-4), pp. 241-252.
Mulligan, G.P. (1983). The Influence of Local Buckling on the Structural Behavior of Singly-Symmetric Cold-Formed Steel Columns. Ph.D. Thesis. Cornell University. Ithaca, New York.
Peköz, T. (1969). "Torsional Flexural Buckling of Thin-Walled Section Under Eccentric Load". *Cornell Engineering Research Bulletin,* 69(1).
Peköz, T. (1977). "Post-Buckling Interaction of Plate Elements: Progress Report to Swedish Building Research Council". *Dept. of Structural Eng.*, Cornell University. Ithaca, New York.
Peköz, T. (1987). *Development of a Unified Approach to the Design of Cold-Formed Steel Members*. American Iron and Steel Institute Research Report, CF 87-1.
Plank, R.J. and Wittrick (1974), W.H.,"Buckling under Combined Loading of Thin, Flat-Walled Structures by a Complex Finite Strip Method, *Int Jour Num Meth in Engg,* Vol 8, pp 323 – 339.
Polyzois, D., Charnvarnichborikarn, P. (1993). "Web-Flange Interaction in Cold-Formed Steel Z-Section Columns". *J. of Struct. Eng.* ASCE, 119(9), pp. 2607-2628.
Polyzois, D., Sudharmapal, A.R. (1990). "Cold-Formed Steel Z-Sections with Sloping Edge Stiffness under Axial Load". *J. of Struct. Eng.*, ASCE, 116(2), pp. 392-406
Purnadi, R.W., Tassoulas, J.L., Polyzois, D. (1990). "Study of Cold-Formed Z-section Steel Member under Axial Loading". *10th Int'l. Spec. Conf. on Cold-Formed Steel Structures*. University of Missouri-Rolla, St. Louis, Missouri.
Rasmussen, K.J.R., Hancock, G.J. (1991). "The Flexural Behavior of Thin-Walled Singly Symmetric Columns". *Int'l Conf. on Steel and Aluminum Structures*. Singapore.
Rhodes, J., Harvey, J.M. (1977). "Interaction Behaviour of Plain Channel Columns under Concentric or Eccentric Loading". *Proc. of the 2nd Int'l. Colloquim on the Stability of Steel Structures.* ECCS, Liege, pp. 439-444.
Rhodes, J., Loughlan, J. (1980). "Simple Design Analysis of Lipped Channel Columns". *5th Int'l. Spec. Conf. on Cold-Formed Steel Structures*. University of Missouri-Rolla, St. Louis, Missouri.
Salmi, P. and Talja, A. (1993), "Design of Cold-Formed HSS Channels for Bending and Eccentric Compression",*VTT Research Notes,* 1505, Technical Research Centre of Finland, Espoo.

Schafer, B.W. (1997). Cold-Formed Steel Behavior and Design: Analytical and Numerical Modeling of Elements and Members with Longitudinal Stiffeners. Ph.D. Thesis. Cornell University. Ithaca, New York.
Schafer, B.W. (1998). "A Correction to AISI Specification B2.3 and B4.2 in order to partially alleviate the unconservative prediction of members with edge stiffened elements." Commentary on Ballot S98-90A, *American Iron and Steel Institute*. (Unpublished).
Schardt, R. (1989). *Verallgemeinerte Technische Biegetheorie*. Springer-Verlag, Germany.
Schardt, R. (1994). "Generalized Beam Theory – An Adequate Method for Coupled Stability Problems". *Thin-Walled Structures*, Elsevier, 19(2-4), pp. 161-180
Seah, L.K. (1989). Buckling behaviour of edge stiffeners in thin-walled sections. Ph.D. Thesis. University of Strathclyde, Glasgow.
Seah, L.K., Rhodes, J. (1993). "Simplified Buckling Analysis of Plate with Compound Edge Stiffners". *J. of Eng. Mech.*, ASCE, 119(1), pp. 19-38.
Seah, L.K., Rhodes, J., Lim, B.S., (1993). "Influence of Lips on Thin-Walled Sections". *Thin-Walled Structures*. Elsevier, 16(1-4), pp. 145-178.
Sharp, M.L., (1966). "Longitudinal Stiffeners for Compression Members". *J. of the Structural Div.*, ASCE, 92(ST5), pp. 187-211.
Sridharan, S. (1982),A Semi-Analytical Method for the Post-Local-Torsional Buckling Analysis of Prismatic Plate Structures",*Int Jour Num Meth in Engg*, Vol 18, pp 1685 – 1697.
Standards Australia (1993), "Steel Storage Racking", AS4084.
Standards Australia/Standards New Zealand (1996),"Cold-Formed Steel Structures",AS/NZS 4600.
Takahashi, K. (1988),"A New Buckling Mode of Thin-Walled Columns with Cross-Sectional Distortions", *Solid Mechanics*, - 2 (eds Tooth, A.S. and Spencer, J.), 25, Elsevier, pp 553 – 573.
Thomasson, P. (1978). "Thin-walled C-shaped Panels in Axial Compression". *Swedish Council for Building Research.* D1:1978, Stockholm, Sweden.
Timoshenko, S.P., Gere, J.M. (1936). *Theory of Elastic Stability*. McGraw-Hill.
Uribe, J., Winter, G. (1969). "Cold-Forming Effects in Thin-Walled Steel Members". *Dept. of Struct. Eng.*, Cornell University.
Venkataramaiah, K.R. (1971). "Optimum Edge Stiffeners for Thin-Walled Structural Elements with Edge Stiffeners". *Solid Mechanics Report*, 7, University of Waterloo, Ontario, Canada.
von Kármán, T., Sechler, E.E., Donnell, L.H. (1932). "The Strength of Thin Plates In Compression". *Transactions of the ASME*, 54, pp. 53-57.
Weng, C. (1987). Flexural Buckling of Cold-Formed Steel Columns. Ph.D. Thesis. Cornell University. Ithaca, New York.
Winter, G. (1940). "Tests on Light Studs of Cold-Formed Steel". Third Progress Report. Cornell University. (Unpublished).
Winter, G. (1943). "Tests on Light Studs of Cold-Formed Steel". Second Summary Report. Cornell University. (Unpublished).
Winter, G. (1947) "Strength of Thin Steel Compression Flanges." *Transactions of ASCE*, Paper No. 2305, Trans., 112, 1.
Winter, G. (1949) "Performance of Compression Plates as Parts of Structural Members". Research, Engineering Structures Supplement, *Colston Papers*, vol. II, p. 179, London.
Wittrick, WH (1968a), "General Sinusoidal Stiffness Matrices for Buckling and Vibration Analyses of Thin Flat-Walled Structures",*Int. J.Mech Sci*,Vol 10, pp 949 – 966.
Wittrick, WH (1968b), "A Unified Approach to the Initial Buckling of Stiffened Panels in Compression",*The Aeronautical Quarterly*, August 1968, pp 265 – 283.

Young, B. (1997). The Behaviour and Design of Cold-Formed Channel Columns. Ph.D. Thesis. University of Sydney. Sydney, Australia.
Zaras, J., Rhodes, J. (1988). “Carefully Controlled Compression Tests on Thin-Walled Cold-Formed Sections”. *Applied Solid Mechanics*, Elsevier, 2, pp. 519-551.

B Example: Hand Calculation of Local and Distortional Buckling

C Detailed Elastic Buckling Results

D Example: Design Examples for Considered Methods

E Detailed Ultimate Strength Results

F Recommended Specification Changes

F.1 New commentary language recommended for immediate adoption

F.2 New Effective Width Procedures recommended for interim adoption

F.3 Direct Strength method recommended for interim adoption as an alternative procedure and long-term adoption as design method

Example hand calculations for local and distortional buckling stress of a simple lipped channel column.

Calculations for:

1. Flange Local Buckling (k=4 solution)
2. Web Local Buckling (k=4 solution)
3. Lip Local Buckling (k=0.43 solution)
4. Flange/Lip Local Buckling (Schafer 1997)
5. Flange/Web Local Buckling (Schafer -unpublished)
6. Distortional buckling (Schafer 1997*)
7. Distortional buckling (Lau and Hancock 1987**)
8. AISI edge stiffened element via AISI (1996)

*with corrections, given below, July 1998.
** with corrections given below, January 1999

Specimen Dimensions and Properties:

$h := 2.5$

$b := 1.328$

$d := 0.328$

$\theta := 90 \cdot \frac{\pi}{180}$

$t := 0.0284$

$E := 29500$

$\nu := 0.3$

$f := 50$

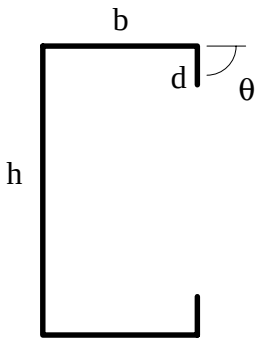

Glossary of Variables:
h = web height
b = flange width
d = lip length
θ = lip angle (radians)
t = thickness
E = Young's modulus
ν = Poisson's ratio
f = compressive stress (necessary for AISI only)

Local Buckling Element Models: Each element is treated separately

1. Flange Local Buckling:

Classical solution for a simply supported plate in pure compression is employed.

$k_{flange} := 4$

$$f_{cr\_flange} := k_{flange} \cdot \frac{\pi^2 \cdot E}{12 \cdot \left(1 - \nu^2\right)} \cdot \left(\frac{t}{b}\right)^2 \qquad f_{cr\_flange} = 48.775$$

2. Web Local Buckling:

Classical solution for a simply supported plate in pure compression is employed.

$k_{web} := 4$

$$f_{cr\_web} := k_{web} \cdot \frac{\pi^2 \cdot E}{12 \cdot \left(1 - \nu^2\right)} \cdot \left(\frac{t}{h}\right)^2 \qquad f_{cr\_web} = 13.763$$

3. Lip Local Buckling:

Classical solution for a plate simply supported on three sides and free along one edge is employed.

$k_{lip} := 0.43$

$$f_{cr\_lip} := k_{lip} \cdot \frac{\pi^2 \cdot E}{12 \cdot \left(1 - \nu^2\right)} \cdot \left(\frac{t}{d}\right)^2 \qquad f_{cr\_lip} = 85.952$$

Note, the local buckling stress of the member can conservatively be predicted by taking the minimum of 1, 2 and 3. In some cases, this calculation will be very conservative since it completely ignores any interaction of the elements.

Local Buckling Interaction Models

4. Flange / Lip Local Buckling

This expression for k, was derived in Schafer (1997). The expression is based on an empirical curve fit to finite strip analysis of an isolated flange and lip. The expression accounts for the beneficial affect of the lip on the flange at intermediate lip lengths and also accounts for the detrimental affect of the lip on the flange at long lip lengths.

$$k_{flange\_lip} := -11.07\cdot\left(\frac{d}{b}\right)^2 + 3.95\cdot\left(\frac{d}{b}\right) + 4 \qquad k_{flange\_lip} = 4.3$$

Note, d/b should be less than 0.6 for this empirical expression. A more general expression for cases when the unstiffened element is under a stress gradient and the edge stiffened element is in pur compression (i.e. the flange of a flexural member) can be found in Schafer (1997).

$$f_{cr\_flange\_lip} := k_{flange\_lip}\cdot\frac{\pi^2\cdot E}{12\cdot\left(1-\nu^2\right)}\cdot\left(\frac{t}{b}\right)^2 \qquad f_{cr\_flange\_lip} = 52.437$$

5. Flange / Web Local Buckling

This expression is newly derived for this work. The expression is based on an empirical curve fit to finite strip analysis of an isolated flange and web. If h/b = 1 The k value is 4. If h/b > 1 the k value is reduced from 4 due to the buckling of the web. If h/b < 1 the k value is increased from 4 due to the restraint provided by the web to the flange.

$$k_{flange\_web} := \begin{cases} \left[\left[2-\left(\frac{b}{h}\right)^{0.4}\right]\cdot 4\cdot\left(\frac{b}{h}\right)^2\right] & \text{if } \frac{h}{b}\geq 1 \\ \left[\left[2-\left(\frac{h}{b}\right)^{0.2}\right]\cdot 4\right] & \text{if } \frac{h}{b}<1 \end{cases} \qquad k_{flange\_web} = 1.381$$

$$f_{cr\_flange\_web} := k_{flange\_web}\cdot\frac{\pi^2\cdot E}{12\cdot\left(1-\nu^2\right)}\cdot\left(\frac{t}{b}\right)^2 \qquad f_{cr\_flange\_web} = 16.84$$

Note, the local buckling stress of the member can be taken as the minimum of 4 and 5. This provides a good estimate of the actual member local buckling stress.

6 and 7: Flange Properties for use in the Distortional Buckling Calculation

The hand methods for distortional buckling prediction require that section properties of the isolated flange be calculated. The expressions here are only applicable for simple lips. More complicated flanges would follow the same procedures, but new expressions would be required

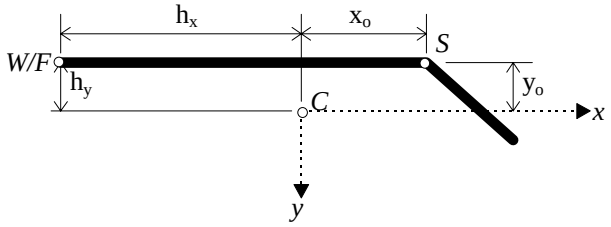

Material Properties:

$$G := \frac{E}{2\cdot(1+\nu)}$$

Properties of the Flange Only:

$$A := (b+d)\cdot t \qquad A = 0.047$$

$$J := \frac{1}{3}\cdot b\cdot t^3 + \frac{1}{3}\cdot d\cdot t^3 \qquad J = 1.264\cdot 10^{-5}$$

$$I_x := \frac{t\cdot\left(t^2\cdot b^2 + 4\cdot b\cdot d^3 - 4\cdot b\cdot d^3\cdot\cos(\theta)^2 + t^2\cdot b\cdot d + d^4 - d^4\cdot\cos(\theta)^2\right)}{12\cdot(b+d)} \qquad I_x = 2.87\cdot 10^{-4}$$

$$I_y := \frac{t\cdot\left(b^4 + 4\cdot d\cdot b^3 + 6\cdot d^2\cdot b^2\cdot\cos(\theta) + 4\cdot d^3\cdot b\cdot\cos(\theta)^2 + d^4\cdot\cos(\theta)^2\right)}{12\cdot(b+d)} \qquad I_y = 8.836\cdot 10^{-3}$$

$$I_{xy} := \frac{t\cdot b\cdot d^2\cdot\sin(\theta)\cdot(b + d\cdot\cos(\theta))}{4\cdot(b+d)} \qquad I_{xy} = 8.135\cdot 10^{-4}$$

$$I_o := \frac{t\cdot b^3}{3} + \frac{b\cdot t^3}{12} + \frac{t\cdot d^3}{3} \qquad I_o = 0.023$$

$$x_o := \frac{b^2 - d^2\cdot\cos(\theta)}{2\cdot(b+d)}$$ x distance from the centroid to the shear center. $x_o = 0.532$

$$y_o := \frac{-d^2\cdot\sin(\theta)}{2\cdot(b+d)}$$ y distance from the centroid to the shear center. $y_o = -0.032$

$$h_x := \frac{-\left(b^2 + 2\cdot d\cdot b + d^2\cdot\cos(\theta)\right)}{2\,(b+d)}$$ x distance from the centroid to the web/flange juncture. $h_x = -0.796$

$$h_y := \frac{-d^2\cdot\sin(\theta)}{2\cdot(b+d)}$$ y distance from the centroid to the web/flange juncture. $h_y = -0.032$

$$C_w := 0 \qquad C_w = 0$$

6. Distortional Buckling (Schafer 1997)

Determine the critical half-wavelength at which distortional buckling occurs:

$$L_{cr} := \left[\frac{6 \cdot \pi^4 \cdot h \cdot \left(1 - \nu^2\right)}{t^3} \cdot \left[I_x \cdot \left(x_o - h_x\right)^2 + C_w - \frac{I_{xy}^2}{I_y} \cdot \left(x_o - h_x\right)^2 \right] \right]^{\frac{1}{4}} \qquad L_{cr} = 12.139$$

If bracing is provided that restricts the distortional mode at some length less than Lcr, then this length should be used in place of Lcr.

Determine the elastic and "geometric" rotational spring stiffness of the flange:

$$k_{\phi fe} := \left(\frac{\pi}{L_{cr}}\right)^4 \cdot \left[E \cdot I_x \cdot \left(x_o - h_x\right)^2 + E \cdot C_w - E \cdot \frac{I_{xy}^2}{I_y} \cdot \left(x_o - h_x\right)^2 \right] + \left(\frac{\pi}{L_{cr}}\right)^2 \cdot G \cdot J$$

$k_{\phi fe} = 0.059$

$$k_{\phi fg} := \left(\frac{\pi}{L_{cr}}\right)^2 \cdot \left[A \cdot \left[\left(x_o - h_x\right)^2 \cdot \left(\frac{I_{xy}}{I_y}\right)^2 - 2 \cdot y_o \cdot \left(x_o - h_x\right) \cdot \left(\frac{I_{xy}}{I_y}\right) + h_x^2 + y_o^2 \right] + I_x + I_y \right]$$

$k_{\phi fg} = 2.68 \cdot 10^{-3}$

Determine the elastic and "geometric" rotational spring stiffness from the web:

$$k_{\phi we} := \frac{E \cdot t^3}{6 \cdot h \cdot \left(1 - \nu^2\right)} \qquad k_{\phi we} = 0.05$$

$$k_{\phi wg} := \left(\frac{\pi}{L_{cr}}\right)^2 \cdot \frac{t \cdot h^3}{60} \qquad k_{\phi wg} = 4.954 \cdot 10^{-4}$$

kϕwg is modified due to an error in Schafer (1997) analysis.

Determine the distortional buckling stress:

$$f_{cr\_dist\_schafer} := \frac{k_{\phi fe} + k_{\phi we}}{k_{\phi fg} + k_{\phi wg}}$$

$f_{cr\_dist\_schafer} = 34.205$

7. Lau and Hancock (1987) Formulation

The notation for Lau and Hancock (1987) is slightly different than in the previous approach. The original notation is employed to aid comparisions to Lau and Hancock (1987).

$x_{bar} := b - x_o \qquad x_{bar} = 0.796 \qquad y_{bar} := -y_o \qquad y_{bar} = 0.032$

The critical half-wavelength for distortional buckling λd is first estimated

$$\lambda_d := 4.80 \cdot \left(\frac{I_x \cdot b^2 \cdot h}{t^3} \right)^{\frac{1}{4}} \qquad \lambda_d = 13.086$$

The next step is to estimate the distortional buckling stress. This estimate is required, because the rotational stiffness is written as a function of the distortional buckling stress. This step requires formulation and solution of a quadratic equation.

Parameters required for the solution:

$$\eta := \left(\frac{\pi}{\lambda_d} \right)^2 \qquad \beta_1 := x_{bar}^2 + \left(\frac{I_x + I_y}{A} \right) \qquad \beta_1 = 0.827$$

$$\alpha_1 := \frac{\eta}{\beta_1} \cdot \left(I_x \cdot b^2 + 0.039 \cdot J \cdot \lambda_d^2 \right) \quad \alpha_2 := \eta \cdot \left(I_y + \frac{2}{\beta_1} \cdot y_{bar} \cdot b \cdot I_{xy} \right) \quad \alpha_3 := \eta \cdot \left(\alpha_1 \cdot I_y - \frac{\eta}{\beta_1} \cdot I_{xy}^2 \cdot b^2 \right)$$

$\alpha_1 = 4.117 \cdot 10^{-5} \qquad \alpha_2 = 5.142 \cdot 10^{-4} \qquad \alpha_3 = 1.628 \cdot 10^{-8}$

The solution to the quadratic has two roots, which are found as:

$$root_{pos}(E, A, \alpha_1, \alpha_2, \alpha_3) := \frac{E}{2 \cdot A} \cdot \left[(\alpha_1 + \alpha_2) + \left[(\alpha_1 + \alpha_2)^2 - 4 \cdot \alpha_3 \right]^{\frac{1}{2}} \right]$$

$$root_{neg}(E, A, \alpha_1, \alpha_2, \alpha_3) := \frac{E}{2 \cdot A} \cdot \left[(\alpha_1 + \alpha_2) - \left[(\alpha_1 + \alpha_2)^2 - 4 \cdot \alpha_3 \right]^{\frac{1}{2}} \right]$$

The smaller of the two roots is of interest. In this case $root_{neg}$ is used.
In cases where the root is negative the distortional buckling stress is set to zero.

note:

$root_{pos}(E, A, \alpha_1, \alpha_2, \alpha_3) = 328.887$

$root_{neg}(E, A, \alpha_1, \alpha_2, \alpha_3) = 19.472$

$f'_{ed} := \max\left(\left[root_{neg}(E, A, \alpha_1, \alpha_2, \alpha_3) \quad 0 \right] \right) \qquad f'_{ed} = 19.472$

(estimated dist. stress, used to estimate kϕ)

Now that the distortional buckling stress has been estimated, the rotational stiffness may be determined:

$$k_\phi := \frac{E \cdot t^3}{5.46 \cdot \left(h + 0.06 \cdot \lambda_d\right)} \cdot \left[1 - \frac{1.11 \cdot f'_{ed}}{E \cdot t^2} \cdot \left(\frac{h^2 \cdot \lambda_d}{h^2 + \lambda_d^2}\right)^2\right]$$

$$k_\phi = 0.03$$

This rotational stiffness is roughly equivalent to the web elastic + web geometric stiffness mentioned in Schafer (1997). If the geometric stiffness of the web is greater than the elastic stiffness of the web, a negative $k\phi$ will result. This does not necessarily imply buckling ensues, because the elastic stiffness of the flange may be great enough to overcome the web contribution.

The original Lau and Hancock (1987) model for columns was updated in Hancock et al. (1996) for beams. The update treats the $k\phi<0$ and the $k\phi>0$ as two different cases. The older model for columns is employed here.

Calculation of the buckling stress:

$$f_{ed} := \left|\begin{array}{l} \alpha_1 \leftarrow \frac{\eta}{\beta_1} \cdot \left(I_x \cdot b^2 + 0.039 \cdot J \cdot \lambda_d^2\right) + \frac{k_\phi}{\beta_1 \cdot \eta \cdot E} \\ \alpha_3 \leftarrow \eta \cdot \left(\alpha_1 \cdot I_y - \frac{\eta}{\beta_1} \cdot I_{xy}^2 \cdot b^2\right) \\ root1 \leftarrow root_{pos}\left(E, A, \alpha_1, \alpha_2, \alpha_3\right) \\ root2 \leftarrow root_{neg}\left(E, A, \alpha_1, \alpha_2, \alpha_3\right) \\ \max((root2 \quad 0)) \end{array}\right.$$

Note that in cases where the negative root is less than zero the distortional buckling stress is set to zero. This is consistent with the approach of Lau and hancock (1987) as employed in the joint Australian/New Zealand standard.

The final result is:

$$f_{cr\_dist\_hancock} := f_{ed}$$

$$f_{cr\_dist\_hancock} = 32.607$$

8. AISI (1996) Calculation for an edge stiffened element

Preliminaries: $S := 1.28 \cdot \sqrt{\frac{E}{f}}$ $I_s := \frac{t \cdot d^3 \cdot \sin(\theta)^2}{12}$

$k_{aisi} :=$ 4 if $\frac{b}{t} \le \frac{S}{3}$

if $\frac{S}{3} < \frac{b}{t} \le S$

$k_u \leftarrow 0.43$

$I_a \leftarrow t^4 \cdot 399 \cdot \left[\frac{\frac{b}{t}}{S} - \left(\frac{k_u}{4}\right)^{\frac{1}{2}}\right]^3$

$n \leftarrow \frac{1}{2}$

$C2 \leftarrow \min\left(\left[\frac{I_s}{I_a} \quad 1\right]\right)$

$C1 \leftarrow 2 - C2$

$k_a \leftarrow \min\left(\left[5.25 - 5 \cdot \frac{d}{b} \quad 4\right]\right)$

$C2^n \cdot (k_a - k_u) + k_u$

if $\frac{b}{t} \ge S$

$k_u \leftarrow 0.43$

$I_a \leftarrow t^4 \cdot \left(115 \cdot \frac{\frac{b}{t}}{S} + 5\right)$

$n \leftarrow \frac{1}{3}$

$C2 \leftarrow \min\left(\left[\frac{I_s}{I_a} \quad 1\right]\right)$

$C1 \leftarrow 2 - C2$

$k_a \leftarrow \min\left(\left[5.25 - 5 \cdot \frac{d}{b} \quad 4\right]\right)$

$C2^n \cdot (k_a - k_u) + k_u$

The AISI calculation for k is based on the slenderness of the flange. Different solutions for k are found depending on how slender the compression flange is. For instance, in case 1, k = 4 because the flange is stocky enough that all edge stiffeners are expected to be adequate.

This is the only k calculated for the flange and thus it accounts for both local and distortional buckling of the flange.

The final result is:

$k_{aisi} = 3.632$

$f_{cr\_aisi} := k_{aisi} \cdot \frac{\pi^2 \cdot E}{12 \cdot (1 - \nu^2)} \cdot \left(\frac{t}{b}\right)^2$

$f_{cr\_aisi} = 44.285$

Summary Results finite strip values are for a 2.5x1.328x0.328x0.0284 lipped C

$f_{cr\_strip\_local} := 18.96$

$f_{cr\_strip\_distortional} := 32.64$

$f_{cr\_flange} = 48.775$

$f_{cr\_web} = 13.763$

$f_{cr\_lip} = 85.952$

$f_{cr\_flange\_lip} = 52.437$

$f_{cr\_flange\_web} = 16.84$

$f_{cr\_dist\_schafer} = 34.205$

$f_{cr\_dist\_hancock} = 32.607$

$f_{cr\_aisi} = 44.285$

This is the order of the plotted values:

$$f_{cr\_all} := \begin{bmatrix} f_{cr\_flange} \\ f_{cr\_web} \\ f_{cr\_lip} \\ f_{cr\_flange\_lip} \\ f_{cr\_flange\_web} \\ f_{cr\_dist\_schafer} \\ f_{cr\_dist\_hancock} \\ f_{cr\_aisi} \\ f_{cr\_strip\_local} \\ f_{cr\_strip\_distortional} \end{bmatrix}$$

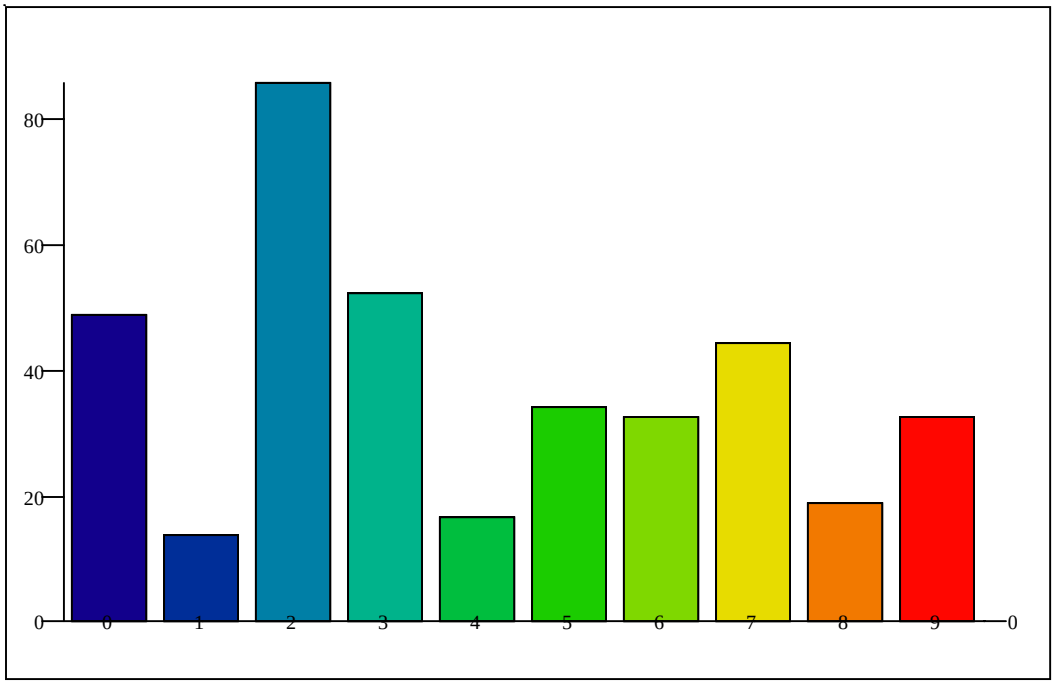

$f_{cr\_all}^{T}$

Basic Data from original source		Centerline Dimensions in mm					Nondimensional Param.				fy	Finite Strip Analysis Results (mm -- MPa)				Hand Calculations (MPa):						dist.	dist.
Group	Member	θ	h	b	d	t	h/t	b/t	d/t	h/b	(MPa)	Llocal	fcrlocal	Ldist	fcrdist	flange	web	lip	flange/lip	flange/web	AISI	Schafer	Hancock
Schafer (1997) Members	C1	90	30	30	2.50	1.00	30	30	3	1	345.00			100	245	815	815	12623	867	815	169	283	269
Schafer (1997) Members	C2	90	30	30	5.00	1.00	30	30	5	1	345.00	30	819	150	398	815	815	3156	887	815	318	444	402
Schafer (1997) Members	C3	45	30	30	2.50	1.00	30	30	3	1	345.00			90	206	815	815	12623	867	815	145	243	233
Schafer (1997) Members	C4	45	30	30	5.00	1.00	30	30	5	1	345.00			150	292	815	815	3156	887	815	251	327	302
Schafer (1997) Members	C5	90	60	30	2.50	1.00	60	30	3	2	345.00			100	186	815	204	12623	867	253	169	174	188
Schafer (1997) Members	C6	90	60	30	5.00	1.00	60	30	5	2	345.00	50	274	200	278	815	204	3156	887	253	318	272	279
Schafer (1997) Members	C7	45	60	30	2.50	1.00	60	30	3	2	345.00			100	160	815	204	12623	867	253	145	152	166
Schafer (1997) Members	C8	45	60	30	5.00	1.00	60	30	5	2	345.00	50	270	150	212	815	204	3156	887	253	251	205	213
Schafer (1997) Members	C9	90	60	60	2.50	1.00	60	60	3	1	345.00			200	59	204	204	12623	211	204	54	69	66
Schafer (1997) Members	C10	90	60	60	5.00	1.00	60	60	5	1	345.00	70	196	300	97	204	204	3156	217	204	87	108	99
Schafer (1997) Members	C11	90	60	60	10.00	1.00	60	60	10	1	345.00	60	211	450	177	204	204	789	222	204	152	200	173
Schafer (1997) Members	C12	45	60	60	2.50	1.00	60	60	3	1	345.00			150	52	204	204	12623	211	204	48	62	60
Schafer (1997) Members	C13	45	60	60	5.00	1.00	60	60	5	1	345.00			250	75	204	204	3156	217	204	74	84	79
Schafer (1997) Members	C14	45	60	60	10.00	1.00	60	60	10	1	345.00	60	210	400	124	204	204	789	222	204	125	140	124
Schafer (1997) Members	C15	90	90	30	2.50	1.00	90	30	3	3	345.00	100	109			815	91	12623	867	123	169	97	118
Schafer (1997) Members	C16	90	90	30	5.00	1.00	90	30	5	3	345.00	70	126			815	91	3156	887	123	318	155	166
Schafer (1997) Members	C17	45	90	30	2.50	1.00	90	30	3	3	345.00	100	101			815	91	12623	867	123	145	86	111
Schafer (1997) Members	C18	45	90	30	5.00	1.00	90	30	5	3	345.00	80	123			815	91	3156	887	123	251	119	135
Schafer (1997) Members	C19	90	90	60	2.50	1.00	90	60	3	2	345.00			200	51	204	91	12623	211	104	54	54	55
Schafer (1997) Members	C20	90	90	60	5.00	1.00	90	60	5	2	345.00	80	116	300	82	204	91	3156	217	104	87	84	82
Schafer (1997) Members	C21	90	90	60	10.00	1.00	90	60	10	2	345.00	80	118	500	147	204	91	789	222	104	152	155	144
Schafer (1997) Members	C22	45	90	60	2.50	1.00	90	60	3	2	345.00			200	47	204	91	12623	211	104	48	49	50
Schafer (1997) Members	C23	45	90	60	5.00	1.00	90	60	5	2	345.00			250	65	204	91	3156	217	104	74	66	65
Schafer (1997) Members	C24	45	90	60	10.00	1.00	90	60	10	2	345.00	80	118	400	105	204	91	789	222	104	125	109	103
Schafer (1997) Members	C25	90	90	90	2.50	1.00	90	90	3	1	345.00			250	25	91	91	12623	93	91	22	30	29
Schafer (1997) Members	C26	90	90	90	5.00	1.00	90	90	5	1	345.00			400	40	91	91	3156	95	91	35	45	42
Schafer (1997) Members	C27	90	90	90	10.00	1.00	90	90	10	1	345.00	90	93	650	78	91	91	789	97	91	60	87	77
Schafer (1997) Members	C28	90	90	90	15.00	1.00	90	90	15	1	345.00	90	94	850	114	91	91	351	99	91	86	129	108
Schafer (1997) Members	C29	45	90	90	2.50	1.00	90	90	3	1	345.00			250	22	91	91	12623	93	91	20	28	27
Schafer (1997) Members	C30	45	90	90	5.00	1.00	90	90	5	1	345.00			350	32	91	91	3156	95	91	30	36	34
Schafer (1997) Members	C31	45	90	90	10.00	1.00	90	90	10	1	345.00	90	92	550	56	91	91	789	97	91	50	63	56
Schafer (1997) Members	C32	45	90	90	15.00	1.00	90	90	15	1	345.00	90	94	700	78	91	91	351	99	91	70	89	76
Commercial Drywall Studs	158ST25	90	41	33	8.09	0.48	85	70	17	1	345.00	40	125	400	189	151	101	275	163	108	151	209	176
Commercial Drywall Studs	212ST25	90	63	33	8.09	0.48	132	70	17	2	345.00	50	57	400	142	151	42	275	163	52	151	150	140
Commercial Drywall Studs	358ST25	90	92	33	8.09	0.48	192	70	17	3	345.00	70	28	400	87	151	20	275	163	27	151	95	97
Commercial Drywall Studs	400ST25	90	101	33	8.09	0.48	212	70	17	3	345.00	80	23			151	16	275	163	22	151	80	81
Commercial Drywall Studs	600ST25	90	152	33	8.09	0.48	318	70	17	5	345.00	100	11			151	7	275	163	11	151	33	0
Commercial Drywall Studs	158ST22	90	41	33	7.97	0.72	56	46	11	1	345.00	40	288	300	293	350	232	646	377	251	308	325	283
Commercial Drywall Studs	212ST22	90	63	33	7.97	0.72	87	46	11	2	345.00	50	131	300	225	350	97	646	377	119	308	235	225
Commercial Drywall Studs	358ST22	90	91	33	7.97	0.72	127	46	11	3	345.00	70	64			350	46	646	377	61	308	148	155
Commercial Drywall Studs	400ST22	90	101	33	7.97	0.72	140	46	11	3	345.00	80	53			350	38	646	377	51	308	126	129
Commercial Drywall Studs	600ST22	90	152	33	7.97	0.72	210	46	11	5	345.00	100	25			350	17	646	377	24	308	51	0
Commercial Drywall Studs	158ST20	90	40	33	7.91	0.84	48	39	9	1	345.00	40	388	300	351	474	313	880	510	338	379	382	337
Commercial Drywall Studs	212ST20	90	63	33	7.91	0.84	75	39	9	2	345.00	50	176	300	265	474	131	880	510	160	379	276	267
Commercial Drywall Studs	358ST20	90	91	33	7.91	0.84	109	39	9	3	345.00	70	86	300	165	474	62	880	510	82	379	175	183
Commercial Drywall Studs	400ST20	90	101	33	7.91	0.84	121	39	9	3	345.00	80	71			474	50	880	510	69	379	148	153
Commercial Drywall Studs	600ST20	90	152	33	7.91	0.84	181	39	9	5	345.00	100	33			474	22	880	510	33	379	60	0
AISI Manual C's	16CS3.75xl35	90	403	92	10.99	3.43	118	27	3	4	345.00	400	67			1023	53	7687	1104	77	304	61	14
AISI Manual C's	16CS3.75xlO5	90	404	93	11.37	2.67	151	35	4	4	345.00	400	43			609	32	4343	657	46	263	43	0
AISI Manual C's	16CS3.75xO9O	90	404	93	11.56	2.29	177	41	5	4	345.00	400	33			444	23	3087	479	34	210	36	0
AISI Manual C's	16CS3.75xO75	90	404	93	11.75	1.91	212	49	6	4	345.00	300	23			306	16	2075	330	24	161	28	0
AISI Manual C's	14CS3.75xl35	90	352	92	10.99	3.43	103	27	3	4	345.00	400	90			1023	70	7687	1104	99	304	85	73
AISI Manual C's	14CS3.75xlO5	90	353	93	11.37	2.67	132	35	4	4	345.00	300	57			609	42	4343	657	59	263	60	41
AISI Manual C's	14CS3.75xO9O	90	353	93	11.56	2.29	155	41	5	4	345.00	300	43			444	31	3087	479	43	210	50	29
AISI Manual C's	14CS3.75xO75	90	354	93	11.75	1.91	186	49	6	4	345.00	300	30			306	21	2075	330	30	161	40	19
AISI Manual C's	14CS3.75xO6O	90	354	94	11.94	1.52	232	62	8	4	345.00	300	20			194	14	1286	210	19	117	30	12
AISI Manual C's	12CS3.75xl35	90	301	92	10.99	3.43	88	27	3	3	345.00	300	124			1023	95	7687	1104	131	304	119	132
AISI Manual C's	12CS3.75xlO5	90	302	93	11.37	2.67	113	35	4	3	345.00	300	80			609	57	4343	657	79	263	85	87

Basic Data from original source		Centerline Dimensions in mm					Nondimensional Param.				fy	Finite Strip Analysis Results (mm -- MPa)				Hand Calculations (MPa):						dist.	dist.
Group	Member	θ	h	b	d	t	h/t	b/t	d/t	h/b	(MPa)	Llocal	fcrlocal	Ldist	fcrdist	flange	web	lip	flange/lip	flange/web	AISI	Schafer	Hancock
AISI Manual C's	12CS3.75xO9O	90	303	93	11.56	2.29	132	41	5	3	345.00	300	60			444	42	3087	479	58	210	70	69
AISI Manual C's	12CS3.75xO75	90	303	93	11.75	1.91	159	49	6	3	345.00	200	42			306	29	2075	330	40	161	56	53
AISI Manual C's	12CS3.75xO6D	90	303	94	11.94	1.52	199	62	8	3	345.00	200	27			194	19	1286	210	25	117	43	39
AISI Manual C's	12CS1.625xIO2	90	302	39	11.40	2.59	117	15	4	8	345.00	300	66			3292	54	4071	3458	84	3107	53	0
AISI Manual C's	12CS1.625xO7l	90	303	39	11.80	1.80	168	22	7	8	345.00	300	35			1532	26	1843	1605	40	1438	34	0
AISI Manual C's	11CS3.75xl35	90	276	92	10.99	3.43	80	27	3	3	345.00	300	149			1023	113	7687	1104	154	304	141	161
AISI Manual C's	11CS3.75xlO5	90	277	93	11.37	2.67	104	35	4	3	345.00	200	95			609	68	4343	657	92	263	101	109
AISI Manual C's	11CS3.75XO90	90	277	93	11.56	2.29	121	41	5	3	345.00	200	70			444	50	3087	479	68	210	83	88
AISI Manual C's	11CS3.75xO75	90	277	93	11.75	1.91	146	49	6	3	345.00	200	49			306	35	2075	330	47	161	66	69
AISI Manual C's	11CS3.75xO6O	90	278	94	11.94	1.52	182	62	8	3	345.00	200	31			194	22	1286	210	30	117	51	52
AISI Manual C's	IOCS3xl35	90	251	73	10.99	3.43	73	21	3	3	345.00	300	181			1629	137	7687	1770	191	743	177	189
AISI Manual C's	10CS3xlO5	90	251	74	11.37	2.67	94	28	4	3	345.00	200	114			965	83	4343	1049	115	365	127	125
AISI Manual C's	IOCS3xO9O	90	252	74	11.56	2.29	110	32	5	3	345.00	200	84			702	61	3087	763	84	352	104	99
AISI Manual C's	1 OCS3xO75	90	252	74	11.75	1.91	132	39	6	3	345.00	200	59			483	42	2075	524	58	270	84	76
AISI Manual C's	1 OCS3xo6O	90	252	75	11.94	1.52	166	49	8	3	345.00	200	38			306	27	1286	332	37	196	64	56
AISI Manual C's	10CS1.625xlO2	90	251	39	11.40	2.59	97	15	4	6	345.00	300	100			3292	78	4071	3458	119	3107	93	0
AISI Manual C's	1OCS1.625xO7l	90	252	39	11.80	1.80	140	22	7	6	345.00	200	53			1532	38	1843	1605	57	1438	60	0
AISI Manual C's	IOCSI.625xO57	90	253	40	11.98	1.45	174	28	8	6	345.00	200	35			970	24	1153	1015	37	767	47	0
AISI Manual C's	9CS3xl35	90	225	73	10.99	3.43	66	21	3	3	345.00	200	226			1629	170	7687	1770	232	743	218	246
AISI Manual C's	9CS3xlO5	90	226	74	11.37	2.67	85	28	4	3	345.00	200	141			965	102	4343	1049	139	365	156	169
AISI Manual C's	9CS3xO9O	90	226	74	11.56	2.29	99	32	5	3	345.00	200	105			702	75	3087	763	102	352	129	136
AISI Manual C's	9CS3xO75	90	227	74	11.75	1.91	119	39	6	3	345.00	200	73			483	52	2075	524	70	270	103	106
AISI Manual C's	9CS3xO6O	90	227	75	11.94	1.52	149	49	8	3	345.00	200	47			306	33	1286	332	45	196	79	80
AISI Manual C's	BCSI.625xlO2	90	201	39	11.40	2.59	77	15	4	5	345.00	200	164			3292	122	4071	3458	181	3107	177	0
AISI Manual C's	SCSI.625XO71	90	201	39	11.80	1.80	112	22	7	5	345.00	150	85			1532	59	1843	1605	87	1438	114	0
AISI Manual C's	8CSI.625xO57	90	202	40	11.98	1.45	139	28	8	5	345.00	150	55			970	38	1153	1015	56	767	89	0
AISI Manual C's	BCS1.625xO45	90	202	40	12.13	1.14	177	35	11	5	345.00	150	35			595	23	701	622	35	509	68	0
AISI Manual C's	5.SCSI.625xlO2	90	137	39	11.40	2.59	53	15	4	4	345.00	100	366			3292	262	4071	3458	366	3107	431	452
AISI Manual C's	5.SCS1.625xO7l	90	138	39	11.80	1.80	76	22	7	3	345.00	100	178			1532	126	1843	1605	175	1438	278	281
AISI Manual C's	5.SCSI.625xO57	90	138	40	11.98	1.45	95	28	8	3	345.00	100	115			970	80	1153	1015	112	767	215	215
AISI Manual C's	5.5CS1.625xO45	90	139	40	12.13	1.14	121	35	11	3	345.00	100	72			595	50	701	622	69	509	165	163
AISI Manual C's	5.5CSI.625xO35	90	139	40	12.26	0.89	156	45	14	3	345.00	100	43			356	30	415	372	42	332	125	123
AISI Manual C's	4CS4xl35	90	98	98	10.99	3.43	29	29	3	1	345.00			400	315	895	895	7687	963	895	241	357	334
AISI Manual C's	4CS4xlOS	90	99	99	11.37	2.67	37	37	4	1	345.00			500	231	533	533	4343	574	533	227	257	238
AISI Manual C's	4CS4xO9O	90	99	99	11.56	2.29	43	43	5	1	345.00	100	385	500	190	389	389	3087	419	389	181	213	195
AISI Manual C's	4CS4xO75	90	100	100	11.75	1.91	52	52	6	1	345.00	100	270	600	154	268	268	2075	289	268	139	172	155
AISI Manual C's	4CS4xO6O	90	100	100	11.94	1.52	66	66	8	1	345.00	100	174	600	119	170	170	1286	184	170	101	133	119
AISI Manual C's	4CSI.625xO7l	90	100	39	8.62	1.80	55	22	5	3	345.00	80	328	200	384	1532	240	3450	1660	314	1057	374	401
AISI Manual C's	4CSI.625xO57	90	100	40	8.80	1.45	69	28	6	3	345.00	80	211	300	283	970	153	2135	1050	201	554	286	303
AISI Manual C's	4CS1.625xO45	90	100	40	8.95	1.14	88	35	8	3	345.00	80	132	300	212	595	95	1286	644	124	418	217	227
AISI Manual C's	4CS1.625xO35	90	101	40	9.08	0.89	113	45	10	2	345.00	80	79	400	159	356	57	756	385	75	292	164	169
AISI Manual C's	3.5CSI.625xO7l	90	87	39	11.80	1.80	48	22	7	2	345.00	70	429	300	521	1532	315	1843	1605	400	1438	546	550
AISI Manual C's	3.5CSI.625xO57	90	87	40	11.98	1.45	60	28	8	2	345.00	70	275	400	409	970	201	1153	1015	255	767	423	421
AISI Manual C's	3.5CSI.625xO451	90	88	40	12.13	1.14	77	35	11	2	345.00	70	171	400	304	595	124	701	622	158	509	324	318
AISI Manual C's	3.5CS1.625xO35	90	88	40	12.26	0.89	99	45	14	2	345.00	70	103	500	231	356	75	415	372	95	332	246	238
AISI Manual C's	3CS3xl35	90	73	73	10.99	3.43	21	21	3	1	345.00			300	570	1629	1629	7687	1770	1629	743	646	601
AISI Manual C's	3CS3xl 05	90	74	74	11.37	2.67	28	28	4	1	345.00			400	419	965	965	4343	1049	965	365	467	427
AISI Manual C's	3CS3xO9O	90	74	74	11.56	2.29	32	32	5	1	345.00	80	700	400	343	702	702	3087	763	702	352	386	351
AISI Manual C's	3CS3xO75	90	74	74	11.75	1.91	39	39	6	1	345.00	80	490	400	281	483	483	2075	524	483	270	312	279
AISI Manual C's	3CS3xO6O	90	75	75	11.94	1.52	49	49	8	1	345.00	80	315	500	214	306	306	1286	332	306	196	242	213
AISI Manual C's	3CS1.625xO7l	90	74	39	8.62	1.80	41	22	5	2	345.00	60	574	200	535	1532	431	3450	1660	528	1057	519	519
AISI Manual C's	3CSI.625xO57	90	75	40	8.80	1.45	52	28	6	2	345.00	60	368	300	390	970	275	2135	1050	337	554	397	393
AISI Manual C's	3CS1.625xO45	90	75	40	8.95	1.14	66	35	8	2	345.00	60	229	300	293	595	170	1286	644	208	418	302	294
AISI Manual C's	3CS1.625xO35	90	75	40	9.08	0.89	85	45	10	2	345.00	60	138	400	221	356	102	756	385	125	292	227	219
AISI Manual C's	2.5CS1.625xO7l	90	62	39	8.62	1.80	34	22	5	2	345.00	50	813	200	598	1532	627	3450	1660	730	1057	602	579
AISI Manual C's	2.5CS1.625xO57	90	62	40	8.80	1.45	43	28	6	2	345.00	50	521	300	446	970	400	2135	1050	464	554	462	439
AISI Manual C's	2.5CSl.625xO45	90	62	40	8.95	1.14	55	35	8	2	345.00	50	323	300	332	595	247	1286	644	286	418	351	329
AISI Manual C's	2.5CS1.625xO35	90	63	40	9.08	0.89	70	45	10	2	345.00	50	194	400	255	356	148	756	385	172	292	265	244

Basic Data from original source		Centerline Dimensions in mm					Nondimensional Param.				fy	Finite Strip Analysis Results (mm -- MPa)				Hand Calculations (MPa):						dist.	dist.
Group	Member	θ	h	b	d	t	h/t	b/t	d/t	h/b	(MPa)	Llocal	fcrlocal	Ldist	fcrdist	flange	web	lip	flange/lip	flange/web	AISI	Schafer	Hancock
AISI Manual C's	1.5CSI.625xO7l	90	36	39	8.62	1.80	20	22	5	1	345.00	40	1602	200	718	1532	1812	3450	1660	1557	1057	819	730
AISI Manual C's	1.5CSI.625xO57	90	37	40	8.80	1.45	25	28	6	1	345.00	40	1037	300	578	970	1145	2135	1050	986	554	631	553
AISI Manual C's	1.5CS1.625xO45	90	37	40	8.95	1.14	32	35	8	1	345.00	40	645	300	418	595	702	1286	644	605	418	482	414
AISI Manual C's	11.5CS1.625xO351	90	37	40	9.08	0.89	42	45	10	1	345.00	40	388	300	318	356	419	756	385	361	292	365	307
AISI Manual Z's	12ZS3.25xl35	50	301	79	17.34	3.43	88	23	5	4	345.00			271	129	1378	95	3087	1494	134	727	135	130
AISI Manual Z's	12ZS3.25xlO5	50	302	80	17.72	2.67	113	30	7	4	345.00	242	80			818	57	1788	886	81	360	98	87
AISI Manual Z's	12ZS3.25xO9O	50	303	80	17.91	2.29	132	35	8	4	345.00	242	59			595	42	1286	644	59	361	81	70
AISI Manual Z's	12ZS3.2SxO75	50	303	81	18.10	1.91	159	42	10	4	345.00	242	41			410	29	874	443	41	277	65	54
AISI Manual Z's	12ZS3.25xO6O	50	303	81	18.29	1.52	199	53	12	4	345.00	243	27			260	19	548	281	26	201	50	41
AISI Manual Z's	10ZS3xi35	50	251	73	17.49	3.43	73	21	5	3	345.00			226	188	1629	137	3033	1756	191	1050	198	217
AISI Manual Z's	IOZS3xlO5	50	251	74	17.72	2.67	94	28	7	3	345.00	201	115			965	83	1788	1040	115	493	143	151
AISI Manual Z's	10ZS3xO9O	50	252	74	17.91	2.29	110	32	8	3	345.00	200	85			702	61	1286	756	84	435	118	123
AISI Manual Z's	1 OZS3xO75	50	252	74	18.10	1.91	132	39	10	3	345.00	200	59			483	42	874	519	58	334	95	97
AISI Manual Z's	iOZS3xO6O	50	252	75	18.29	1.52	166	49	12	3	345.00	200	38			306	27	548	329	37	242	73	74
AISI Manual Z's	9ZS3xi35	50	225	73	17.34	3.43	66	21	5	3	345.00	180	232	400	241	1629	170	3087	1757	232	1038	239	268
AISI Manual Z's	9ZS3xlO5	50	226	74	17.72	2.67	85	28	7	3	345.00	181	142			965	102	1788	1040	139	493	173	190
AISI Manual Z's	9ZS3xO9O	50	226	74	17.91	2.29	99	32	8	3	345.00	181	105			702	75	1286	756	102	435	143	156
AISI Manual Z's	9ZS3xO75	50	227	74	18.10	1.91	119	39	10	3	345.00	181	73			483	52	874	519	70	334	115	124
AISI Manual Z's	9ZS3xO6O	50	227	75	18.29	1.52	149	49	12	3	345.00	182	47			306	33	548	329	45	242	89	95
AISI Manual Z's	8ZS2.5xlO5	50	201	61	17.72	2.67	75	23	7	3	345.00	160	181			1411	130	1788	1485	179	1018	221	243
AISI Manual Z's	8ZS2.5xO9O	50	201	61	17.91	2.29	88	27	8	3	345.00	161	133			1023	95	1286	1077	131	644	182	199
AISI Manual Z's	8ZS2.5xO75	50	201	62	18.10	1.91	106	32	10	3	345.00	161	93			702	66	874	738	91	484	147	158
AISI Manual Z's	8ZS2.5xO6O	50	202	62	18.29	1.52	132	41	12	3	345.00	161	60			444	42	548	466	58	350	113	121
AISI Manual Z's	8ZS2.5xO48	50	202	62	18.44	1.22	166	51	15	3	345.00	162	38			281	27	345	295	37	254	88	93
AISI Manual Z's	BZS2xiOS	50	201	48	17.72	2.67	75	18	7	4	345.00	160	181			2253	130	1788	2227	186	1921	218	211
AISI Manual Z's	8ZS2xO9O	50	201	49	17.91	2.29	88	21	8	4	345.00	161	134			1629	95	1286	1609	136	1387	181	171
AISI Manual Z's	8ZS2xO75	50	201	49	18.10	1.91	106	26	10	4	345.00	161	94			1114	66	874	1099	94	881	145	136
AISI Manual Z's	8ZS2xO6O	50	202	49	18.29	1.52	132	32	12	4	345.00	161	61			702	42	548	692	60	532	112	104
AISI Manual Z's	BZS2xO48	50	202	50	18.44	1.22	166	41	15	4	345.00	162	39			444	27	345	437	38	376	87	80
AISI Manual Z's	7ZS2xlO5	50	175	48	17.72	2.67	66	18	7	4	345.00	140	237			2253	170	1788	2227	239	1921	286	315
AISI Manual Z's	7ZS2xO9O	50	176	49	17.91	2.29	77	21	8	4	345.00	140	175			1629	124	1286	1609	175	1387	237	258
AISI Manual Z's	7ZS2xO75	50	176	49	18.10	1.91	92	26	10	4	345.00	141	122			1114	86	874	1099	121	881	190	205
AISI Manual Z's	7ZS2xO6O	50	176	49	18.29	1.52	116	32	12	4	345.00	141	79			702	55	548	692	77	532	147	157
AISI Manual Z's	7ZS2xO48	50	177	50	18.44	1.22	145	41	15	4	345.00	141	50			444	35	345	437	49	376	114	121
AISI Manual Z's	6ZS2xl 05	50	150	48	17.72	2.67	56	18	7	3	345.00	120	322	300	353	2253	233	1788	2227	318	1921	373	413
AISI Manual Z's	6ZS2xG9O	50	150	49	17.91	2.29	66	21	8	3	345.00	120	238	400	287	1629	170	1286	1609	232	1387	308	338
AISI Manual Z's	6ZS2xO75	50	150	49	18.10	1.91	79	26	10	3	345.00	120	165	400	225	1114	118	874	1099	160	881	247	269
AISI Manual Z's	6ZS2xO6O	50	151	49	18.29	1.52	99	32	12	3	345.00	121	106	500	172	702	75	548	692	102	532	191	206
AISI Manual Z's	6ZS2xO48	50	151	50	18.44	1.22	124	41	15	3	345.00	121	68	500	131	444	48	345	437	65	376	148	158
AISI Manual Z's	5ZS2xO9O	50	125	49	17.91	2.29	55	21	8	3	345.00	100	340	400	374	1629	247	1286	1609	324	1387	394	414
AISI Manual Z's	5ZS2xO75	50	125	49	18.10	1.91	66	26	10	3	345.00	100	236	400	294	1114	170	874	1099	224	881	316	330
AISI Manual Z's	5ZS2xO6O	50	125	49	18.29	1.52	82	32	12	3	345.00	100	150	500	226	702	108	548	692	142	532	244	251
AISI Manual Z's	5ZS2xO48	50	126	50	18.44	1.22	103	41	15	3	345.00	100	96	500	172	444	69	345	437	90	376	190	193
AISI Manual Z's	5ZS2xO36	50	126	50	18.59	0.91	138	55	20	3	345.00	100	54	600	124	247	39	191	243	51	209	138	138
AISI Manual Z's	4ZS2xO9O	50	99	49	17.91	2.29	43	21	8	2	345.00	80	524	400	473	1629	389	1286	1609	486	1387	495	488
AISI Manual Z's	4ZS2xO75	50	100	49	18.10	1.91	52	26	10	2	345.00	80	363	400	369	1114	268	874	1099	334	881	397	388
AISI Manual Z's	4ZS2xO6O	50	100	49	18.29	1.52	66	32	12	2	345.00	80	231	400	287	702	170	548	692	212	532	307	296
AISI Manual Z's	4ZS2xO48	50	100	50	18.44	1.22	82	41	15	2	345.00	80	147	500	217	444	108	345	437	135	376	238	226
AISI Manual Z's	4ZS2xO36	50	101	50	18.59	0.91	110	55	20	2	345.00	80	82	600	157	247	61	191	243	75	209	174	162
AISI Manual Z's	3ZS1.75xO9O	50	74	42	17.91	2.29	32	18	8	2	345.00	60	927	300	623	2157	702	1286	1985	843	1686	687	649
AISI Manual Z's	3ZSI.75xO75	50	74	43	18.10	1.91	39	22	10	2	345.00	60	640	300	506	1471	483	874	1353	579	1149	551	515
AISI Manual Z's	3ZS1.75xO6O	50	75	43	18.29	1.52	49	28	12	2	345.00	60	406	400	379	925	306	548	850	366	721	425	391
AISI Manual Z's	3ZS1.75xO48	50	75	43	18.44	1.22	62	35	15	2	345.00	60	258	400	294	584	194	345	536	232	455	330	299
AISI Manual Z's	3ZS1.75xO36	50	75	44	18.59	0.91	82	48	20	2	345.00	60	144	500	210	324	108	191	297	130	252	241	213

Design Examples: Concentrically Loaded Lipped Channel Column

The following 11 examples include the methodology for all methods considered in the report: Distortional Buckling of Columns. In brief, the 11 methods include:

A. AISI (1996) Methods and Simple Modifications
- **A1. Current AISI (1996) Method**
- **A2. AISI (1996) with a Distortional Check**

B. New Methods which include only Local+Euler Check and Distortional Check
- **B1. Effective width "element" based method**
- **B2. Hand Implementation of Direct Strength "member" based method**
- **B3. Numerical Implementation of Direct Strength "member" based method**

C. New methods which include Local+Euler Check and Dist+Euler Check
- **C1 - C3 same as B methods with interactions listed above**

D. New methods which include Local+Euler, Dist+Euler, and Local+Dist Check
- **D1 - D3 same as B and C methods with interactions listed above**

Specimen Dimensions and Properties:

$h := 5.034 \cdot in$

$b := 1.992 \cdot in$

$d := 0.735 \cdot in$

$t := 0.031 \cdot in$

$E := 29500 \cdot ksi$

$\nu := 0.3$

$f_y := 35.1 \cdot ksi$

$K_x := 1$

$K_y := 1$

$K_t := 0.5$

$L_x := 75 \cdot in$

$L_y := 75 \cdot in$

$L_t := 75 \cdot in$

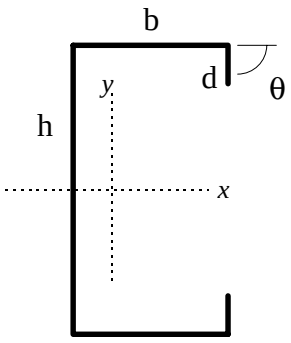

Dimensions of the above example are based on Loughlan (1979) specimen #L6

Glossary of Variables:

h = web height
b = flange width
d = lip length
θ = lip angle (radians)
t = thickness
E = Young's modulus
ν = Poisson's ratio
fy = yield stress

K_x = x-axis effective length
K_y = y axis effective length
K_t = torsion effective length
L_x = x-axis unbraced length
L_y = y-axis unbraced length
L_t = torsion unbraced length

$\theta := 90 \cdot \frac{\pi}{180}$

The following solution only applies for θ = 90, due to explicit formulas used in the calculation of C_w for overall (Euler) buckling. Those formulas only apply to lipped C's.

Whole Section Material and Gross Properties Required for Overall Buckling Analysis of Lipped Channel

Material Property: $G := \frac{E}{2\cdot(1+\nu)}$ $G = 1.135\cdot10^{4}\ \circ ksi$

Gross Section Properties:

This is a series of "canned" formulas for gross property calculations of a lipped channel. They do not apply to other cross-section geometry. The C_w formula is from Yu, Cold-Formed Steel Design.

$A := t\cdot(h+2\cdot b+2\cdot d)$ $A = 0.325\ \circ in^2$

$J := \frac{1}{3}\cdot h\cdot t^3 + 2\cdot\frac{1}{3}\cdot b\cdot t^3 + 2\cdot\frac{1}{3}\cdot d\cdot t^3$ $J = 1.041\cdot10^{-4}\ \circ in^4$

$y_{cg} := \frac{1}{2}\cdot h$ $y_{cg} = 2.517\ \circ in$

$I_x := \frac{1}{12}\cdot\left(h^3\cdot t\right) + \frac{1}{2}\cdot b\cdot t\cdot h^2 + \frac{2}{3}\cdot d^3\cdot t + \frac{1}{2}\cdot d\cdot t\cdot h^2 - d^2\cdot t\cdot h + \frac{1}{6}\cdot b\cdot t^3$ $I_x = 1.325\ \circ in^4$

$x_{cg} := \frac{b\cdot(b+2\cdot d)}{h+2\cdot b+2\cdot d}$ $x_{cg} = 0.658\ \circ in$

$I_y := \frac{1}{12}\cdot h\cdot t^3 + \frac{2}{3}\cdot t\cdot b^3 + \frac{1}{6}\cdot d\cdot t^3 + 2\cdot d\cdot t\cdot b^2 - (h\cdot t+2\cdot b\cdot t+2\cdot d\cdot t)\cdot b^2\cdot\frac{(b+2\cdot d)^2}{(h+2\cdot b+2\cdot d)^2}$ $I_y = 0.204\ \circ in^4$

$x_o := \frac{b\cdot t\cdot(b+2\cdot d)}{A} + \frac{b\cdot t}{12\cdot I_x}\cdot\left(6\cdot d\cdot h^2 + 3\cdot b\cdot h^2 - 8\cdot d^3\right)$ $x_o = 1.668\ \circ in$

$m := x_o - x_{cg}$ $m = 1.01\ \circ in$

$C_{wterm1} := \frac{x_{cg}\cdot A\cdot h^2}{t}\cdot\left(\frac{b^2}{3} + m^2 - m\cdot b\right)$ $C_{wterm1} = 57.823\ \circ in^6$

$C_{wterm2} := \frac{A}{3\cdot t}\cdot\left[m^2\cdot h^3 + b^2\cdot d^2\cdot(2\cdot d+3\cdot h)\right] - \frac{I_x\cdot m^2}{t}\cdot(2\cdot h+4\cdot d)$ $C_{wterm2} = 12.11\ \circ in^6$

$C_{wterm3} := \frac{m\cdot d^2}{3}\cdot\left[8\cdot b^2\cdot d + 2\cdot m\cdot(2\cdot d\cdot(d-h)+b\cdot(2\cdot d-3\cdot h))\right]$ $C_{wterm3} = -8.058\ \circ in^6$

$C_{wterm4} := \frac{b^2\cdot h^2}{6}\cdot\left[(3\cdot d+b)\cdot(4\cdot d+h) - 6\cdot d^2\right] - \frac{m^2\cdot h^4}{4}$ $C_{wterm4} = 342.735\ \circ in^6$

$C_w := \frac{t^2}{A}\cdot\left(C_{wterm1} + C_{wterm2} + C_{wterm3} + C_{wterm4}\right)$ $C_w = 1.196\ \circ in^6$

Flange Only Properties Required for Distortional Buckling Calculation

Hand methods for distortional buckling prediction require that section properties of the isolated flange be calculated. The expressions here are only applicable for simple lips. More complicated flanges would follow the same procedures, but new expressions would be required.

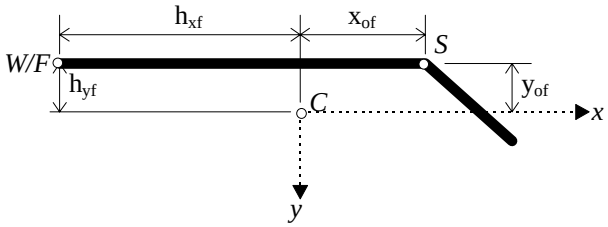

Material Properties:

$$G := \frac{E}{2\cdot(1+\nu)}$$

Properties of the Flange Only:

$$A_f := (b+d)\cdot t \qquad A_f = 0.085\,in^2$$

$$J_f := \frac{1}{3}\cdot b\cdot t^3 + \frac{1}{3}\cdot d\cdot t^3 \qquad J_f = 2.708\cdot 10^{-5}\,in^4$$

$$I_{xf} := \frac{t\cdot\left(t^2\cdot b^2 + 4\cdot b\cdot d^3 - 4\cdot b\cdot d^3\cdot\cos(\theta)^2 + t^2\cdot b\cdot d + d^4 - d^4\cdot\cos(\theta)^2\right)}{12\cdot(b+d)} \qquad I_{xf} = 3.279\cdot 10^{-3}\,in^4$$

$$I_{yf} := \frac{t\cdot\left(b^4 + 4\cdot d\cdot b^3 + 6\cdot d^2\cdot b^2\cdot\cos(\theta) + 4\cdot d^3\cdot b\cdot\cos(\theta)^2 + d^4\cdot\cos(\theta)^2\right)}{12\cdot(b+d)} \qquad I_{yf} = 0.037\,in^4$$

$$I_{xyf} := \frac{t\cdot b\cdot d^2\cdot\sin(\theta)\cdot(b+d\cdot\cos(\theta))}{4\cdot(b+d)} \qquad I_{xyf} = 6.092\cdot 10^{-3}\,in^4$$

$$I_{of} := \frac{t\cdot b^3}{3} + \frac{b\cdot t^3}{12} + \frac{t\cdot d^3}{3} \qquad I_{of} = 0.086\,in^4$$

$$x_{of} := \frac{b^2 - d^2\cdot\cos(\theta)}{2\cdot(b+d)}$$ x distance from the centroid to the shear center. $x_{of} = 0.728\,in$

$$y_{of} := \frac{-d^2\cdot\sin(\theta)}{2\cdot(b+d)}$$ y distance from the centroid to the shear center. $y_{of} = -0.099\,in$

$$h_{xf} := \frac{-\left(b^2 + 2\cdot d\cdot b + d^2\cdot\cos(\theta)\right)}{2\,(b+d)}$$ x distance from the centroid to the web/flange juncture. $h_{xf} = -1.264\,in$

$$h_{yf} := \frac{-d^2\cdot\sin(\theta)}{2\cdot(b+d)}$$ y distance from the centroid to the web/flange juncture. $h_{yf} = -0.099\,in$

$$C_{wf} := 0\cdot in^6 \qquad C_{wf} = 0\,in^6$$

All flange properties are given the subscript 'f' to distinguish them from the overall properties of the column

Overall (Global, Long-wavelength) Buckling Modes as per AISI (1996)

Elastic Flexural Buckling about the x-axis:

$r_x := \sqrt{\frac{I_x}{A}}$ $\quad r_x = 2.018 \cdot in$

$F_{ex} := \frac{\pi^2 \cdot E}{\left(\frac{K_x \cdot L_x}{r_x}\right)^2}$ $\quad F_{ex} = 210.876 \cdot ksi$

Slenderness is:

$\frac{K_x \cdot L_x}{r_x} = 37.158$

Elastic Flexural Buckling about the y-axis:

$r_y := \sqrt{\frac{I_y}{A}}$ $\quad r_y = 0.791 \cdot in$

$F_{ey} := \frac{\pi^2 \cdot E}{\left(\frac{K_y \cdot L_y}{r_y}\right)^2}$ $\quad F_{ey} = 32.417 \cdot ksi$

Slenderness is:

$\frac{K_y \cdot L_y}{r_y} = 94.77$

Elastic Flexural-torsional buckling

$\sigma_{ex} := F_{ex}$ $\quad r_o := \sqrt{r_x^2 + r_y^2 + x_o^2}$ $\quad r_o = 2.735 \cdot in$

$\sigma_t := \frac{1}{A \cdot r_o^2} \cdot \left[G \cdot J + \frac{\pi^2 \cdot E \cdot C_w}{\left(K_t \cdot L_t\right)^2} \right]$ $\quad \beta := 1 - \left(\frac{x_o}{r_o}\right)^2$ $\quad \sigma_t = 102.279 \cdot ksi$

$\beta = 0.628$

$F_{et} := \frac{1}{2 \cdot \beta} \cdot \left[\sigma_{ex} + \sigma_t - \sqrt{\left(\sigma_{ex} + \sigma_t\right)^2 - 4 \cdot \beta \cdot \sigma_{ex} \cdot \sigma_t} \right]$ $\quad F_{et} = 82.543 \cdot ksi$

The controlling long-wavelength buckling load is the minimum:

$F_e := \min\left(\left[F_{ex} \;\; F_{ey} \;\; F_{et}\right]\right)$ $\quad F_e = 32.417 \cdot ksi$

$mode\_is := \begin{cases} \text{"x-axis flexure"} & \text{if } F_e = F_{ex} \\ \text{"y-axis flexure"} & \text{if } F_e = F_{ey} \\ \text{"flexural-torsional"} & \text{if } F_e = F_{et} \end{cases}$ $\quad mode\_is = \text{"y-axis flexure"}$

Note, columns with different effective lengths (K) or braced lengths (Lx, Ly, Lt) are treated in the usual fashion regardless of the design method considered.

A1. Ultimate Strength per Current AISI (1996) Procedure

Determine the long column nominal buckling stress Fn (per AISI section C4):

$$\lambda_c := \sqrt{\frac{f_y}{F_e}} \qquad \lambda_c = 1.041$$

$$F_n := \begin{cases} \left(0.658^{\lambda_c^2} \cdot f_y\right) & \text{if } \lambda_c \le 1.5 \\ \left(\frac{0.877}{\lambda_c^2} \cdot f_y\right) & \text{if } \lambda_c > 1.5 \end{cases} \qquad F_n = 22.31 \cdot ksi$$

Determine the effective area (calculated at the nominal buckling stress, Fn):

Determine the effective width of the web:

The buckling coefficient and stress are:

$$k_{web} := 4$$

$$f_{cr\_web} := k_{web} \cdot \frac{\pi^2 \cdot E}{12 \cdot \left(1 - \nu^2\right)} \cdot \left(\frac{t}{h}\right)^2 \qquad f_{cr\_web} = 4.044 \cdot ksi$$

The slenderness is:

$$\lambda := \frac{1.052}{\sqrt{k_{web}}} \cdot \left(\frac{h}{t}\right) \cdot \sqrt{\frac{F_n}{E}} \qquad \lambda = 2.349 \qquad \text{or} \qquad \lambda := \sqrt{\frac{F_n}{f_{cr\_web}}} \qquad \lambda = 2.349$$

the two expressions for λ are equivalent.

The reduction factor is:

$$\rho := \begin{cases} 1 & \text{if } \lambda \le 0.673 \\ \frac{\left(1 - \frac{0.22}{\lambda}\right)}{\lambda} & \text{if } \lambda > 0.673 \end{cases} \qquad \rho = 0.386$$

The effective width of the web:

$$h_{eff} := \rho \cdot h \qquad h_{eff} = 1.943 \cdot in$$

A1. Ultimate Strength per Current AISI (1996) Procedure (continued)

Determine the effective width of the flange:

Preliminaries: $S := 1.28\cdot\sqrt{\frac{E}{F_n}}$ $I_s := \frac{t\cdot d^3\cdot\sin(\theta)^2}{12}$

$$k_{aisi} := \begin{cases} 4 & \text{if } \frac{b}{t}\le\frac{S}{3} \\ & \text{if } \frac{S}{3}<\frac{b}{t}\le S \\ & \quad \left| \begin{array}{l} k_u \leftarrow 0.43 \\ I_a \leftarrow t^4\cdot 399\cdot\left[\frac{\frac{b}{t}}{S}-\left(\frac{k_u}{4}\right)^{\frac{1}{2}}\right]^3 \\ n \leftarrow \frac{1}{2} \\ C2 \leftarrow \min\left(\left[\frac{I_s}{I_a}\ \ 1\right]\right) \\ C1 \leftarrow 2 - C2 \\ k_a \leftarrow \min\left(\left[5.25-5\cdot\frac{d}{b}\ \ 4\right]\right) \\ C2^n\cdot\left(k_a-k_u\right)+k_u \end{array} \right. \\ & \text{if } \frac{b}{t}\ge S \\ & \quad \left| \begin{array}{l} k_u \leftarrow 0.43 \\ I_a \leftarrow t^4\cdot\left(115\cdot\frac{\frac{b}{t}}{S}+5\right) \\ n \leftarrow \frac{1}{3} \\ C2 \leftarrow \min\left(\left[\frac{I_s}{I_a}\ \ 1\right]\right) \\ C1 \leftarrow 2 - C2 \\ k_a \leftarrow \min\left(\left[5.25-5\cdot\frac{d}{b}\ \ 4\right]\right) \\ C2^n\cdot\left(k_a-k_u\right)+k_u \end{array} \right. \end{cases}$$

Once kaisi is determined from the equations on the left, the effective width of the flange is readily calculated:

The buckling coefficient and stress are:

$k_{aisi} = 3.405$

$f_{cr\_aisi} := k_{aisi}\cdot\frac{\pi^2\cdot E}{12\cdot\left(1-\nu^2\right)}\cdot\left(\frac{t}{b}\right)^2$

$f_{cr\_aisi} = 21.988\cdot ksi$

The slenderness is:

$\lambda := \frac{1.052}{\sqrt{k_{aisi}}}\cdot\left(\frac{b}{t}\right)\cdot\sqrt{\frac{F_n}{E}}$ $\lambda = 1.007$

or $\lambda := \sqrt{\frac{F_n}{f_{cr\_aisi}}}$ $\lambda = 1.007$

The reduction factor is:

$$\rho := \begin{cases} 1 & \text{if } \lambda\le 0.673 \\ \frac{\left(1-\frac{0.22}{\lambda}\right)}{\lambda} & \text{if } \lambda > 0.673 \end{cases} \qquad \rho = 0.776$$

The effective width of the flange:

$b_{eff} := \rho\cdot b$ $b_{eff} = 1.546\cdot in$

A1. Ultimate Strength per Current AISI (1996) Procedure (continued)

Determine the effective width of the lip

The effective width of the lip is first determined as an unstiffened element in pure compression, labeled as ds_p. Then a second reduction using the C2 term from the flange expressions must also be applied.

First reduction:

$k_{lip} := 0.43$

$f_{cr\_lip} := k_{lip} \cdot \frac{\pi^2 \cdot E}{12 \cdot \left(1 - \nu^2\right)} \cdot \left(\frac{t}{d}\right)^2$

$f_{cr\_lip} = 20.395 \cdot ksi$

$\lambda := \frac{1.052}{\sqrt{k_{lip}}} \cdot \left(\frac{d}{t}\right) \cdot \sqrt{\frac{F_n}{E}}$ or $\lambda := \sqrt{\frac{F_n}{f_{cr\_lip}}}$

$\lambda = 1.046$

$$\rho := \begin{cases} 1 & \text{if } \lambda \le 0.673 \\ \frac{\left(1 - \frac{0.22}{\lambda}\right)}{\lambda} & \text{if } \lambda > 0.673 \end{cases}$$

$\rho = 0.755$

$d_{s\_p} := \rho \cdot d$

$d_{s\_p} = 0.555 \cdot in$

Second reduction

$$C_2 := \begin{cases} 1 & \text{if } \frac{b}{t} \le \frac{S}{3} \\ I_a \leftarrow t^4 \cdot 399 \cdot \left[\frac{\frac{b}{t}}{S} - \left(\frac{0.43}{4}\right)^{\frac{1}{2}}\right]^3 & \text{if } \frac{S}{3} < \frac{b}{t} \le S \\ \min\left(\left[\frac{I_s}{I_a} \quad 1\right]\right) & \\ I_a \leftarrow t^4 \cdot \left(115 \cdot \frac{\frac{b}{t}}{S} + 5\right) & \text{if } \frac{b}{t} \ge S \\ \min\left(\left[\frac{I_s}{I_a} \quad 1\right]\right) & \end{cases}$$

$C_2 = 1$

$d_{eff} := C_2 \cdot d_{s\_p}$

$d_{eff} = 0.555 \cdot in$

Determine the effective area and the Ultimate Strength:

The Effective area is:

$A_e := t \cdot \left(h_{eff} + 2 \cdot b_{eff} + 2 \cdot d_{eff}\right)$ $A_e = 0.19 \cdot in^2$ vs. $A = 0.325 \cdot in^2$

The ultimate strength is:

$P_{n\_A1} := A_e \cdot F_n$ $P_{n\_A1} = 4.249 \cdot k$

A2. AISI (1996) with a Distortional Check

Step 1: Complete design method A1.

Step 2: Perform the Distortional Check

Calculate the distortional buckling stress, via hand method of Schafer (1997)

Determine the critical half-wavelength at which distortional buckling occurs:

$$L_{cr} := \left[\frac{6\cdot\pi^4\cdot h\cdot\left(1-\nu^2\right)}{t^3}\cdot\left[I_{xf}\cdot\left(x_{of}-h_{xf}\right)^2+C_{wf}-\frac{I_{xyf}^2}{I_{yf}}\cdot\left(x_{of}-h_{xf}\right)^2\right]\right]^{\frac{1}{4}} \qquad L_{cr} = 30.007\cdot in$$

If bracing is provided that restricts the distortional mode at some length less than Lcr, then the shorter bracing length should be used in place of Lcr in the following calculations.

Determine the elastic and "geometric" rotational spring stiffness of the flange:

$$k_{\phi fe} := \left(\frac{\pi}{L_{cr}}\right)^4\cdot\left[E\cdot I_{xf}\cdot\left(x_{of}-h_{xf}\right)^2+E\cdot C_{wf}-E\cdot\frac{I_{xyf}^2}{I_{yf}}\cdot\left(x_{of}-h_{xf}\right)^2\right]+\left(\frac{\pi}{L_{cr}}\right)^2\cdot G\cdot J_f$$

$$k_{\phi fe} = 0.035\cdot k$$

$$k_{\phi fg} := \left(\frac{\pi}{L_{cr}}\right)^2\cdot\left[A_f\cdot\left[\left(x_{of}-h_{xf}\right)^2\cdot\left(\frac{I_{xyf}}{I_{yf}}\right)^2-2\cdot y_{of}\cdot\left(x_{of}-h_{xf}\right)\cdot\left(\frac{I_{xyf}}{I_{yf}}\right)+h_{xf}^2+y_{of}^2\right]+I_{xf}+I_{yf}\right]$$

$$k_{\phi fg} = 2.092\cdot 10^{-3}\cdot in^2$$

Determine the elastic and "geometric" rotational spring stiffness from the web:

$$k_{\phi we} := \frac{E\cdot t^3}{6\cdot h\cdot\left(1-\nu^2\right)} \qquad k_{\phi we} = 0.032\cdot k \qquad k_{\phi wg} := \left(\frac{\pi}{L_{cr}}\right)^2\cdot\frac{t\cdot h^3}{60} \qquad k_{\phi wg} = 7.224\cdot 10^{-4}\cdot in^2$$

kϕwg is modified due to an error in Schafer (1997) analysis.

Determine the distortional buckling stress:

$$f_{cr\_dist} := \frac{k_{\phi fe}+k_{\phi we}}{k_{\phi fg}+k_{\phi wg}} \qquad f_{cr\_dist} = 23.921\cdot ksi$$

A2. AISI (1996) with a Distortional Check (continued)

Calculate the strength reduction factor (ρ) for distortional buckling

Find the reduction factor for the distortional stress

$$\lambda_d := \sqrt{\frac{f_y}{f_{cr\_dist}}} \qquad \lambda_d = 1.211$$

$$R_d := \min\left(\left[1 \quad \frac{1.17}{\lambda_d + 1} + 0.3\right]\right) \qquad R_d = 0.829$$

Winter's curve is used to find the strength reduction factor; but the distortional stress is reduced by Rd to account for lower post-buckling capacity in the distortional mode.

The increased slenderness is

$$\lambda := \sqrt{\frac{f_y}{R_d \cdot f_{cr\_dist}}} \qquad \lambda = 1.33$$

note that fy, not Fn is used in the strength provisions for distortional buckling in method A2, this is because distortional interaction with long column Euler buckling is ignored in this method.

The reduction factor is:

$$\rho := \begin{cases} 1 & \text{if } \lambda \le 0.673 \\ \left(1 - 0.22 \cdot \sqrt{\frac{R_d \cdot f_{cr\_dist}}{f_y}}\right) \cdot \sqrt{\frac{R_d \cdot f_{cr\_dist}}{f_y}} & \text{if } \lambda > 0.561 \end{cases} \qquad \rho = 0.627$$

An alternative, but similar method to calculate the strength reduction factor (ρ)

The alternative reduction factor is:

$$\rho_{alt} := \begin{cases} 1 & \text{if } \lambda_d \le 0.561 \\ \left[1 - 0.25 \cdot \left(\frac{f_{cr\_dist}}{f_y}\right)^{0.6}\right] \cdot \left(\frac{f_{cr\_dist}}{f_y}\right)^{0.6} & \text{if } \lambda > 0.561 \end{cases} \qquad \rho_{alt} = 0.637$$

this method for calculation of ρ is used in methods B2 and B3 and is provided for comparison only.

The Effective area for distortional buckling is:

$$A_e := \rho \cdot A \qquad A_e = 0.204 \cdot in^2 \qquad \text{vs.} \qquad A = 0.325 \cdot in^2$$

The strength prediction for the distortional check is

$$P_{n\_A2dist\_check} := A_e \cdot f_y \qquad P_{n\_A2dist\_check} = 7.16 \cdot k$$

The ultimate strength is the minimum:

$$P_{n\_A2} := \min\left(\left[P_{n\_A1} \quad P_{n\_A2dist\_check}\right]\right) \qquad P_{n\_A2} = 4.249 \cdot k$$

$$ultimate\_is := \begin{cases} \text{"local limited to Fn (L+E)"} & \text{if } P_{n\_A2} = P_{n\_A1} \\ \text{"distortional"} & \text{if } P_{n\_A2} = P_{n\_A2dist\_check} \end{cases}$$

ultimate_is = "local limited to Fn (L+E)"

B1. Effective width "element" based method with L+E and D Checks

L=local buckling D=distortional buckling E=Euler (long wavelength) buckling a "+" indicates that interaction in these modes is considered in the design method.

Determine the effective width of the flange web and lip considering L+E, thus all eff. width calculations are limited to the long column nominal stress Fn

Effective Width of the Web

The plate buckling coefficient is OR the web local buckling stress is

$k_{web} := 4$

$f_{cr\_w} := k_{web} \cdot \frac{\pi^2 \cdot E}{12 \cdot \left(1 - \nu^2\right)} \cdot \left(\frac{t}{h}\right)^2$ $f_{cr\_w} = 4.044 \cdot ksi$

The slenderness is

$\lambda := \frac{1.052}{\sqrt{k_{web}}} \cdot \left(\frac{h}{t}\right) \cdot \sqrt{\frac{F_n}{E}}$ $\lambda = 2.349$ $\lambda := \sqrt{\frac{F_n}{f_{cr\_w}}}$ $\lambda = 2.349$

The reduction factor is:

$$\rho := \begin{cases} 1 & \text{if } \lambda \le 0.673 \\ \frac{\left(1 - \frac{0.22}{\lambda}\right)}{\lambda} & \text{if } \lambda > 0.673 \end{cases} \qquad \rho = 0.386$$

The effective width of the web:

$h_{eff} := \rho \cdot h$ $h_{eff} = 1.943 \cdot in$

Effective Width of the Flange

The plate buckling coefficient is* OR the flange local buckling stress is

$k_{flange} := 4$

$f_{cr\_f} := k_{flange} \cdot \frac{\pi^2 \cdot E}{12 \cdot \left(1 - \nu^2\right)} \cdot \left(\frac{t}{b}\right)^2$ $f_{cr\_f} = 25.829 \cdot ksi$

The slenderness is

$\lambda := \frac{1.052}{\sqrt{k_{flange}}} \cdot \left(\frac{b}{t}\right) \cdot \sqrt{\frac{F_n}{E}}$ $\lambda = 0.929$ $\lambda := \sqrt{\frac{F_n}{f_{cr\_f}}}$ $\lambda = 0.929$

The reduction factor is:

$$\rho := \begin{cases} 1 & \text{if } \lambda \le 0.673 \\ \frac{\left(1 - \frac{0.22}{\lambda}\right)}{\lambda} & \text{if } \lambda > 0.673 \end{cases} \qquad \rho = 0.821$$

The effective width of the flange:

$b_{eff} := \rho \cdot b$ $b_{eff} = 1.636 \cdot in$

* note that a k of 4 is used for the flange instead of the AISI rules from B4.2. This implies that only local buckling is considered in this calculation, and distortional buckling will thus be checked separately.

B1. Effective width "element" based method with L+E and D Checks (continued)

Effective Width of the Lip

The plate buckling coefficient is* OR the lip local buckling stress is

$k_{lip} := 0.43$

$f_{cr\_l} := k_{lip} \cdot \frac{\pi^2 \cdot E}{12 \cdot \left(1 - \nu^2\right)} \cdot \left(\frac{t}{d}\right)^2$ $f_{cr\_l} = 20.395\,ksi$

The slenderness is

$\lambda := \frac{1.052}{\sqrt{k_{lip}}} \cdot \left(\frac{d}{t}\right) \cdot \sqrt{\frac{F_n}{E}}$ $\lambda = 1.046$ $\lambda := \sqrt{\frac{F_n}{f_{cr\_l}}}$ $\lambda = 1.046$

The reduction factor is:

$$\rho := \begin{cases} 1 & \text{if } \lambda \le 0.673 \\ \dfrac{\left(1 - \frac{0.22}{\lambda}\right)}{\lambda} & \text{if } \lambda > 0.673 \end{cases} \qquad \rho = 0.755$$

The effective width of the lip:

$d_{eff} := \rho \cdot d$ $d_{eff} = 0.555\,in$

The Effective area is:

$A_e := t \cdot \left(h_{eff} + 2 \cdot b_{eff} + 2 \cdot d_{eff}\right)$ $A_e = 0.196\,in^2$ $A_{e\_B1local} := A_e$

The strength prediction for local buckling (L) considering long column (E) interaction is

$P_{n\_B1local} := A_e \cdot F_n$ $P_{n\_B1local} = 4.374\,k$

Check distortional buckling (calculations are identical to distortional check in method A2)

The strength prediction for the distortional check from A2 is

$P_{n\_A2dist\_check} = 7.16\,k$

The ultimate strength is the minimum:

$P_{n\_B1} := \min\left(\left[P_{n\_B1local} \quad P_{n\_A2dist\_check}\right]\right)$ $P_{n\_B1} = 4.374\,k$

$$ultimate\_is := \begin{cases} \text{"local (k=4 sol'n) limited to Fn (L+E)"} & \text{if } P_{n\_B1} = P_{n\_B1local} \\ \text{"distortional"} & \text{if } P_{n\_B1} = P_{n\_A2dist\_check} \end{cases}$$

ultimate_is = "local (k=4 sol'n) limited to Fn (L+E)"

B2. Hand Based Direct Strength "member" method with L+E and D Checks

L=local buckling D=distortional buckling E=Euler (long wavelength) buckling a "+" indicates that interaction in these modes is considered in the design method.

In the member methods (B2-B3, C2-C3, D2-D3) solutions are written in terms of load, P.

Calculate the **elastic buckling loads** by hand

Long Column Buckling (Euler buckling) see before method A1 for details of hand calculation

$P_{cre} := A \cdot F_e$ $P_{cre} = 10.54\,k$

Distortional Buckling see method A2 for details of hand calculation

$P_{crd} := A \cdot f_{cr\_dist}$ $P_{crd} = 7.777\,k$

Local buckling (based on hand expressions for flange/web and flange/lip interaction)

Flange/Web Local Buckling

The plate buckling coefficient for the flange/web interaction expressions are written in terms of the flange:

$$k_{flange\_web} := \begin{cases} \left[2 - \left(\frac{b}{h}\right)^{0.4}\right] \cdot 4 \cdot \left(\frac{b}{h}\right)^2 & \text{if } \frac{h}{b} \geq 1 \\ \left[2 - \left(\frac{h}{b}\right)^{0.2}\right] \cdot 4 & \text{if } \frac{h}{b} < 1 \end{cases} \qquad k_{flange\_web} = 0.82$$

$$f_{cr\_fw} := k_{flange\_web} \cdot \frac{\pi^2 \cdot E}{12 \cdot \left(1 - \nu^2\right)} \cdot \left(\frac{t}{b}\right)^2 \qquad f_{cr\_fw} = 5.298\,ksi$$

Flange/Lip Local Buckling

The plate buckling coefficient for the flange/lip interaction expression is also written in terms of the flange:

$$k_{flange\_lip} := -11.07 \cdot \left(\frac{d}{b}\right)^2 + 3.95 \cdot \left(\frac{d}{b}\right) + 4 \qquad k_{flange\_lip} = 3.95$$

$$f_{cr\_fl} := k_{flange\_lip} \cdot \frac{\pi^2 \cdot E}{12 \cdot \left(1 - \nu^2\right)} \cdot \left(\frac{t}{b}\right)^2 \qquad f_{cr\_fl} = 25.508\,ksi$$

Local buckling stress

$f_{cr\_local} := \min\left(\left[f_{cr\_fw} \;\; f_{cr\_fl}\right]\right)$ $f_{cr\_local} = 5.298\,ksi$

Local buckling load

$P_{crl} := A \cdot f_{cr\_local}$ $P_{crl} = 1.722\,k$

Calculate the column squash load

$P_y := A \cdot f_y$ $P_y = 11.412\,k$

B2. Hand Based Direct Strength "member" method with L+E and D Checks (continued)

Calculate the nominal long column (Euler) strength

$$\lambda_c := \sqrt{\frac{P_y}{P_{cre}}} \qquad \lambda_c = 1.041$$

$$P_{ne} := \begin{cases} \left(0.658^{\lambda_c^2} \cdot P_y\right) & \text{if } \lambda_c \le 1.5 \\ \left(\frac{0.877}{\lambda_c^2} \cdot P_y\right) & \text{if } \lambda_c > 1.5 \end{cases} \qquad P_{ne} = 7.253 \cdot k$$

Consider local and long column (Euler) interaction, calculate the strength

$$\lambda := \sqrt{\frac{P_{ne}}{P_{crl}}} \qquad \lambda = 2.052$$

$$P_{nl} := \begin{cases} P_{ne} & \text{if } \lambda \le 0.7776 \\ \left[1 - 0.15 \cdot \left(\frac{P_{crl}}{P_{ne}}\right)^{0.4}\right] \cdot \left(\frac{P_{crl}}{P_{ne}}\right)^{0.4} \cdot P_{ne} & \text{if } \lambda > 0.776 \end{cases} \qquad P_{nl} = 3.737 \cdot k$$

Consider distortional, calculate the strength

$$\lambda := \sqrt{\frac{P_y}{P_{crd}}} \qquad \lambda = 1.211$$

note Py, not Pne is used in the calculation. Thus disotortional and overall interaction is ignored.

$$P_{nd} := \begin{cases} P_y & \text{if } \lambda \le 0.561 \\ \left[1 - 0.25 \cdot \left(\frac{P_{crd}}{P_y}\right)^{0.6}\right] \cdot \left(\frac{P_{crd}}{P_y}\right)^{0.6} \cdot P_y & \text{if } \lambda > 0.561 \end{cases} \qquad P_{nd} = 7.266 \cdot k$$

The ultimate strength is the minimum:

$$P_{n\_B2} := \min\left(\left[P_{nl} \quad P_{nd}\right]\right) \qquad P_{n\_B2} = 3.737 \cdot k$$

$$\text{ultimate\_is} := \begin{cases} \text{"local limited to long column Pne (L+E)"} & \text{if } P_{n\_B2} = P_{nl} \\ \text{"distortional"} & \text{if } P_{n\_B2} = P_{nd} \end{cases}$$

ultimate_is = "local limited to long column Pne (L+E)"

B3. Numerical Implementation of Direct Strength "member" method with L+E and D Checks

L=local buckling D=distortional buckling E=Euler (long wavelength) buckling a "+" indicates that interaction in these modes is considered in the design method.

Finite Strip Analysis of the member (the raw data is imported from Matlab):

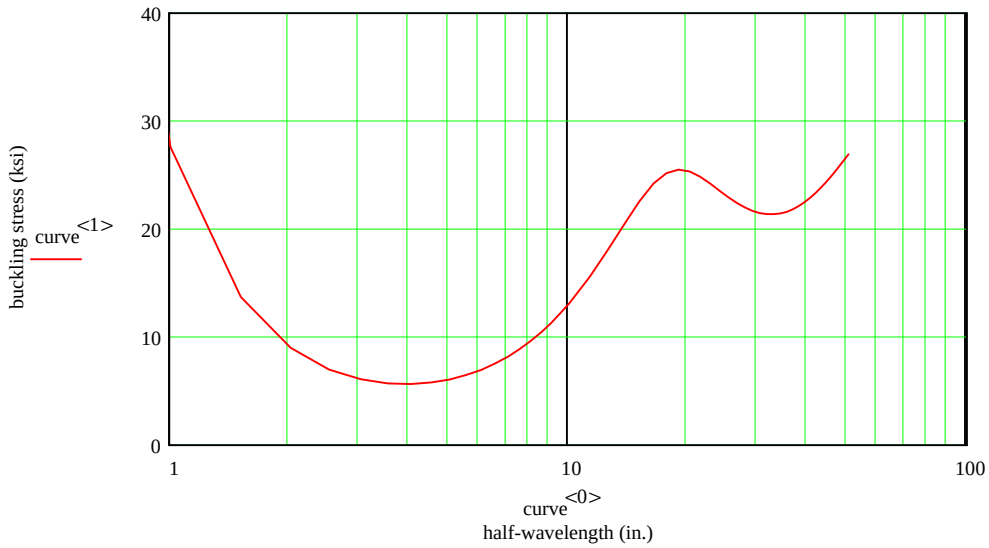

Buckling stresses from the finite strip analysis:

$f_{cr\_locals} := 5.65 \cdot ksi$ These values are manually entered from the curve.

$f_{cr\_dists} := 21.4 \cdot ksi$

$f_{cr\_longs} := F_e$ Since the analysis was stopped at approximately 50 in. the hand solution for overall buckling of the column will be employed.

Elastic Buckling Loads (subscript "s" is added to distinguish from the hand based methods)

Local $P_{crls} := A \cdot f_{cr\_locals}$ $P_{crls} = 1.837 \cdot k$

Dist. $P_{crds} := A \cdot f_{cr\_dists}$ $P_{crds} = 6.958 \cdot k$

Long $P_{cres} := A \cdot f_{cr\_longs}$ $P_{cres} = 10.54 \cdot k$

B3. Numerical Implementation of Direct Strength "member" method with L+E and D Checks (continued)

Calculate the nominal long column strength

$$\lambda_c := \sqrt{\frac{P_y}{P_{cres}}} \qquad \lambda_c = 1.041$$

$$P_{nes} := \begin{cases} \left(0.658^{\lambda_c^2} \cdot P_y\right) & \text{if } \lambda_c \le 1.5 \\ \left(\frac{0.877}{\lambda_c^2} \cdot P_y\right) & \text{if } \lambda_c > 1.5 \end{cases} \qquad P_{nes} = 7.253 \cdot k$$

Consider local and long column (Euler) interaction, calculate the strength

$$\lambda := \sqrt{\frac{P_{nes}}{P_{crls}}} \qquad \lambda = 1.987$$

$$P_{nls} := \begin{cases} P_{nes} & \text{if } \lambda \le 0.776 \\ \left[1 - 0.15 \cdot \left(\frac{P_{crls}}{P_{nes}}\right)^{0.4}\right] \cdot \left(\frac{P_{crls}}{P_{nes}}\right)^{0.4} \cdot P_{nes} & \text{if } \lambda > 0.776 \end{cases} \qquad P_{nls} = 3.825 \cdot k$$

Consider distortional, calculate the strength

$$\lambda := \sqrt{\frac{P_y}{P_{crds}}} \qquad \lambda = 1.281$$

note Py, not Pne is used in the calculation. Thus disotortional and overall interaction is ignored.

$$P_{nds} := \begin{cases} P_y & \text{if } \lambda \le 0.561 \\ \left[1 - 0.25 \cdot \left(\frac{P_{crds}}{P_y}\right)^{0.6}\right] \cdot \left(\frac{P_{crds}}{P_y}\right)^{0.6} \cdot P_y & \text{if } \lambda > 0.561 \end{cases} \qquad P_{nds} = 6.905 \cdot k$$

The ultimate strength is the minimum:

$$P_{n\_B3} := \min\left(\left[P_{nls} \;\; P_{nds}\right]\right) \qquad P_{n\_B3} = 3.825 \cdot k$$

$$\text{ultimate\_is} := \begin{cases} \text{"local limited to long column Pnes (L+E)"} & \text{if } P_{n\_B3} = P_{nls} \\ \text{"distortional"} & \text{if } P_{n\_B3} = P_{nds} \end{cases}$$

ultimate_is = "local limited to long column Pnes (L+E)"

C1. Effective width "element" based method with L+E and D+E Checks

Note, the presented solution for method C1 is in a different format, than that suggested in Appendix F.2. The results are identical, see example C1 (alternate) for solution in the same form as Appendix F.2

Calculations for C1 are nearly identical to B1 except that now the distortional buckling strength check includes the possibility of interaction with the long column (Euler) buckling modes, and thus effective width in both the distortional mode is limited to Fn (instead of Fy).

Strength in local mode from calculation in B1 $P_{n\_B1local} = 4.374 \cdot k$

Strength in distortional mode considering possibility of long column (Euler) interaction

Calculate the strength reduction factor (ρ) for distortional buckling

Find the reduction factor for the distortional stress

$$\lambda_d := \sqrt{\frac{F_n}{f_{cr\_dist}}} \qquad \lambda_d = 0.966$$

$$R_d := \min\left(\left[1 \quad \frac{1.17}{\lambda_d + 1} + 0.3\right]\right) \qquad R_d = 0.895$$

Winter's curve is used to find the strength reduction factor; but the distortional stress is reduced by Rd to account for lower post-buckling capacity in the distortional mode.

The increased slenderness is $\lambda := \sqrt{\frac{F_n}{R_d \cdot f_{cr\_dist}}} \qquad \lambda = 1.021$

The reduction factor is:

$$\rho := \begin{cases} 1 & \text{if } \lambda \le 0.673 \\ \left(1 - 0.22 \cdot \sqrt{\frac{R_d \cdot f_{cr\_dist}}{F_n}}\right) \cdot \sqrt{\frac{R_d \cdot f_{cr\_dist}}{F_n}} & \text{if } \lambda > 0.561 \end{cases} \qquad \rho = 0.769$$

Alternative method for the strength reduction factor (ρ) used in C2 and C3 and provided here for the purposes of comparison only.

$$\rho_{alt} := \begin{cases} 1 & \text{if } \lambda_d \le 0.561 \\ \left[1 - 0.25 \cdot \left(\frac{f_{cr\_dist}}{F_n}\right)^{0.6}\right] \cdot \left(\frac{f_{cr\_dist}}{F_n}\right)^{0.6} & \text{if } \lambda_d > 0.561 \end{cases} \qquad \rho_{alt} = 0.771$$

The Effective area for distortional buckling is (same reduction for all elements):

$A_e := \rho \cdot A$ $\qquad A_e = 0.25 \cdot in^2$ vs. $A = 0.325 \cdot in^2$

The strength prediction for the distortional check is

$P_{n\_C1dist\_check} := A_e \cdot F_n \qquad P_{n\_C1dist\_check} = 5.575 \cdot k$

The ultimate strength is the minimum:

$P_{n\_C1} := \min\left(\left[P_{n\_B1local} \quad P_{n\_C1dist\_check}\right]\right) \qquad P_{n\_C1} = 4.374 \cdot k$

$$ultimate\_is := \begin{cases} \text{"local limited to long column Pne (L+E)"} & \text{if } P_{n\_C1} = P_{n\_B1local} \\ \text{"distortional limited to long column Pne (D+E)"} & \text{if } P_{n\_C1} = P_{n\_C1dist\_check} \end{cases}$$

ultimate_is = "local limited to long column Pne (L+E)"

C1 - Alternate. Effective width "element" based method with L+E and D+E Checks

Appendix F.2 provides a proposed method for incorporating method C1 into the AISI Specification. The format is different than that presented in the previous example for C1, but the result is the same. For completeness, this example is provided in the same format as presented in Appendix F.2 and proposed for adoption - however, the final results are identical to method C1 presented above.

Step 1. Determine the effective area for local buckling (consider long column interaction - follow method B1)

$A_{e\_B1local} = 0.196 \cdot in^2$

Step 2. Determine the distortional buckling effective area (as described in Appendix F.2)

Determine the long column nominal stress (same as in method A1)

$F_n = 22.31 \cdot ksi$

Determine the elastic distortional buckling stress (same as fcr_dist in method A2)

$f_{ed} := f_{cr\_dist}$ $\quad f_{ed} = 23.921 \cdot ksi$

Determine the reduced elastic distortional buckling stress

$\lambda_d := \sqrt{\frac{F_n}{f_{ed}}}$ $\quad \lambda_d = 0.966$

$R_d := \min\left(\left[1 \quad \frac{1.17}{\lambda_d + 1} + 0.3\right]\right)$ $\quad R_d = 0.895$

$f_d := R_d \cdot f_{ed}$ $\quad f_d = 21.414 \cdot ksi$

Determine the effective width of each element, subjected to distortional buckling

Flange

$k_{d\_flange} := f_d \cdot \frac{12 \cdot \left(1 - \nu^2\right)}{\pi^2 E} \cdot \left(\frac{b}{t}\right)^2$ $\quad k_{d\_flange} = 3.316$

$\lambda := \frac{1.052}{\sqrt{k_{d\_flange}}} \cdot \left(\frac{b}{t}\right) \cdot \sqrt{\frac{F_n}{E}}$ $\quad \lambda = 1.021$

$\rho := \begin{cases} 1 & \text{if } \lambda \le 0.673 \\ \frac{\left(1 - \frac{0.22}{\lambda}\right)}{\lambda} & \text{if } \lambda > 0.673 \end{cases}$ $\quad \rho = 0.768$

$b_{eff} := \rho \cdot b$ $\quad b_{eff} = 1.531 \cdot in$

C1 - Alternate. Effective width "element" based method with L+E and D+E Checks (continued)

Web

$$k_{d\_web} := f_d \cdot \frac{12 \cdot \left(1 - \nu^2\right)}{\pi^2 E} \cdot \left(\frac{h}{t}\right)^2 \qquad k_{d\_web} = 21.179$$

$$\lambda := \frac{1.052}{\sqrt{k_{d\_web}}} \cdot \left(\frac{h}{t}\right) \cdot \sqrt{\frac{F_n}{E}} \qquad \lambda = 1.021$$

$$\rho := \begin{cases} 1 & \text{if } \lambda \le 0.673 \\ \dfrac{\left(1 - \dfrac{0.22}{\lambda}\right)}{\lambda} & \text{if } \lambda > 0.673 \end{cases} \qquad \rho = 0.768$$

$$h_{eff} := \rho \cdot h \qquad h_{eff} = 3.869 \cdot in$$

Lip

$$k_{d\_lip} := f_d \cdot \frac{12 \cdot \left(1 - \nu^2\right)}{\pi^2 E} \cdot \left(\frac{d}{t}\right)^2 \qquad k_{d\_lip} = 0.451$$

$$\lambda := \frac{1.052}{\sqrt{k_{d\_lip}}} \cdot \left(\frac{d}{t}\right) \cdot \sqrt{\frac{F_n}{E}} \qquad \lambda = 1.021$$

$$\rho := \begin{cases} 1 & \text{if } \lambda \le 0.673 \\ \dfrac{\left(1 - \dfrac{0.22}{\lambda}\right)}{\lambda} & \text{if } \lambda > 0.673 \end{cases} \qquad \rho = 0.768$$

$$d_{eff} := \rho \cdot d \qquad h_{eff} = 3.869 \cdot in$$

The Effective area for distortional buckling is:

$$A_{e\_dist} := t \cdot \left(h_{eff} + 2 \cdot b_{eff} + 2 \cdot d_{eff}\right) \qquad A_{e\_dist} = 0.25 \cdot in^2$$

The governinig effective area is:

$$A_e := \min\left(\left[A_{e\_B1local} \quad A_{e\_dist}\right]\right) \qquad A_e = 0.196 \cdot in^2$$

$$ultimate\_is := \begin{cases} \text{"local limited to long column (L+E)"} & \text{if } A_e = A_{e\_B1local} \\ \text{"distortional limited to long column (D+E)"} & \text{if } A_e = A_{e\_dist} \end{cases}$$

ultimate_is = "local limited to long column (L+E)"

Capacity is $P_{n\_C1alt} := A_e \cdot F_n \qquad P_{n\_C1alt} = 4.374 \cdot k$

C2. Hand Based Direct Strength "member" method with L+E and D+E Checks

L=local buckling D=distortional buckling E=Euler (long wavelength) buckling a "+" indicates that interaction in these modes is considered in the design method.

Local Buckling considering long column interaction (same as B2)

$P_{nl} = 3.737 \cdot k$

Distortional Buckling considering long column interaction

$$\lambda := \sqrt{\frac{P_{ne}}{P_{crd}}} \qquad \lambda = 0.966$$

$$P_{nd2} := \begin{cases} P_{ne} & \text{if } \lambda \le 0.561 \\ \left[1 - 0.25 \cdot \left(\frac{P_{crd}}{P_{ne}}\right)^{0.6}\right] \cdot \left(\frac{P_{crd}}{P_{ne}}\right)^{0.6} \cdot P_{ne} & \text{if } \lambda > 0.561 \end{cases} \qquad P_{nd2} = 5.592 \cdot k$$

note a "2" is added to the subscript of Pnd to distinguish from the calculation method used in example B2, which ignores long column (Euler) interaction, but is otherwise performed in a similar manner.

The ultimate strength is the minimum:

$$P_{n\_C2} := \min\left(\left[P_{nl} \quad P_{nd2}\right]\right) \qquad P_{n\_C2} = 3.737 \cdot k$$

$$\text{ultimate\_is} := \begin{cases} \text{"local limited to long column Pne (L+E)"} & \text{if } P_{n\_C2} = P_{nl} \\ \text{"distortional limited to long column Pne (D+E)"} & \text{if } P_{n\_C2} = P_{nd2} \end{cases}$$

ultimate_is = "local limited to long column Pne (L+E)"

C3. Hand Based Direct Strength "member" method with L+E and D+E Checks

L=local buckling D=distortional buckling E=Euler (long wavelength) buckling a "+" indicates that interaction in these modes is considered in the design method.

Local Buckling considering long column interaction (same as B3)

$P_{nls} = 3.825 \cdot k$

Distortional Buckling considering long column interaction

$$\lambda := \sqrt{\frac{P_{nes}}{P_{crds}}} \qquad \lambda = 1.021$$

$$P_{nd2s} := \begin{cases} P_{nes} & \text{if } \lambda \le 0.561 \\ \left[1 - 0.25 \cdot \left(\frac{P_{crds}}{P_{nes}}\right)^{0.6}\right] \cdot \left(\frac{P_{crds}}{P_{nes}}\right)^{0.6} \cdot P_{nes} & \text{if } \lambda > 0.561 \end{cases} \qquad P_{nd2s} = 5.35 \cdot k$$

The ultimate strength is the minimum:

$$P_{n\_C3} := \min\left(\left[P_{nls} \;\; P_{nd2s}\right]\right) \qquad P_{n\_C3} = 3.825 \cdot k$$

$$\text{ultimate\_is} := \begin{cases} \text{"local limited to long column Pnes (L+E)"} & \text{if } P_{n\_C3} = P_{nls} \\ \text{"distortional limited to long column Pnes (D+E)"} & \text{if } P_{n\_C3} = P_{nd2s} \end{cases}$$

ultimate_is = "local limited to long column Pnes (L+E)"

D1. Effective width "element" based method with L+E, D+E and L+D Checks

L=local buckling D=distortional buckling E=Euler (long wavelength) buckling a "+" indicates that interaction in these modes is considered in the design method.

This design method is the same as C1 with the addition of a local + distortional check

Check local + distortional interaction

Find the limiting, nominal, distortional stress (Fnd)

Local and long column (Euler) interaction is completed by calculating the effective width for local buckling at the nominal long column stress (Fn). Local and distortional interaction is completed in a similar manner by calculating the effective width for local buckling at the nominal distortional stress (Fnd)

Distortional slenderness is

$$\lambda := \sqrt{\frac{f_y}{f_{cr\_dist}}} \qquad \lambda = 1.211$$

$$F_{nd} := \begin{cases} 1 & \text{if } \lambda \le 0.561 \\ \left[1 - 0.25 \cdot \left(\frac{f_{cr\_dist}}{f_y}\right)^{0.6}\right] \cdot \left(\frac{f_{cr\_dist}}{f_y}\right)^{0.6} \cdot f_y & \text{if } \lambda > 0.561 \end{cases} \qquad F_{nd} = 22.348 \cdot ksi$$

Determine the effective width of the flange web and lip considering L+D, thus all eff. width calculations are limited to the distortional nominal stress Fnd

Effective Width of the Web

The plate buckling coefficient is

$$k_{web} := 4$$

The slenderness is

$$\lambda := \frac{1.052}{\sqrt{k_{web}}} \cdot \left(\frac{h}{t}\right) \cdot \sqrt{\frac{F_{nd}}{E}} \qquad \lambda = 2.351$$

The reduction factor is:

$$\rho := \begin{cases} 1 & \text{if } \lambda \le 0.673 \\ \frac{\left(1 - \frac{0.22}{\lambda}\right)}{\lambda} & \text{if } \lambda > 0.673 \end{cases} \qquad \rho = 0.386$$

The effective width of the web:

$$h_{eff} := \rho \cdot h \qquad h_{eff} = 1.941 \cdot in$$

D1. Effective width "element" based method with L+E, D+E and L+D Checks (continued)

Effective Width of the Flange

The plate buckling coefficient is

$k_{flange} := 4$

The slenderness is

$$\lambda := \frac{1.052}{\sqrt{k_{flange}}} \cdot \left(\frac{b}{t}\right) \cdot \sqrt{\frac{F_{nd}}{E}} \qquad \lambda = 0.93$$

The reduction factor is:

$$\rho := \begin{cases} 1 & \text{if } \lambda \le 0.673 \\ \dfrac{\left(1 - \dfrac{0.22}{\lambda}\right)}{\lambda} & \text{if } \lambda > 0.673 \end{cases} \qquad \rho = 0.821$$

The effective width of the flange:

$b_{eff} := \rho \cdot b \qquad b_{eff} = 1.635 \cdot in$

Effective Width of the Lip

The plate buckling coefficient is $k_{lip} := 0.43$

The slenderness is

$$\lambda := \frac{1.052}{\sqrt{k_{lip}}} \cdot \left(\frac{d}{t}\right) \cdot \sqrt{\frac{F_{nd}}{E}} \qquad \lambda = 1.047$$

The reduction factor is:

$$\rho := \begin{cases} 1 & \text{if } \lambda \le 0.673 \\ \dfrac{\left(1 - \dfrac{0.22}{\lambda}\right)}{\lambda} & \text{if } \lambda > 0.673 \end{cases} \qquad \rho = 0.754$$

The effective width of the lip:

$d_{eff} := \rho \cdot d \qquad d_{eff} = 0.555 \cdot in$

The Effective area is:

$A_e := t \cdot \left(h_{eff} + 2 \cdot b_{eff} + 2 \cdot d_{eff}\right) \qquad A_e = 0.196 \cdot in^2$ vs. $A = 0.325 \cdot in^2$

The strength prediction for local buckling (L) considering long column (E) interaction is

$P_{n\_D1localdist} := A_e \cdot F_{nd} \qquad P_{n\_D1localdist} = 4.378 \cdot k$

The ultimate strength is the minimum:

$P_{n\_D1} := \min\left(\left[P_{n\_B1local} \;\; P_{n\_A2dist\_check} \;\; P_{n\_D1localdist}\right]\right) \qquad P_{n\_D1} = 4.374 \cdot k$

$$ultimate\_is := \begin{cases} \text{"local (k=4 sol'n) limited to Fn (L+E)"} & \text{if } P_{n\_D1} = P_{n\_B1local} \\ \text{"distortional"} & \text{if } P_{n\_D1} = P_{n\_A2dist\_check} \\ \text{"local limited to distortional Fnd (L+D)"} & \text{if } P_{n\_D1} = P_{n\_D1localdist} \end{cases}$$

ultimate_is = "local (k=4 sol'n) limited to Fn (L+E)"

D2. Hand Based Direct Strength "member" method with L+E, D+E and L+D Checks

L=local buckling D=distortional buckling E=Euler (long wavelength) buckling a "+" indicates that interaction in these modes is considered in the design method.

Local Buckling considering long column interaction (same as B2)

$P_{nl} = 3.737 \cdot k$

Distortional Buckling considering long column interaction

$P_{nd2} = 5.592 \cdot k$

Local Buckling considering distortional interaction

Consider distortional alone, calculate the strength (done previoulsy in B2)

$P_{nd} = 7.266 \cdot k$

Now consider local limited to nominal distortional load

$$\lambda := \sqrt{\frac{P_{nd}}{P_{crl}}} \qquad \lambda = 2.054$$

$$P_{nld} := \begin{cases} P_{nd} & \text{if } \lambda \le 0.776 \\ \left[1 - 0.15 \cdot \left(\frac{P_{crl}}{P_{nd}}\right)^{0.4}\right] \cdot \left(\frac{P_{crl}}{P_{nd}}\right)^{0.4} \cdot P_{nd} & \text{if } \lambda > 0.776 \end{cases} \qquad P_{nld} = 3.741 \cdot k$$

The ultimate strength is the minimum:

$$P_{n\_D2} := \min\left(\left[P_{nl} \quad P_{nd2} \quad P_{nld}\right]\right) \qquad P_{n\_D2} = 3.737 \cdot k$$

$$ultimate\_is := \begin{cases} \text{"local limited to long column Pne (L+E)"} & \text{if } P_{n\_D2} = P_{nl} \\ \text{"distortional limited to long column Pne (D+E)"} & \text{if } P_{n\_D2} = P_{nd2} \\ \text{"local limited to distortional Pnd (L+D)"} & \text{if } P_{n\_D2} = P_{nld} \end{cases}$$

ultimate_is = "local limited to long column Pne (L+E)"

D3. Numerical Implementation of Direct Strength "member" method with L+E, D+E and L+D Checks

L=local buckling D=distortional buckling E=Euler (long wavelength) buckling a "+" indicates that interaction in these modes is considered in the design method.

Local Buckling considering long column interaction (same as B3)

$P_{nls} = 3.825 \cdot k$

Distortional Buckling considering long column interaction (same as C3)

$P_{nd2s} = 5.35 \cdot k$

Local Buckling considering distortional interaction

Consider distortional alone, calculate the strength (done previously in B3)

$P_{nds} = 6.905 \cdot k$

Now consider local limited to nominal distortional load

$$\lambda := \sqrt{\frac{P_{nds}}{P_{crls}}} \qquad \lambda = 1.939$$

$$P_{nlds} := \begin{cases} P_{nds} & \text{if } \lambda \le 0.776 \\ \left[1 - 0.15 \cdot \left(\frac{P_{crls}}{P_{nds}}\right)^{0.4}\right] \cdot \left(\frac{P_{crls}}{P_{nds}}\right)^{0.4} \cdot P_{nds} & \text{if } \lambda > 0.776 \end{cases} \qquad P_{nlds} = 3.707 \cdot k$$

The ultimate strength is the minimum:

$$P_{n\_D3} := \min\left(\left[P_{nls} \quad P_{nd2s} \quad P_{nlds}\right]\right) \qquad P_{n\_D3} = 3.707 \cdot k$$

$$ultimate\_is := \begin{cases} \text{"local limited to long column Pne (L+E)"} & \text{if } P_{n\_D3} = P_{nls} \\ \text{"distortional limited to long column Pne (D+E)"} & \text{if } P_{n\_D3} = P_{nd2s} \\ \text{"local limited to distortional Pnd (L+D)"} & \text{if } P_{n\_D3} = P_{nlds} \end{cases}$$

ultimate_is = "local limited to distortional Pnd (L+D)"

Summary

A. AISI (1996) Methods and Simple Modifications
- **A1. Current AISI (1996) Method**
- **A2. AISI (1996) with a Distortional Check**

B. New Methods which include only Local+Euler Check and Distortional Check
- **B1. Effective width "element" based method**
- **B2. Hand Implementation of Direct Strength "member" based method**
- **B3. Numerical Implementation of Direct Strength "member" based method**

C. New methods which include Local+Euler Check and Dist+Euler Check
- **C1 - C3 same as B methods with interactions listed above**

D. New methods which include Local+Euler, Dist+Euler, and Local+Dist Check
- **D1 - D3 same as B and C methods with interactions listed above**

$P_{n\_A1} = 4.249 \cdot k$

$P_{n\_A2} = 4.249 \cdot k$

$P_{n\_B1} = 4.374 \cdot k$

$P_{n\_B2} = 3.737 \cdot k$

$P_{n\_B3} = 3.825 \cdot k$

$P_{n\_C1} = 4.374 \cdot k$

$P_{n\_C2} = 3.737 \cdot k$

$P_{n\_C3} = 3.825 \cdot k$

$P_{n\_D1} = 4.374 \cdot k$

$P_{n\_D2} = 3.737 \cdot k$

$P_{n\_D3} = 3.707 \cdot k$

Predicted Nominal Capacity $P_{test} := 3.8 \cdot k$

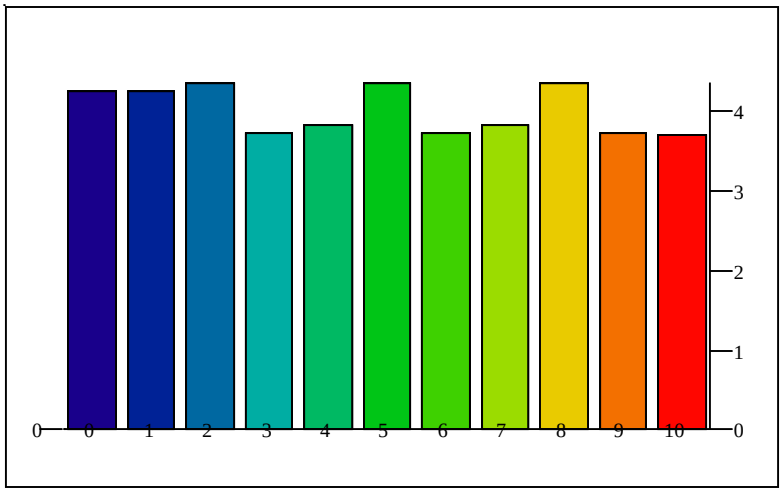

$\frac{P_{n\_all}}{k}$

Test to Predicted Ratio for Loughlan (1979) #L6

$R_{tp} =$

	0	
0	0.894	A1
1	0.894	A2
2	0.869	B1
3	1.017	B2
4	0.993	B3
5	0.869	C1
6	1.017	C2
7	0.993	C3
8	0.869	D1
9	1.017	D2
10	1.025	D3

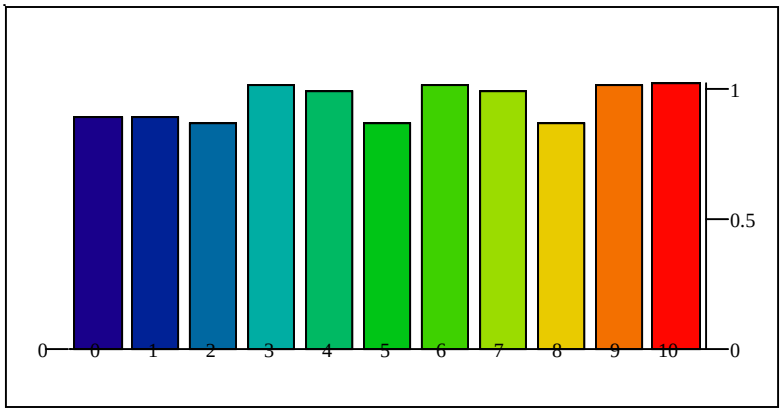

R_{tp}

see the text for complete discussion of the analyzed design methods.

Researcher	Specimen ID	h (mm)	b (mm)	d (mm)	t (mm)	L (mm)	fy (MPa)	P (kN)	fcr_local (MPa)	fcr_dist (MPa)	test to predicted ratios for studied methods											AISI comparison	
											A1	A2	B1	B2	B3	C1	C2	C3	D1	D2	D3	C1/A1	C3/A1
Mulligan (1983) Pekoz (1987)	GM1	155	80	18	1.14	1600	223	43.6	54	130	0.94	0.94	0.94	1.06	1.02	0.94	1.06	1.02	1.18	1.35	1.32	1.00	0.91
Mulligan (1983) Pekoz (1987)	GM2	129	80	16	1.14	1905	221	46.3	76	137	1.05	1.05	1.05	1.14	1.10	1.05	1.14	1.10	1.27	1.38	1.34	1.00	0.96
Mulligan (1983) Pekoz (1987)	GM3	156	80	16	1.17	3073	221	36.5	56	121	0.96	0.96	0.96	1.08	1.05	0.96	1.08	1.05	0.99	1.12	1.10	1.00	0.91
Mulligan (1983) Pekoz (1987)	GM4	154	80	17	1.14	3073	221	37.4	54	125	1.01	1.01	1.01	1.15	1.11	1.01	1.15	1.11	1.04	1.18	1.15	1.00	0.91
Mulligan (1983) Pekoz (1987)	GM5	155	79	18	1.24	1905	224	52.5	64	144	1.01	1.01	1.01	1.15	1.11	1.01	1.15	1.11	1.20	1.37	1.34	1.00	0.91
Mulligan (1983) Pekoz (1987)	GM6	230	80	17	1.14	1829	225	42.7	25	71	0.94	0.94	0.94	1.14	1.12	0.94	1.14	1.12	1.39	1.67	1.69	0.99	0.83
Mulligan (1983) Pekoz (1987)	GM7	231	80	17	1.14	2413	223	38.9	25	70	0.93	0.93	0.93	1.14	1.12	0.93	1.14	1.12	1.27	1.53	1.55	1.00	0.83
Mulligan (1983) Pekoz (1987)	GM8	231	80	17	1.12	2997	223	33.8	24	69	0.93	0.93	0.93	1.14	1.12	0.93	1.14	1.12	1.14	1.38	1.40	1.00	0.83
Mulligan (1983) Pekoz (1987)	GM9	229	80	18	1.22	2413	228	48.0	29	81	1.00	1.00	1.00	1.23	1.21	1.00	1.23	1.21	1.31	1.59	1.60	1.00	0.83
Mulligan (1983) Pekoz (1987)	GM10	113	113	19	1.22	2515	236	48.9	89	111	0.98	0.98	0.98	0.92	0.91	0.98	0.94	1.00	1.14	1.08	1.11	1.00	0.98
Mulligan (1983) Pekoz (1987)	GM11	221	113	19	1.22	1908	219	54.7	30	74	0.98	0.98	0.98	1.10	1.06	0.98	1.10	1.06	1.49	1.69	1.65	1.00	0.92
Mulligan (1983) Pekoz (1987)	GM12	222	112	19	1.22	2517	244	53.8	30	75	0.95	0.95	0.95	1.07	1.04	0.95	1.07	1.04	1.42	1.61	1.57	1.00	0.92
Mulligan (1983) Pekoz (1987)	GM13	221	113	19	1.22	2520	234	52.5	30	74	0.95	0.95	0.95	1.06	1.03	0.95	1.06	1.03	1.40	1.59	1.55	1.00	0.92
Thomasson (1978) Pekoz (1987)	A71	299	100	20	0.64	2690	391	16.0	5	26	0.85	0.85	0.85	0.95	0.94	0.85	0.95	0.94	1.63	1.96	2.00	1.00	0.91
Thomasson (1978) Pekoz (1987)	A74	300	101	21	0.64	2690	395	16.2	5	27	0.85	0.85	0.85	0.95	0.93	0.85	0.95	0.93	1.61	1.93	1.98	1.00	0.92
Thomasson (1978) Pekoz (1987)	A75	299	101	20	0.64	2690	398	15.5	5	26	0.82	0.82	0.82	0.91	0.89	0.82	0.91	0.89	1.57	1.88	1.92	1.00	0.91
Thomasson (1978) Pekoz (1987)	A76	300	100	20	0.66	2690	288	14.5	5	26	0.81	0.81	0.81	0.92	0.90	0.81	0.92	0.90	1.49	1.81	1.85	1.00	0.89
Thomasson (1978) Pekoz (1987)	A101	300	101	20	0.94	2690	464	36.9	10	39	0.89	0.89	0.89	1.05	1.03	0.89	1.05	1.03	1.56	1.90	1.94	1.00	0.87
Thomasson (1978) Pekoz (1987)	A102	300	101	20	0.94	2690	460	35.0	10	39	0.85	0.85	0.85	0.99	0.98	0.85	0.99	0.98	1.48	1.81	1.84	1.00	0.87
Thomasson (1978) Pekoz (1987)	A103	299	101	20	0.94	2690	460	37.1	10	39	0.90	0.90	0.90	1.05	1.03	0.90	1.05	1.03	1.56	1.91	1.95	1.00	0.87
Thomasson (1978) Pekoz (1987)	A104	298	100	20	0.97	2690	475	34.5	10	16													
Thomasson (1978) Pekoz (1987)	A151	299	100	20	1.45	2690	382	76.5	24	64	0.89	0.89	0.89	1.09	1.07	0.97	1.09	1.07	1.36	1.66	1.68	0.92	0.83
Thomasson (1978) Pekoz (1987)	A152	300	100	20	1.42	2690	379	69.8	23	62	0.84	0.84	0.84	1.03	1.01	0.91	1.03	1.01	1.31	1.59	1.61	0.92	0.83
Thomasson (1978) Pekoz (1987)	A153	300	100	21	1.37	2690	395	71.2	22	62	0.90	0.90	0.90	1.10	1.08	0.95	1.10	1.08	1.38	1.70	1.72	0.95	0.83
Thomasson (1978) Pekoz (1987)	A154	301	100	23	1.40	2690	393	72.9	23	68	0.88	0.88	0.88	1.07	1.05	0.89	1.07	1.05	1.30	1.60	1.63	0.99	0.83
Thomasson (1978) Pekoz (1987)	A156	299	100	20	1.40	2690	381	68.9	23	61	0.85	0.85	0.85	1.04	1.02	0.92	1.04	1.02	1.32	1.61	1.63	0.92	0.83
Loughlan (1979) Pekoz (1987)	L1	102	51	19	0.81	1905	242	13.9	63	195	0.70	0.70	0.68	0.75	0.73	0.68	0.75	0.73	0.68	0.75	0.73	1.03	0.96
Loughlan (1979) Pekoz (1987)	L2	254	50	19	0.79	1295	242	16.0	11	33	0.74	0.74	0.72	0.92	0.92	0.74	0.92	0.92	1.24	1.57	1.73	1.01	0.81
Loughlan (1979) Pekoz (1987)	L3	103	63	25	0.79	1905	242	15.7	57	187	0.73	0.73	0.70	0.71	0.68	0.70	0.71	0.68	0.73	0.75	0.74	1.04	1.07
Loughlan (1979) Pekoz (1987)	L4	102	63	25	0.81	1600	242	16.8	61	193	0.71	0.71	0.68	0.69	0.66	0.68	0.69	0.66	0.74	0.76	0.75	1.04	1.07
Loughlan (1979) Pekoz (1987)	L5	102	63	26	0.79	1295	242	18.2	58	191	0.78	0.78	0.74	0.74	0.71	0.74	0.74	0.71	0.84	0.85	0.84	1.05	1.09
Loughlan (1979) Pekoz (1987)	L6	128	51	19	0.79	1905	242	16.9	39	147	0.88	0.88	0.86	1.00	0.98	0.86	1.00	0.98	0.86	1.00	1.02	1.03	0.90
Loughlan (1979) Pekoz (1987)	L7	126	50	19	0.79	1600	242	17.7	40	151	0.87	0.87	0.84	0.98	0.95	0.84	0.98	0.95	0.90	1.05	1.06	1.03	0.91
Loughlan (1979) Pekoz (1987)	L8	126	51	19	0.79	1295	242	19.2	40	151	0.87	0.87	0.84	0.97	0.95	0.84	0.97	0.95	0.97	1.13	1.14	1.03	0.91
Loughlan (1979) Pekoz (1987)	L9	128	63	25	0.79	1905	242	19.3	38	154	0.89	0.89	0.85	0.92	0.90	0.85	0.92	0.90	0.93	1.02	1.02	1.04	1.00
Loughlan (1979) Pekoz (1987)	L10	127	63	26	0.79	1600	242	20.3	39	158	0.90	0.90	0.85	0.91	0.88	0.85	0.91	0.88	0.97	1.05	1.05	1.05	1.01
Loughlan (1979) Pekoz (1987)	L11	127	63	26	0.81	1295	242	20.7	41	162	0.84	0.84	0.80	0.86	0.83	0.80	0.86	0.83	0.94	1.02	1.02	1.05	1.01
Loughlan (1979) Pekoz (1987)	L12	152	51	19	0.81	1905	242	14.9	30	115	0.75	0.75	0.73	0.88	0.86	0.73	0.88	0.86	0.77	0.93	0.95	1.03	0.87
Loughlan (1979) Pekoz (1987)	L13	152	51	20	0.81	1600	242	15.7	30	119	0.73	0.73	0.70	0.84	0.83	0.70	0.84	0.83	0.80	0.96	0.99	1.04	0.88
Loughlan (1979) Pekoz (1987)	L14	152	50	19	0.81	1295	242	17.1	30	115	0.75	0.75	0.72	0.87	0.86	0.72	0.87	0.86	0.88	1.07	1.10	1.03	0.87
Loughlan (1979) Pekoz (1987)	L15	154	63	25	0.79	1905	235	21.8	27	126	1.02	1.02	0.98	1.10	1.08	0.98	1.10	1.08	1.11	1.27	1.29	1.04	0.94
Loughlan (1979) Pekoz (1987)	L16	154	63	26	0.81	1600	242	23.0	28	132	0.97	0.97	0.92	1.04	1.01	0.92	1.04	1.01	1.09	1.25	1.27	1.05	0.96
Loughlan (1979) Pekoz (1987)	L17	152	63	26	0.79	1295	242	23.6	28	130	1.00	1.00	0.95	1.06	1.03	0.95	1.06	1.03	1.18	1.34	1.36	1.05	0.97
Loughlan (1979) Pekoz (1987)	L18	178	50	19	0.79	1905	242	13.9	21	81	0.75	0.75	0.72	0.90	0.89	0.72	0.90	0.89	0.82	1.01	1.07	1.03	0.84
Loughlan (1979) Pekoz (1987)	L19	177	50	19	0.79	1600	242	15.1	21	82	0.74	0.74	0.72	0.89	0.88	0.72	0.89	0.88	0.89	1.10	1.16	1.03	0.85
Loughlan (1979) Pekoz (1987)	L20	178	50	20	0.81	1295	242	16.3	22	86	0.71	0.71	0.69	0.84	0.83	0.69	0.84	0.83	0.90	1.11	1.17	1.04	0.86
Loughlan (1979) Pekoz (1987)	L21	178	63	25	0.79	1905	242	17.2	20	102	0.79	0.79	0.76	0.89	0.87	0.76	0.89	0.87	0.91	1.08	1.11	1.04	0.91
Loughlan (1979) Pekoz (1987)	L22	178	63	25	0.79	1600	242	19.7	20	102	0.86	0.86	0.83	0.96	0.94	0.83	0.96	0.94	1.05	1.23	1.27	1.04	0.92
Loughlan (1979) Pekoz (1987)	L23	177	63	26	0.79	1295	242	18.4	21	105	0.78	0.78	0.74	0.85	0.84	0.74	0.85	0.84	0.97	1.13	1.17	1.05	0.93
Loughlan (1979) Pekoz (1987)	L24	152	49	18	1.63	1905	233	65.8	120	242	1.22	1.22	1.22	1.25	1.23	1.22	1.25	1.23	1.22	1.25	1.23	1.00	0.99
Loughlan (1979) Pekoz (1987)	L25	152	62	25	1.65	1905	233	71.2	120	283	0.94	0.94	0.94	1.03	1.01	0.94	1.03	1.01	0.94	1.03	1.01	1.00	0.93
Loughlan (1979) Pekoz (1987)	L26	152	62	25	1.68	1600	233	72.9	124	289	0.87	0.87	0.87	0.97	0.95	0.87	0.97	0.95	0.87	0.97	0.95	1.00	0.92
Loughlan (1979) Pekoz (1987)	L27	151	62	25	1.65	1295	233	73.8	122	285	0.87	0.87	0.86	0.97	0.94	0.86	0.97	0.94	0.88	0.99	0.99	1.01	0.92
Loughlan (1979) Pekoz (1987)	L28	178	49	18	1.63	1905	233	51.2	88	175	0.95	0.95	0.95	0.99	0.98	0.95	0.99	0.98	0.95	0.99	0.98	1.00	0.97
Loughlan (1979) Pekoz (1987)	L29	178	49	18	1.65	1600	233	56.0	91	178	0.91	0.91	0.91	0.96	0.96	0.91	0.96	0.96	0.91	0.96	0.99	1.00	0.95

Researcher	Specimen ID	h (mm)	b (mm)	d (mm)	t (mm)	L (mm)	fy (MPa)	P (kN)	fcr_local (MPa)	fcr_dist (MPa)	test to predicted ratios for studied methods											AISI comparison	
											A1	A2	B1	B2	B3	C1	C2	C3	D1	D2	D3	C1/A1	C3/A1
Loughlan (1979) Pekoz (1987)	L30	176	49	18	1.65	1295	233	60.5	93	183	0.88	0.88	0.88	0.96	0.95	0.88	0.96	0.95	0.95	1.01	1.06	1.00	0.93
Loughlan (1979) Pekoz (1987)	L31	178	62	25	1.63	1905	233	75.6	87	223	1.01	1.01	1.01	1.15	1.13	1.01	1.15	1.13	1.01	1.15	1.14	1.00	0.89
Loughlan (1979) Pekoz (1987)	L32	178	62	25	1.63	1600	233	75.6	87	223	0.94	0.94	0.94	1.08	1.07	0.94	1.08	1.07	0.97	1.11	1.14	1.00	0.88
Loughlan (1979) Pekoz (1987)	L33	177	62	25	1.63	1295	233	80.1	88	225	0.95	0.95	0.94	1.10	1.08	0.94	1.10	1.08	1.03	1.18	1.20	1.01	0.88
Mulligan (1983) Stubs	SLC/1 60x30	81	40	9	1.22	304	226	46.3	225	296	1.17	1.17	1.12	1.16	1.13	1.14	1.16	1.16	1.27	1.28	1.25	1.02	1.01
Mulligan (1983) Stubs	SLC/1 90x30	115	40	9	1.22	304	226	44.7	116	183	1.09	1.09	1.08	1.16	1.14	1.10	1.16	1.14	1.37	1.44	1.44	1.00	0.96
Mulligan (1983) Stubs	SLC/1 120x30	153	41	9	1.22	278	226	45.1	66	100	1.08	1.14	1.14	1.18	1.24	1.16	1.18	1.26	1.60	1.68	1.77	0.93	0.86
Mulligan (1983) Stubs	SLC/1 60x60	79	81	17	1.20	458	230	58.7	171	279	1.12	1.12	1.12	1.06	1.04	1.12	1.06	1.04	1.23	1.17	1.16	1.00	1.07
Mulligan (1983) Stubs	SLC/2 60x60	78	80	17	1.21	458	230	60.5	178	283	1.14	1.14	1.14	1.08	1.06	1.14	1.08	1.06	1.25	1.19	1.18	1.00	1.07
Mulligan (1983) Stubs	SLC/1 120x60	150	81	17	1.20	457	230	57.8	63	184	1.04	1.04	1.04	1.17	1.13	1.04	1.17	1.13	1.24	1.39	1.42	1.00	0.92
Mulligan (1983) Stubs	SLC/2 120x60	150	81	16	1.20	457	230	60.5	63	171	1.11	1.11	1.10	1.23	1.19	1.10	1.23	1.19	1.35	1.51	1.53	1.01	0.93
Mulligan (1983) Stubs	SLC/1 180x60	227	80	17	1.20	559	230	56.9	29	77	1.02	1.02	1.02	1.24	1.22	1.02	1.24	1.22	1.47	1.78	1.99	1.00	0.84
Mulligan (1983) Stubs	SLC/2 180x60	227	81	17	1.19	685	230	56.9	28	76	1.04	1.04	1.04	1.26	1.24	1.04	1.26	1.24	1.60	1.93	2.01	1.00	0.84
Mulligan (1983) Stubs	SLC/1 240x60	299	81	17	1.19	559	230	56.9	17	41	1.02	1.02	1.02	1.29	1.29	1.02	1.29	1.30	1.71	2.13	2.56	1.00	0.79
Mulligan (1983) Stubs	SLC/2 240x60	300	81	17	1.19	914	239	53.4	17	41	0.96	1.10	1.10	1.21	1.20	1.13	1.21	1.22	1.86	2.28	2.38	0.85	0.78
Mulligan (1983) Stubs	SLC/3 240x60	299	81	17	1.20	558	230	56.0	17	42	0.99	0.99	0.99	1.25	1.25	0.99	1.25	1.26	1.66	2.06	2.47	1.00	0.79
Mulligan (1983) Stubs	SLC/1 60x90	80	113	19	1.14	648	223	51.2	88	166	1.07	1.07	1.07	1.05	1.01	1.07	1.05	1.01	1.28	1.27	1.24	1.00	1.06
Mulligan (1983) Stubs	SLC/2 60x90	79	113	19	1.14	647	223	52.5	88	166	1.10	1.10	1.10	1.08	1.04	1.10	1.08	1.04	1.31	1.30	1.27	1.00	1.06
Mulligan (1983) Stubs	SLC/1 90x90	114	113	19	1.13	647	225	52.9	76	155	1.07	1.07	1.07	0.99	0.98	1.07	0.99	0.98	1.34	1.27	1.26	1.00	1.09
Mulligan (1983) Stubs	SLC/2 90x90	113	113	19	1.14	647	225	53.4	78	156	1.06	1.06	1.06	0.99	0.97	1.06	0.99	0.97	1.33	1.26	1.25	1.00	1.09
Mulligan (1983) Stubs	SLC/1 180x90	280	144	33	1.55	891	412	138.6	30	122	1.03	1.03	1.03	1.09	1.05	1.03	1.09	1.05	1.39	1.53	1.75	1.00	0.98
Mulligan (1983) Stubs	SLC/2 180x90	280	145	33	1.55	892	412	139.7	30	122	1.03	1.03	1.03	1.10	1.06	1.03	1.10	1.06	1.40	1.54	1.76	1.00	0.98
Mulligan (1983) Stubs	SLC/3 180x90	223	113	19	1.22	647	368	67.6	30	91	0.89	0.89	0.87	0.95	0.91	0.87	0.95	0.91	1.34	1.52	1.63	1.03	0.97
Mulligan (1983) Stubs	SLC/4 180x90	222	114	18	1.28	648	199	61.4	33	92	1.04	1.04	1.02	1.15	1.11	1.02	1.15	1.11	1.42	1.59	1.65	1.02	0.94
Mulligan (1983) Stubs	SLC/5 180x90	222	114	19	1.29	648	199	64.9	34	98	1.06	1.06	1.06	1.19	1.15	1.06	1.19	1.15	1.42	1.60	1.68	1.00	0.92
Mulligan (1983) Stubs	SLC/1 270x90	330	114	18	1.27	762	199	60.5	15	40	1.03	1.03	1.01	1.22	1.20	1.01	1.22	1.20	1.72	2.07	2.31	1.02	0.85
Mulligan (1983) Stubs	SLC/2 270x90	329	114	18	1.28	971	203	62.3	16	41	1.04	1.09	1.09	1.23	1.21	1.12	1.23	1.21	1.89	2.26	2.32	0.93	0.86
Mulligan (1983) Stubs	SLC/1 360x90	440	112	19	1.24	762	201	55.6	8	21	0.96	0.96	0.96	1.20	1.33	0.97	1.20	1.34	1.88	2.34	2.88	0.99	0.71
Miller and Pekoz (1994)	LC-1	89	34	10	1.93	1307	366	50.3	473	548	0.87	0.87	0.87	0.87	0.86	0.87	0.87	0.86	0.87	0.87	0.86	1.00	1.01
Miller and Pekoz (1994)	LC-2	89	34	11	1.92	1310	366	45.8	470	568	0.78	0.78	0.78	0.78	0.77	0.78	0.78	0.77	0.78	0.78	0.77	1.00	1.01
Miller and Pekoz (1994)	LC-3	89	34	11	1.94	1310	366	47.6	479	575	0.80	0.80	0.80	0.80	0.79	0.80	0.80	0.79	0.80	0.80	0.79	1.00	1.01
Miller and Pekoz (1994)	LC-4	151	34	7	0.90	1310	302	15.8	38	53	0.92	0.92	0.92	1.03	1.03	1.08	1.08	1.15	1.14	1.21	1.27	0.85	0.80
Miller and Pekoz (1994)	LC-6	151	34	8	0.89	1308	302	13.3	37	58	0.76	0.76	0.76	0.86	0.86	0.85	0.86	0.91	0.91	0.99	1.04	0.89	0.83
Miller and Pekoz (1994)	LC-7	151	33	8	0.90	1307	302	15.1	38	58	0.90	0.90	0.90	0.99	0.99	0.99	0.99	1.06	1.03	1.11	1.17	0.91	0.84
Miller and Pekoz (1994)	LC-10	89	35	11	1.92	1308	366	97.9	469	562	1.09	1.09	1.09	1.02	1.00	1.09	1.05	1.06	1.09	1.05	1.06	1.00	1.02
Miller and Pekoz (1994)	LC-14	151	34	8	0.91	2531	302	6.5	39	59	1.01	1.01	1.01	0.94	0.94	1.01	0.94	0.94	1.01	0.94	0.94	1.00	1.07
Miller and Pekoz (1994)	LC-15	151	34	8	0.90	2534	302	14.5	38	58	0.78	0.78	0.78	0.89	0.89	0.89	0.89	0.95	0.97	1.06	1.11	0.88	0.82
Miller and Pekoz (1994)	LC-17	90	34	11	1.92	2532	366	55.6	460	559	1.06	1.06	1.06	1.06	1.06	1.06	1.06	1.06	1.06	1.06	1.06	1.00	1.00
Miller and Pekoz (1994)	LC-18	90	35	11	1.92	2532	366	49.8	459	554	0.93	0.93	0.93	0.93	0.93	0.93	0.93	0.93	0.93	0.93	0.93	1.00	1.00
Miller and Pekoz (1994)	LC-19	90	35	11	1.92	2531	366	26.7	459	554	1.50	1.50	1.50	1.50	1.50	1.50	1.50	1.50	1.50	1.50	1.50	1.00	1.00
Miller and Pekoz (1994)	LC-21	90	34	11	1.91	1300	366	54.1	455	555	0.92	0.92	0.92	0.92	0.90	0.92	0.92	0.90	0.92	0.92	0.90	1.00	1.02
Miller and Pekoz (1994)	LC-22	90	35	11	1.92	1313	366	52.5	459	554	0.86	0.86	0.86	0.86	0.84	0.86	0.86	0.84	0.86	0.86	0.84	1.00	1.02
Miller and Pekoz (1994)	LC-23	90	35	11	1.91	1318	366	50.3	454	550	0.83	0.83	0.83	0.83	0.81	0.83	0.83	0.81	0.83	0.83	0.81	1.00	1.02
Miller and Pekoz (1994)	LC-24	90	35	11	1.92	1305	366	103.6	459	554	1.15	1.15	1.15	1.07	1.06	1.15	1.11	1.12	1.15	1.11	1.12	1.00	1.02
Miller and Pekoz (1994)	LC-25	151	34	8	0.90	1310	366	24.2	38	58	0.86	0.95	0.95	0.96	1.02	1.06	1.06	1.14	1.51	1.66	1.75	0.81	0.75
Miller and Pekoz (1994)	LC-30	90	35	11	1.92	2532	366	27.4	459	554	1.55	1.55	1.55	1.55	1.55	1.55	1.55	1.55	1.55	1.55	1.55	1.00	1.00
Miller and Pekoz (1994)	LC-31	90	35	11	1.91	2532	366	22.5	454	550	1.28	1.28	1.28	1.28	1.28	1.28	1.28	1.28	1.28	1.28	1.28	1.00	1.00
Z-Section Columns																							
Polyzois and Charnvarnichborikarn	38-0.0-1	116.6	45.2	0	1.5	458	345	52.96	116.877	116.877	1.09	1.17	1.17	1.17	1.09	1.24	1.24	1.15	1.38	1.33	1.41	0.88	0.94
Polyzois and Charnvarnichborikarn	38-0.0-2	115.5	45.5	0	1.5	458	345	49.17	117.56	117.5605	1.01	1.08	1.08	1.08	1.01	1.14	1.14	1.07	1.27	1.23	1.31	0.88	0.94
Polyzois and Charnvarnichborikarn	38-0.0-3	116.3	45.5	0	1.5	457.2	345	52.93	116.613	116.6127	1.09	1.17	1.17	1.17	1.09	1.23	1.23	1.15	1.37	1.33	1.41	0.88	0.94
Polyzois and Charnvarnichborikarn	38-6.4-1	114.8	52.3	14.5	1.5	457.2	345	84.11	171.424	349.1	1.00	1.00	0.92	1.04	1.02	0.95	1.04	1.02	1.12	1.25	1.17	1.05	0.99
Polyzois and Charnvarnichborikarn	38-6.4-2	115.6	52.9	14.8	1.5	458	345	77.65	169.012	350.952	0.91	0.91	0.84	0.96	0.93	0.87	0.96	0.93	1.03	1.15	1.08	1.05	0.98
Polyzois and Charnvarnichborikarn	38-6.4-3	115.3	52.8	14.2	1.5	457.7	345	85.89	169.82	339.7036	1.03	1.03	0.94	1.06	1.04	0.98	1.06	1.04	1.16	1.29	1.21	1.05	0.99

											test to predicted ratios for studied methods											AISI comparison	
Researcher	**Specimen ID**	**h (mm)**	**b (mm)**	**d (mm)**	**t (mm)**	**L (mm)**	**fy (MPa)**	**P (kN)**	**fcr_local (MPa)**	**fcr_dist (MPa)**	**A1**	**A2**	**B1**	**B2**	**B3**	**C1**	**C2**	**C3**	**D1**	**D2**	**D3**	**C1/A1**	**C3/A1**
Polyzois and Charnvarnichborikarn	38-12.7-1	115.6	52.9	20.6	1.5	457.2	345	79.66	169.325	441.0982	0.85	0.85	0.83	0.93	0.91	0.83	0.93	0.91	0.92	1.03	1.00	1.03	0.94
Polyzois and Charnvarnichborikarn	38-12.7-2	115.9	53.2	21.1	1.5	457.2	345	88.56	168.409	444.1084	0.94	0.94	0.92	1.03	1.01	0.92	1.03	1.01	1.01	1.14	1.10	1.03	0.94
Polyzois and Charnvarnichborikarn	38-12.7-3	115	52.3	20.6	1.5	457.7	345	67.86	171.206	445.1763	0.73	0.73	0.71	0.80	0.78	0.71	0.80	0.78	0.78	0.88	0.85	1.03	0.94
Polyzois and Charnvarnichborikarn	38-19.1-1	115.3	52.3	26.9	1.5	458	345	80.55	170.394	488.4826	0.88	0.88	0.82	0.90	0.88	0.82	0.90	0.88	0.85	0.93	0.94	1.06	1.00
Polyzois and Charnvarnichborikarn	38-19.1-2	115.5	52.8	26.7	1.5	457.2	345	88.11	169.668	485.8655	0.95	0.95	0.90	0.98	0.96	0.90	0.98	0.96	0.93	1.02	1.03	1.06	1.00
Polyzois and Charnvarnichborikarn	38-19.1-3	115.4	52.9	26.7	1.5	457.7	345	92.87	169.911	486.6304	1.01	1.01	0.95	1.04	1.01	0.95	1.04	1.01	0.98	1.08	1.09	1.06	1.00
Polyzois and Charnvarnichborikarn	38-25.4-1	115	52.6	32.8	1.5	457.7	345	93.01	170.893	557.7216	1.04	1.04	0.94	0.99	0.97	0.94	0.99	0.97	0.94	0.99	1.01	1.10	1.07
Polyzois and Charnvarnichborikarn	38-25.4-2	116.1	52.9	33.1	1.5	457.2	345	85.89	167.747	552.0763	0.96	0.96	0.87	0.92	0.89	0.87	0.92	0.89	0.87	0.92	0.94	1.10	1.07
Polyzois and Charnvarnichborikarn	38-25.4-3	115.8	52.6	33	1.5	457.7	345	81.21	168.673	551.7394	0.91	0.91	0.82	0.87	0.84	0.82	0.87	0.84	0.82	0.87	0.89	1.10	1.07
Polyzois and Charnvarnichborikarn	51.0.0-1	117.4	58.2	0	1.5	457.2	345	49.84	88.1694	88.16935	0.99	1.06	1.06	1.06	1.05	1.10	1.10	1.09	1.21	1.20	1.43	0.90	0.91
Polyzois and Charnvarnichborikarn	51.0.0-2	117.4	58.2	0	1.5	457.7	345	52.73	88.1694	88.16935	1.04	1.12	1.12	1.12	1.11	1.16	1.16	1.15	1.28	1.27	1.51	0.90	0.91
Polyzois and Charnvarnichborikarn	51.0.0-3	117.2	57.7	0	1.5	457.7	345	52.96	89.3027	89.30272	1.05	1.13	1.13	1.13	1.11	1.16	1.16	1.15	1.29	1.28	1.51	0.90	0.91
Polyzois and Charnvarnichborikarn	51-6.4-1	116.1	65	14.7	1.5	457.7	345	77.79	163.742	343.2307	0.90	0.90	0.82	0.88	0.85	0.84	0.88	0.85	1.02	1.12	1.00	1.07	1.05
Polyzois and Charnvarnichborikarn	51-6.4-2	115.4	65.3	14.5	1.5	457.7	345	78.77	165.49	342.0292	0.91	0.91	0.84	0.89	0.86	0.86	0.89	0.86	1.04	1.13	1.01	1.07	1.06
Polyzois and Charnvarnichborikarn	51-6.4-3	115.3	64.7	14.7	1.5	457.7	345	73.38	165.973	347.9863	0.85	0.85	0.77	0.83	0.80	0.79	0.83	0.80	0.96	1.05	0.94	1.07	1.05
Polyzois and Charnvarnichborikarn	51-12.7-1	114.5	65.3	20.6	1.5	457.2	345	78.32	168.223	442.1679	0.79	0.79	0.77	0.85	0.82	0.77	0.85	0.82	0.87	0.95	0.90	1.02	0.97
Polyzois and Charnvarnichborikarn	51-12.7-2	115	65	20.8	1.5	457.2	345	67.2	166.965	441.0846	0.68	0.68	0.66	0.73	0.70	0.66	0.73	0.70	0.74	0.81	0.77	1.02	0.96
Polyzois and Charnvarnichborikarn	51-12.7-3	114	65	20.3	1.5	457.2	345	89.22	169.699	443.3529	0.90	0.90	0.88	0.97	0.93	0.88	0.97	0.93	1.00	1.09	1.03	1.01	0.96
Polyzois and Charnvarnichborikarn	51-19.1-1	116.1	65.1	27.2	1.5	457.7	345	71.2	163.981	531.0268	0.72	0.72	0.69	0.74	0.71	0.69	0.74	0.71	0.71	0.76	0.76	1.04	1.02
Polyzois and Charnvarnichborikarn	51-19.1-2	116.1	65.1	27.5	1.5	457.7	345	89.36	163.975	537.0634	0.91	0.91	0.87	0.92	0.89	0.87	0.92	0.89	0.89	0.95	0.94	1.04	1.02
Polyzois and Charnvarnichborikarn	51-19.1-3	116.1	65.3	27	1.5	457.7	345	83.22	163.92	527.3896	0.84	0.84	0.81	0.86	0.83	0.81	0.86	0.83	0.84	0.89	0.88	1.04	1.02
Polyzois and Charnvarnichborikarn	51-25.4-1	115.8	65	32.5	1.5	457.7	345	80.77	164.584	575.0345	0.83	0.83	0.78	0.81	0.78	0.78	0.81	0.78	0.78	0.81	0.82	1.07	1.07
Polyzois and Charnvarnichborikarn	51-25.4-2	115.3	65	33	1.4	458	345	77.21	144.524	543.5859	0.91	0.91	0.84	0.86	0.83	0.84	0.86	0.83	0.84	0.86	0.88	1.08	1.09
Polyzois and Charnvarnichborikarn	51-25.4-3	115.6	65.6	33.1	1.5	457.7	345	86.33	164.871	579.7639	0.89	0.89	0.83	0.85	0.82	0.83	0.85	0.82	0.83	0.85	0.86	1.07	1.08
Polyzois and Charnvarnichborikarn	63-0.0-1	117.9	70.4	0	1.5	458	345	53.62	65.825	65.82497	1.04	1.14	1.14	1.14	1.19	1.17	1.17	1.22	1.27	1.28	1.70	0.89	0.85
Polyzois and Charnvarnichborikarn	63-0.0-2	118.2	70.4	0	1.5	458	345	55.4	65.7661	65.76609	1.08	1.18	1.18	1.18	1.23	1.21	1.21	1.26	1.31	1.32	1.75	0.89	0.85
Polyzois and Charnvarnichborikarn	63-0.0-3	116.6	70.6	0	1.5	458	345	54.29	65.7726	65.77262	1.05	1.16	1.16	1.16	1.21	1.19	1.18	1.24	1.28	1.29	1.73	0.89	0.85
Polyzois and Charnvarnichborikarn	63-6.4-1	115.4	78.8	14.3	1.5	458	345	70.31	160.67	312.0451	0.82	0.82	0.73	0.74	0.70	0.75	0.75	0.70	0.94	0.99	0.85	1.09	1.16
Polyzois and Charnvarnichborikarn	63-6.4-2	116.1	78.3	14.5	1.5	458	345	78.32	159.133	315.0381	0.90	0.90	0.81	0.82	0.79	0.82	0.82	0.79	1.04	1.10	0.95	1.10	1.15
Polyzois and Charnvarnichborikarn	63-6.4-3	116.3	77.7	14.2	1.5	458	345	88.11	158.835	308.5292	1.03	1.03	0.92	0.93	0.89	0.94	0.94	0.89	1.18	1.25	1.08	1.09	1.15
Polyzois and Charnvarnichborikarn	63-12.7-1	114.8	78	20.6	1.4	457.7	345	72.98	141.903	362.1081	0.79	0.79	0.79	0.83	0.79	0.79	0.83	0.79	0.90	0.95	0.92	1.00	1.01
Polyzois and Charnvarnichborikarn	63-12.7-2	114.9	78	21.1	1.5	457.7	345	85	162.609	409.5519	0.82	0.82	0.81	0.85	0.81	0.81	0.85	0.81	0.91	0.96	0.92	1.01	1.00
Polyzois and Charnvarnichborikarn	63-12.7-3	114.5	78	20.8	1.5	457.7	345	82.99	163.633	409.541	0.80	0.80	0.80	0.83	0.80	0.80	0.83	0.80	0.90	0.95	0.90	1.00	1.00
Polyzois and Charnvarnichborikarn	63-19.1-1	114.6	78	27.2	1.5	457.7	345	82.77	163.341	508.592	0.80	0.80	0.78	0.80	0.76	0.78	0.80	0.76	0.81	0.82	0.82	1.03	1.05
Polyzois and Charnvarnichborikarn	63-19.1-2	115.6	78	27	1.5	457.7	345	89	160.805	497.0054	0.86	0.86	0.84	0.86	0.82	0.84	0.86	0.82	0.87	0.89	0.89	1.03	1.05
Polyzois and Charnvarnichborikarn	63-19.1-3	115.6	78	27	1.5	457.7	345	85	160.805	497.0054	0.82	0.82	0.80	0.82	0.79	0.80	0.82	0.79	0.83	0.85	0.85	1.03	1.05
Polyzois and Charnvarnichborikarn	63-25.4-1	114.5	78.2	32.8	1.4	457.7	345	84.55	142.184	526.5667	0.94	0.94	0.90	0.88	0.84	0.90	0.88	0.84	0.90	0.88	0.90	1.05	1.12
Polyzois and Charnvarnichborikarn	63-25.4-2	114.8	78.2	33	1.5	457.7	345	84.06	162.415	562.0575	0.83	0.83	0.79	0.78	0.75	0.79	0.78	0.75	0.79	0.78	0.79	1.05	1.11
Polyzois and Charnvarnichborikarn	63-25.4-3	115.4	78.6	33.3	1.4	457.7	345	80.1	140.032	519.6032	0.89	0.89	0.85	0.83	0.80	0.85	0.83	0.80	0.85	0.83	0.86	1.05	1.12
Polyzois and Charnvarnichborikarn	-	203.8	76	0	1.5	609.3	345	55.18	39.3975	39.39746	1.04	1.29	1.29	1.29	1.18	1.33	1.33	1.22	1.68	1.75	1.83	0.78	0.85
Polyzois and Charnvarnichborikarn	-	202.9	75.2	0	1.5	609.3	345	47.17	39.9065	39.90651	0.89	1.10	1.10	1.10	1.01	1.14	1.14	1.04	1.44	1.49	1.56	0.78	0.85
Polyzois and Charnvarnichborikarn	-	203.3	77.1	3.6	1.5	610.1	345	58.07	43.6732	43.67317	0.90	1.22	1.22	1.22	1.15	1.26	1.26	1.18	1.60	1.70	1.74	0.72	0.77
Polyzois and Charnvarnichborikarn	-	201.2	76.8	4.1	1.5	609.6	345	49.62	46.4016	46.40163	0.76	1.01	1.01	1.01	0.95	1.04	1.04	0.98	1.32	1.41	1.43	0.73	0.77
Polyzois and Charnvarnichborikarn	-	201.9	75.7	5.15	1.5	609.9	345	54.74	51.3264	51.32641	0.81	1.03	1.03	1.03	0.99	1.07	1.07	1.02	1.38	1.49	1.47	0.76	0.79
Polyzois and Charnvarnichborikarn	-	202.4	75.7	5.3	1.5	609.6	345	54.96	51.8619	51.86188	0.81	1.03	1.03	1.03	0.99	1.06	1.06	1.02	1.37	1.48	1.46	0.76	0.79
Polyzois and Charnvarnichborikarn	-	201.1	74.9	9.4	1.5	609.6	345	67.64	56.4726	77.8667	0.89	0.97	0.97	0.97	0.96	0.99	0.99	0.99	1.33	1.52	1.49	0.89	0.90
Polyzois and Charnvarnichborikarn	-	202.4	76.2	9.6	1.5	609.9	345	70.31	55.7349	77.6901	0.92	0.99	0.99	0.99	0.99	1.02	1.02	1.02	1.37	1.57	1.54	0.90	0.90
Polyzois and Charnvarnichborikarn	-	202.7	74.7	15.7	1.5	610.1	345	84.11	56.1952	115.3263	0.92	0.92	0.90	1.00	0.98	0.92	1.00	0.98	1.31	1.55	1.57	1.00	0.94
Polyzois and Charnvarnichborikarn	-	201.3	75	15.8	1.5	609.6	345	81.21	56.9237	117.0984	0.89	0.89	0.86	0.96	0.94	0.88	0.96	0.94	1.26	1.49	1.50	1.00	0.94
Polyzois and Charnvarnichborikarn	-	203.4	76.2	22.6	1.5	609.6	345	91.49	55.8878	158.1927	0.88	0.88	0.87	1.04	1.01	0.87	1.04	1.01	1.14	1.38	1.48	1.01	0.86
Polyzois and Charnvarnichborikarn	-	203.2	76.4	22.8	1.5	609.3	345	90.78	55.9804	159.8541	0.87	0.87	0.86	1.03	1.00	0.86	1.03	1.00	1.13	1.36	1.46	1.01	0.87
Polyzois and Charnvarnichborikarn	-	204.3	75.8	28.5	1.5	609.6	345	92.12	55.5166	185.9957	0.89	0.89	0.86	1.01	0.99	0.86	1.01	0.99	1.02	1.21	1.38	1.03	0.90
Polyzois and Charnvarnichborikarn	-	204.5	75.8	28.5	1.5	609.6	345	92.78	55.4136	185.5881	0.90	0.90	0.87	1.02	1.00	0.87	1.02	1.00	1.03	1.22	1.39	1.03	0.90
Polyzois and Charnvarnichborikarn	-	205.2	74.9	35	1.5	610.1	345	102.8	55.1586	205.5439	1.02	1.02	0.96	1.10	1.08	0.96	1.10	1.08	1.05	1.21	1.45	1.06	0.94
Polyzois and Charnvarnichborikarn	-	201.7	75.2	34.8	1.5	609.9	345	94.56	56.9626	214.0431	0.93	0.93	0.88	1.01	0.99	0.88	1.01	0.99	0.96	1.11	1.32	1.06	0.95

Researcher	Specimen ID	h (mm)	b (mm)	d (mm)	t (mm)	L (mm)	fy (MPa)	P (kN)	fcr_local (MPa)	fcr_dist (MPa)	test to predicted ratios for studied methods											AISI comparison	
											A1	A2	B1	B2	B3	C1	C2	C3	D1	D2	D3	C1/A1	C3/A1
Polyzois and Charnvarnichborikarn	-	202.2	74.9	41.1	1.5	609.9	345	104.13	56.7268	227.0378	1.05	1.05	0.96	1.08	1.06	0.96	1.08	1.06	1.00	1.12	1.38	1.09	1.00
Polyzois and Charnvarnichborikarn	-	201.9	75.2	40.9	1.5	609.9	345	97.46	56.863	227.8079	0.98	0.98	0.90	1.01	0.99	0.90	1.01	0.99	0.94	1.05	1.29	1.09	1.00
Polyzois and Charnvarnichborikarn	-	200.6	75.4	54.1	1.5	610.1	345	103.69	57.477	249.9819	1.12	1.12	0.95	1.01	0.99	0.95	1.01	0.99	0.95	1.01	1.26	1.18	1.14
Polyzois and Charnvarnichborikarn	-	202.4	74.4	54.3	1.5	609.9	345	93.01	56.5949	243.1791	1.01	1.01	0.85	0.91	0.89	0.85	0.91	0.89	0.85	0.91	1.15	1.19	1.14
Polyzois and Charnvarnichborikarn	-	205.1	75.5	0	1.5	1220	345	51.18	39.2246	39.22458	1.09	1.20	1.20	1.20	1.10	1.37	1.37	1.25	1.57	1.63	1.70	0.80	0.87
Polyzois and Charnvarnichborikarn	-	203.2	75.7	0	1.5	1219	345	56.52	39.6564	39.65643	1.20	1.32	1.32	1.32	1.21	1.50	1.50	1.38	1.72	1.79	1.87	0.80	0.87
Polyzois and Charnvarnichborikarn	-	200.2	73.5	6.1	1.5	1220	345	55.85	55.5712	57.65107	0.90	0.99	0.99	0.99	0.96	1.12	1.12	1.09	1.33	1.45	1.42	0.80	0.82
Polyzois and Charnvarnichborikarn	-	201.5	73.7	6.1	1.5	1219	345	51.84	54.8533	58.1709	0.83	0.92	0.92	0.92	0.88	1.04	1.04	1.00	1.24	1.35	1.31	0.80	0.83
Polyzois and Charnvarnichborikarn	-	201.1	73.4	6.1	1.5	1220	345	57.41	55.0803	58.4471	0.92	1.02	1.02	1.02	0.98	1.15	1.15	1.11	1.37	1.49	1.45	0.80	0.83
Polyzois and Charnvarnichborikarn	-	201.9	73.9	6.1	1.5	1219	345	56.52	54.6308	57.9271	0.90	1.00	1.00	1.00	0.96	1.13	1.13	1.09	1.35	1.47	1.43	0.80	0.83
Polyzois and Charnvarnichborikarn	-	202.2	74.5	8.9	1.5	1220	345	60.97	55.7998	74.3934	0.90	0.90	0.90	0.90	0.89	1.01	1.01	1.00	1.24	1.40	1.37	0.89	0.90
Polyzois and Charnvarnichborikarn	-	202.7	74.7	8.7	1.5	1220	345	63.64	55.4745	72.8491	0.94	0.95	0.95	0.95	0.94	1.07	1.07	1.05	1.31	1.48	1.45	0.88	0.89
Polyzois and Charnvarnichborikarn	-	200.1	73.6	15.5	1.5	1220	345	86.33	57.6684	116.7028	1.05	1.05	0.95	1.14	1.12	1.05	1.14	1.12	1.36	1.61	1.61	0.99	0.93
Polyzois and Charnvarnichborikarn	-	201.4	74.9	14.7	1.5	1219	345	75.21	56.8292	110.1133	0.93	0.93	0.84	0.99	0.98	0.94	0.99	0.98	1.21	1.43	1.43	0.99	0.96
Polyzois and Charnvarnichborikarn	-	202	74.7	21.1	1.5	1220	345	93.23	56.7145	143.953	0.99	0.99	0.98	1.18	1.16	0.98	1.18	1.16	1.28	1.55	1.57	1.01	0.85
Polyzois and Charnvarnichborikarn	-	201.7	74.5	21.6	1.5	1220	345	92.56	56.8993	146.8438	0.98	0.98	0.97	1.17	1.15	0.97	1.17	1.15	1.26	1.52	1.55	1.01	0.85
Polyzois and Charnvarnichborikarn	-	202.3	74.7	28	1.5	1220	345	95.45	56.6433	170.1019	1.01	1.01	0.98	1.15	1.13	0.98	1.15	1.13	1.21	1.43	1.47	1.03	0.89
Polyzois and Charnvarnichborikarn	-	202.3	74.7	27.5	1.5	1218	345	87.22	56.6389	168.4684	0.92	0.92	0.89	1.06	1.04	0.89	1.06	1.04	1.11	1.32	1.36	1.03	0.89
Polyzois and Charnvarnichborikarn	-	202.3	74.2	34.3	1.5	1220	345	91.45	56.7195	183.8017	0.98	0.98	0.92	1.07	1.05	0.92	1.07	1.05	1.10	1.28	1.34	1.06	0.93
Polyzois and Charnvarnichborikarn	-	202.3	74.2	34.3	1.5	1219	345	99.24	56.7195	183.8018	1.06	1.06	1.00	1.16	1.14	1.00	1.16	1.14	1.20	1.39	1.46	1.06	0.93
Polyzois and Charnvarnichborikarn	-	202.3	75	40.4	1.5	1220	345	92.34	56.6662	194.2872	1.00	1.00	0.92	1.04	1.02	0.92	1.04	1.02	1.08	1.23	1.29	1.09	0.98
Polyzois and Charnvarnichborikarn	-	201.5	74.7	40.7	1.5	1219	345	95.45	57.1165	195.9231	1.04	1.04	0.95	1.07	1.05	0.95	1.07	1.05	1.12	1.26	1.33	1.09	0.99
Polyzois and Charnvarnichborikarn	-	202	74.7	53.4	1.5	1220	345	96.79	56.791	214.498	1.11	1.11	0.95	1.01	0.99	0.95	1.01	0.99	1.08	1.16	1.24	1.17	1.12
Polyzois and Charnvarnichborikarn	-	202.5	74.5	53.9	1.5	1218	345	100.35	56.5382	214.2484	1.16	1.16	0.98	1.05	1.03	0.98	1.05	1.03	1.11	1.20	1.28	1.18	1.12

Appendix F.1 For Immediate Consideration: New Commentary Language

B4.2 Uniformly Compressed Elements with an Edge Stiffener

An edge stiffener is used to provide a continuous support along a longitudinal edge of the compression flange to improve the buckling stress. Even though in most cases, the edge stiffener takes the form of a simple lip, other types of edge stiffeners can also be used for cold-formed steel members.

In order to provide necessary support for the compression element, the edge stiffener must possess sufficient rigidity. Otherwise it may buckle perpendicular to the plane of the element to be stiffened. This mode of buckling first termed "stiffener buckling" by Desmond, Pekoz and Winter (1981a) has come to be termed distortional buckling.

Both theoretical and experimental studies on the local and distortional stability of compression flanges stiffened by edge stiffeners have been carried out in the past. The design requirements included in Section B4.2 of the 1986 AISI *Specification* were based on the investigations on adequately stiffened and partially stiffened elements conducted by Desmond, Pekoz and Winter (1981a), with additional research work of Pekoz and Cohen (Pekoz, 1986b). These design provisions were developed on the basis of the critical buckling criterion and the postbuckling strength criterion.

Specification Section B4.2 recognizes that the necessary stiffener rigidity depends upon the slenderness (w/t) of the plate element being stiffened. Thus, Cases I, II and III each contains different definitions for an adequate stiffener moment of inertia.

The interaction of the plate elements, as well as the degree of edge support, full or partial, is compensated for in the expressions for k, d_s, and A_s (Pekoz, 1986b). In the 1996 edition of the AISI *Specification* (AISI, 1996), the design equations for buckling coefficient were changed for further clarity. In Case II, the equation for k_a = 5.25-5 (D/w) ∨ 4.0 is applicable only for simple lip stiffeners because the term D/w is meaningless for other types of edge stiffeners. It should be noted that the provisions in this section were based on research dealing only with simple lip stiffeners and extension to other types of stiffeners was purely intuitive. The requirement of 140°> θ > 40° for the applicability of these provisions was also decided on an intuitive basis. For design examples, see Part I of the *Manual* (AISI, 1996).

Test data on flexural members to verify the accuracy of the simple lip stiffener design was collected from a number of sources, both university and industry. These tests showed good correlation with the equations in Section B4.2. ~~However, proprietary testing conducted in 1989 revealed that lip lengths with a d/t ratio of greater than 14 gave unconservative results.~~

~~A review of the original research data showed a lack of data for simple stiffening lips with d/t ratios greater than 14. Therefore, pending further research, an upper limit of 14 is recommended.~~

Test data on compression members also showed good overall correlation with the equations in Section B4.2 (Schafer 2000). However, compression members with high web slenderness (approximately h/t > 200) and/or narrow flanges (approximately h/b > 2) may yield unconservative solutions with current methods due to local buckling interaction. Compression members with low web slenderness and wide flanges (shapes approaching square, approximately b/h > 3/4) may yield unconservative solutions due to distortional buckling. In addition, the provisions of

B4.2 may be overly conservative for members with long lips (d/b > 0.25). Current research on beams and columns; Hancock (1985), Hancock et al. (1994, 1996), Schafer and Peköz (1998), Schafer (2000) indicate that more exact calculation of the plate buckling coefficient, k, for both local and distortional buckling may be completed by hand or computational methods.

References

Hancock, G.J. (1985). "Distortional Buckling of Steel Storage Rack Columns". *J. of Structural Eng*., ASCE, 111(12), pp. 2770-2783

Hancock, G.J., Kwon, Y.B., Bernard, E.S. (1994). "Strength Design Curves for Thin-Walled Sections Undergoing Distortional Buckling". *J. of Constructional Steel Research*, Elsevier, 31(2-3), pp. 169-186.

Hancock, G.J., Rogers, C.A., Schuster, R.M. (1996). "Comparison of the Distortional Buckling Method for Flexural Members with Tests." *Proceedings of the Thirteenth International Specialty Conference on Cold-Formed Steel Structures*, St. Louis, MO.

Schafer, B.W. (2000). "Distortional Buckling of Cold-Formed Steel Columns." *Final Report to the American Iron and Steel Institute*, Washington, D.C.

Schafer, B.W., and Peköz, T., (1998). "Laterally Braced Cold-Formed Steel Flexural Members with Edge Stiffened Flanges." *Proceedings of the Fourteenth International Specialty Conference on Cold-Formed Steel Structures*, St. Louis, MO.

Appendix F.2 For Interim Adoption: New Effective Width Method

- Delete all content in existing section B4.2
- New B4.2 section:

B4.2 Uniformly Compressed Elements with an Edge Stiffener

Note, all members that contain elements with an edge stiffener must also be checked for distortional buckling of the member, see provisions of B7.

(a) *Strength Determination*

The effective width, b, shall be determined in accordance with Section B2.1a, except that k shall be taken as 4.0 and w as defined in Figure B4-2.

(b) *Deflection Determination*

The effective width, b_d, used in computing deflection shall be determined as in Section B4.2a, except that f_d is substituted for f.

- New B7 section:

B7 Effective Width of Elements Subject to Distortional Buckling

Elements that form a member which include an edge stiffened element in compression must be checked for distortional buckling. Effective width calculations for **local buckling** should be completed by sections B2 through B5. In addition, effective width calculations for **distortional buckling** should be completing by the guidelines below. The minimum effective area or effective moment of inertia governs the design.

(a) *Strength Determination*

The effective width, b, of all elements that form a member which includes an edge stiffened element in compression, shall be determined in accordance with Section B2.1a, except that k shall be taken as k_d determined below

Determine the elastic distortional buckling stress, f_{ed}, per expressions in Table B7.1. See the commentary for aid in calculation of the section properties for use in the expressions.

Determine the reduced elastic distortional buckling stress

$$f_d = R_d f_{ed} \qquad (Eq.\ \text{B7-11})$$

$$R_d = \min\left(1, \frac{1.17}{\lambda_d + 1} + 0.3\right) \qquad (Eq.\ \text{B7-12})$$

$$\lambda_d = \sqrt{F_n / f_{ed}} \qquad (Eq.\ \text{B7-13})$$

where

F_n is per section C3 for flexural members, and C4 for compression members

Determine k_d for distortional buckling

for elements of width, w, that are a portion of a uniformly compressed member

$$k_d = f_d \frac{12\left(1-\nu^2\right)}{\pi^2 E}\left(\frac{w}{t}\right)^2 \qquad (Eq.\ \text{B7-14})$$

for elements of width, w, that are a portion of a flexural member

determine *f*, the distortional stress at the compression fiber of the element of interest, by using f_d for the distortional stress at the extreme compression fiber of the flexural member (i.e., $f = f_d$ at the extreme compression fiber). then k_d may be calculated as

$$k_d = f \frac{12\left(1-\nu^2\right)}{\pi^2 E}\left(\frac{w}{t}\right)^2 \qquad (Eq.\ \text{B7-15})$$

Table B7.1 Calculation of Distortional Buckling Stress (f_{ed})

DISTORTIONAL BUCKLING

$$f_{ed} = \frac{k_{\phi fe} + k_{\phi we}}{\tilde{k}_{\phi fg} + \tilde{k}_{\phi wg}} \qquad \text{(Eq. B7-1)}$$

$$L = min\left(L_{cr}, L_m\right) \qquad \text{(Eq. B7-2)}$$

Flange Rotational "Stiffness":

$$\left(k_{\phi f}\right)_e = \left(\frac{\pi}{L}\right)^4 \left(EI_{xf}\left(x_o - h_x\right)^2 + EC_{wf} - E\frac{I_{xyf}^2}{I_{yf}}\left(x_o - h_x\right)^2 \right) + \left(\frac{\pi}{L}\right)^2 GJ_f \qquad \text{(Eq. B7-3)}$$

$$\left(\tilde{k}_{\phi f}\right)_g = \left(\frac{\pi}{L}\right)^2 \left[A_f \left(\left(x_o - h_x\right)^2 \left(\frac{I_{xyf}}{I_{yf}}\right)^2 - 2y_o\left(x_o - h_x\right)\left(\frac{I_{xyf}}{I_{yf}}\right) + h_x^2 + y_o^2 \right) + I_{xf} + I_{yf} \right] \qquad \text{(Eq. B7-4)}$$

Flexural Member: Critical Length and Web Rotational Stiffness

$$L_{cr} = \left(\frac{4\pi^4 h\left(1-\nu^2\right)}{t^3} \left(I_{xf}\left(x_o - h_x\right)^2 + C_{wf} - \frac{I_{xyf}^2}{I_{yf}}\left(x_o - h_x\right)^2 \right) + \frac{\pi^4 h^4}{720} \right)^{1/4} \qquad \text{(Eq. B7-5)}$$

$$k_{\phi we} = \frac{Et^3}{12\left(1-\nu^2\right)} \left(\frac{3}{h} + \left(\frac{\pi}{L}\right)^2 \frac{19h}{60} + \left(\frac{\pi}{L}\right)^4 \frac{h^3}{240} \right) \qquad \text{(Eq. B7-6)}$$

$$\tilde{k}_{\phi wg} = \frac{ht\pi^2}{13440} \left(\frac{\left(45360\left(1-\xi_{web}\right)+62160\right)\left(\frac{L}{h}\right)^2 + 448\pi^2 + \left(\frac{h}{L}\right)^2 \left(53+3\left(1-\xi_{web}\right)\right)\pi^4}{\pi^4 + 28\pi^2\left(\frac{L}{h}\right)^2 + 420\left(\frac{L}{h}\right)^4} \right) \qquad \text{(Eq. B7-7)}$$

Compression Member: Critical Length and Web Rotational Stiffness

$$L_{cr} = \left(\frac{6\pi^4 h\left(1-\nu^2\right)}{t^3} \left(I_{xf}\left(x_o - h_x\right)^2 + C_{wf} - \frac{I_{xyf}^2}{I_{yf}}\left(x_o - h_x\right)^2 \right) \right)^{1/4} \qquad \text{(Eq. B7-8)}$$

$$k_{\phi we} = \frac{Et^3}{6h\left(1-\nu^2\right)} \qquad \text{(Eq. B7-9)}$$

$$\tilde{k}_{\phi wg} = \left(\frac{\pi}{L}\right)^2 \frac{th^3}{60} \qquad \text{(Eq. B7-10)}$$

E = Modulus of Elasticity
G = Shear Modulus
ν = Poisson's Ratio
t = plate thickness
h = web depth
$\xi = (f_1 - f_2)/f_1$ stress gradient in the web
L_m = Distance between restraints which limit rotation of the flange about the flange/web junction

A_f, I_{xf}, I_{yf}, C_{wf}, J_f = Section properties of the compression flange (flange and edge stiffener) about x, y axes respectively, where the x, y axes are located at the centroid of flange with x-axis parallel with flat portion of the flange
x_o = x distance from the flange/web junction to the centroid of the flange.
h_x = x distance from the centroid of the flange to the shear center of the flange

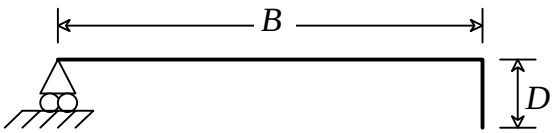

$$A = (B + D)t$$

$$J = \tfrac{1}{3} Bt^3 + \tfrac{1}{3} Dt^3$$

$$I_x = \frac{t\left(t^2 B^2 + 4BD^3 + t^2 BD + D^4\right)}{12(B + D)}$$

$$I_y = \frac{t\left(B^4 + 4DB^3\right)}{12(B + D)}$$

$$I_{xy} = \frac{tB^2 D^2}{4(B + D)}$$

$$I_o = \frac{tB^3}{3} + \frac{Bt^3}{12} + \frac{tD^3}{3}$$

$$x_o = \frac{B^2}{2(B + D)}$$

$$h_y = y_o = \frac{-D^2}{2(B + D)}$$

$$h_x = \frac{-\left(B^2 + 2DB\right)}{2(B + D)}$$

$$x_o - h_x = B$$

$$C_w = 0$$

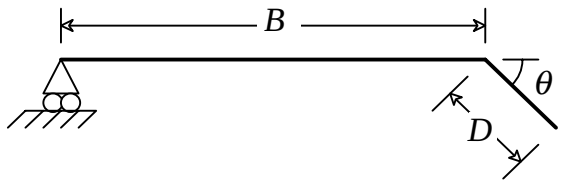

$$A = (B + D)t$$

$$J = \tfrac{1}{3} Bt^3 + \tfrac{1}{3} Dt^3$$

$$I_x = \frac{t\left(t^2 B^2 + 4BD^3 - 4BD^3 \cos^2(\theta) + t^2 BD + D^4 - D^4 \cos^2(\theta)\right)}{12(B + D)}$$

$$I_y = \frac{t\left(B^4 + 4DB^3 + 6D^2 B^2 \cos(\theta) + 4D^3 B \cos^2(\theta) + D^4 \cos^2(\theta)\right)}{12(B + D)}$$

$$I_{xy} = \frac{tBD^2 \sin(\theta)\left(B + D\cos(\theta)\right)}{4(B + D)}$$

$$I_o = \frac{tB^3}{3} + \frac{Bt^3}{12} + \frac{tD^3}{3}$$

$$x_o = \frac{B^2 - D^2 \cos(\theta)}{2(B + D)}$$

$$h_y = y_o = \frac{-D^2 \sin(\theta)}{2(B + D)}$$

$$h_x = \frac{-\left(B^2 + 2DB + D^2 \cos(\theta)\right)}{2(B + D)}$$

$$x_o - h_x = B$$

$$C_w = 0$$

Figure C-B7-1 Element Properties for a Simple Lip Stiffener

Appendix F.3 For Long-term Adoption and Interim Adoption as an Alternative Procedure: Direct Strength

An outline of the Direct Strength method (methods C2 and C3 in this report) follows:

G. Alternative Design Procedure: Direct Strength

G1 Columns

G1.1 Nominal long column buckling load

$P_{ne} = \left(0.658^{\lambda_c^2}\right) P_y$ for $\lambda_c \le 1.5$ and (*Eq.* G1.1-1)

$= \left[\frac{0.877}{\lambda_c^2}\right] P_y$ for $\lambda_c > 1.5$ (*Eq.* G1.1-2)

$\lambda_c = \sqrt{P_y / P_{cre}}$ (*Eq.* G1.1-3)

$P_y = A_g F_y$ (*Eq.* G1.1-4)

$P_{cre} = A_g F_e$ (*Eq.* G1.1-5)

F_e = the least of the elastic flexural, torsional and torsional-flexural buckling stress determined according to Section C4.1 through C4.3

G2.1 Local buckling strength

$P_{nl} = P_{ne}$ for $\lambda_l \le 0.776$ and (*Eq.* G1.2-1)

$= \left(1 - 0.15\left(\frac{P_{crl}}{P_{ne}}\right)^{0.4}\right)\left(\frac{P_{crl}}{P_{ne}}\right)^{0.4} P_{ne}$ for $\lambda_l > 0.776$ (*Eq.* G1.2-2)

$\lambda_l = \sqrt{P_{ne} / P_{crl}}$ (*Eq.* G1.2-3)

P_{crl} = Elastic local column buckling load*

G3.1 Distortional buckling strength

$P_{nd} = P_{ne}$ for $\lambda_d \le 0.561$ and (*Eq.* G1.3-1)

$= \left(1 - 0.25\left(\frac{P_{crd}}{P_{ne}}\right)^{0.6}\right)\left(\frac{P_{crd}}{P_{ne}}\right)^{0.6} P_{ne}$ for $\lambda_d > 0.561$ (*Eq.* G1.3-2)

$\lambda_d = \sqrt{P_{ne} / P_{crd}}$ (*Eq.* G1.3-3)

P_{crd} = Elastic distortional column buckling load*

G4.1 Nominal Capacity

P_n = minimum of P_{nl} , P_{nd} (*Eq.* G1.4-1)

$\Omega = 1.80$ (ASD)

$\phi = 0.85$ (LRFD)

* Elastic buckling loads may be determined by expressions in Appendix … *{an Appendix should be added to the Specification that provides closed-form expressions for local and distortional buckling similar to those expressions given in Appendix B of this report and used in Appendix D method C2 of this report}* In lieu of those expressions the elastic buckling load may be determined by rational analysis.